Studying magnesium transport in the common goldfish (*Carassius auratus*) using molecular and potentiometric approaches: Role and characterization of the magnesium transporter solute carrier 41a1 (SLC41a1)

Vladimir Ivaylov Kodzhahinchev

A thesis submitted to the Faculty of Graduate Studies in partial fulfillment of the requirements for the degree of Masters of Science

Graduate Program in Biology
York University
Toronto, Ontario

December 2016

Abstract

This thesis examined how magnesium transporter solute carrier 41a1 (SLC41a1) is regulated at the transcriptional level in the stenohaline goldfish (Carassius auratus) in response to environmental (ion-poor water exposures and temperature variation) and dietary manipulations (feeding a low, regular and high magnesium content diet). SLC41a1 mRNA behaved contrary to my hypotheses that expression levels would be innversely proportional to magnesium availability in the diet and environment. This suggests SLC41a1 participates in magnesium secretion, rather than absorption as proposed in mammals.

Finally, the scanning ion-selective electrode technique (SIET) was used as an alternative to radioisotope approaches in magnesium transport study. SIET found transport zonation along the gastrointestinal (GI) tract for magnesium, suggestive of mostly passive transport kinetics for magnesium at the 1st GI tract segment. Furthermore, a decrease in magnesium transport at the 1st and 8th GI tract segments was observed in response to 10^{-4}M ouabain, but not 10^{-4}M cobalt(III)hexamine-chloride.

Acknowledgments

The following thesis was completed solely by me with the exception of the following collaborations. The experiments shown in Figures 12 and 14 were completed with D. Kovacevic. I extracted all of the tissues used in both experiments, while we completed the cDNA synthesis together. Finally, D. ran the qPCR plates using my designed primers, while I troubleshot, ran the statistics and constructed the graphs. Figure 16 was completed with A. Biancolin. I sampled all of the tissues for segment 1, while the two of us worked together on the other 7 segments (I troubleshot and assisted A.). I ran the statistics and constructed the graph. Finally, Dr. Carol Bucking provided the entirety of Figure 17, including the data and statistical analysis.

I am eternally grateful to my supervisor, Dr. Carol Bucking, for having taken me under her wing for the past 3.5 years. It is through her seemingly limitless patience, wisdom and kindness that I have been able to survive both an undergraduate thesis and (hopefully) a Master's thesis.

I would also like to thank my present and past lab mates, (in turns of appearance) Leah, Dom, Julie, Salma, Tehmeena, Melanie and Pranav, all of whom have been critical to maintaining my sanity throughout graduate school, either by offering a helping hand, a thoughtful comment, or a warm cup of coffee. I would especially like to thank Drago and Andrew, the two undergraduate thesis students I had the pleasure of collaborating with over the past year.

Next, I would also like to thank Dr. Andrew Donini, for being a very kind and helpful advisor. Much of this thesis would not have been possible without him sharing knowledge (and access) of the SIET and ISME systems. I would also like to thank the members of the Donini lab, namely Lidiya, Gil, Andrea, Sima and Heath, for being wonderful people, every one of which has had to show me how to pull reference electrodes on multiple occasions.

I would also like to thank Dr. Scott Kelly for agreeing to be a part of my defence committee, and much more importantly, inspiring my initial interest in animal physiology. I would like to extend this gratitude to Kelly lab members, Anna, Julia, Chun and Dennis, all of whom have helped me on numerous occasions (many of which involved me locking myself out of room 022).

I would also like to thank Andreea of the Paluzzi lab for always being a good sport about sharing the SIET room over the past year and a half and not getting too mad at me for occasionally stealing her electrodes.

I'd especially like to thank Carm for always brightening my day and making the past 4 months of writing this thesis bearable.

Finally and most importantly, I would like to thank my family for their continuous support and love. Without the numerous sacrifices of my parents, Ivaylo and Margarita and the kindness of my sister, Marlena, I would not be the same person I am today.

Table of contents

List of tables

List of figures

List of abbreviations

(2-hydroxyethyl)ethylenediaminetriacetic acid - HEDTA
4-(2-hydroxyethyl)-1-piperazineethanesulfonic acid - HEPES
Chinese hamster ovary kidney cell - CHOK
Cobalt(III)-hexaammine chloride - Co3Hex
Cystic fibrosis transmembrane conductance regulator - CFTR
Cyclin M - Cnnm
Dechlorinated tap water - DTW
Diisothiocyanatostilbene-2,2'-disulfonic acid - DIDS
Epithelial Na^+ channel - ENaC
Fluorescence resonance energy transfer - FRET
Freshwater - FW
Gastrointestinal - GI
Human embryonic kidney - HEK
Hypocalcaemia - HSH
Ion-poor water - IPW
Ion-selective micro-electrode - ISME
Magnesium transporter E - MgtE
Mitochondria-rich cell - MRC
Na^+/H^+ exchanger - NHE
Na^+/K^+ ATPase - NKA
Na^+/K^+ exchanger - NKCC
Na^+/Mg^{2+} exchanger - NME
Pavement cell - PVC
Peanut lectin-insensitive - PNA^-
Peanut lectin-sensitive - PNA^+
Quantitative polymerase chain reaction - qPCR
Scanning ion-selective electrode technique - SIET
Seawater - SW
Solute carrier - SLC
Tight junctions - TJ
Transient receptor potential melastatin - TRPM
Tricaine mesylate - MS-222
Two-electrode voltage-clamp - TEVC

Chapter 1: General background

1.1 Fish physiology and its importance

Currently estimated at around 33,000 distinct species, fish make up almost half the diversity of all vertebrate life. Playing an important and intricate role in the ecological systems of their aquatic habitats, preserving fish diversity and abundance is of paramount importance. Fish also play an important global economic role, as worldwide aquaculture and fish capture are major business endeavours generating US$99.2 billion and US$93.4 billion, per year respectively (FAO 2016). Altogether, due to their diversity and basal vertebrate phylogeny, economic importance, and general ease of laboratory maintenance, fish are extensively used in diverse areas of scientific research. Thus, the uses and importance of fish for ecology, scientific discovery and the world economy makes in-depth knowledge of fish physiology a worthwhile pursuit.

1.2 General osmo- and ionregulation overview

The majority of freshwater (FW) fish are stenohaline, and live within a narrow water salinity limit (approximately 0 - 0.5 parts per thousand), with large fluctuations proving detrimental or even lethal. As such, they must regulate the osmotic pressures of their extracellular fluids (e.g. their plasma) to facilitate normal cellular function in a dilute environment (Marshall and Grosell 2005). Overall, FW fish face two constant threats: the passive, diffusive loss of ions down their concentration gradient to the external environment and the passive intake of water through osmosis into their tissues. With no compensation, the internal fluid composition would eventually match the external environment proving lethal to the animals. Hence, they must rely on several osmoregulatory strategies to overcome these challenges and survive. Generally, the gill and skin form selective barriers that restrict ion and water movement through tight junctions (TJs) between cells (Kolosov et al. 2013). Despite this, ion loss and water gain remain a diminished but

constant threat to FW fish. Thus, to maintain homeostasis, the gill actively uptakes ions from the dilute environment, while the kidney forms copious amounts of dilute urine, actively reabsorbing ions and ridding the body of water (illustrated in Figure 1). Traditionally, when forming osmo- and ionregulating paradigms, fish physiologists studied unfed, adult animals. Under these conditions, the GI tract is likely not involved in the ion and water balance, as fish in FW are assumed to not drink water continuously (Fuentes and Eddy 1997). Atlantic salmon smolts transferred to seawater (SW) provide an example of this, as drinking at a rate of 2.4 ml kg^{-1} h^{-1} only commenced 4-6 hours after an abrupt transfer from FW to SW (Usher et al. 1988). However upon feeding this organ provides an ion load extracted from the diet (Bucking and Wood 2006a; Bucking and Wood 2007; Bucking and Wood 2009) along with possibly providing an additional route of water loss (Bucking and Wood 2006b).

1.3 The gills, GI tract, and integument form a regulated biological barrier

1.3.1 Paracellular movement

The gills, integument, and GI tract of fish comprise the barrier between the FW fish body and the dilute external environment. Therefore, the rate of diffusion across these epithelia depend on their permeability to solutes. The "leakiness" of these tissues is largely dependent on the permeability of the TJ found between these epithelial cells. Briefly, transmembrane proteins (such as members of the claudin and occludin families) link to the actin cytoskeleton of epithelial cells via cytosolic TJ proteins such as ZO-1 (Chasiotis et al. 2012; Kolosov et al. 2013). These proteins are expressed in both tissue-specific and region-specific manner and are regulated by a variety of factors, including water salinity, diet and hormones (reviewed in detail by Chasiotis et al. 2012; Kolosov et al. 2013).

FW gills lack "leaky" junctions as found in fish from other environments (such as SW) (Laurent and Perry 1990; Sardet et al. 1979; Wilson and Laurent 2002). Furthermore, FW gill cell cultures containing only pavement cells (PVCs) have been shown to have a lower trans-epithelial resistance than do PVC-mitochondria rich cell (MRC) cultures (reviewed by Wood et al. 2002). This suggests that the barrier properties of the FW gill are formed by both cells types and their junctions. The integument of FW fish is similar to gill epithelium, in that its barrier-forming properties are crucial to maintaining homeostasis and providing a "shield" to external pathogens (Kolosov et al. 2013). Teleost skin is made up of an epidermis (the outer layer, composed of a layer of stratified squamous cells overlaying a basal layer of columnar cells) and dermis (the inner layer, primarily made up of connective tissues and blood vessels) tightly linked by a stratum germinativum which adheres to a basal lamina (Kolosov et al. 2013). Similar to the gill, environmental conditions seemingly regulate the expression of putative barrier forming claudins (e.g. cldn-3a, -3c, -8c, -27a, -27c) in the skin, as they have been shown to be upregulated in animals acclimated to hyperosmotic environments (Bagherie-Lachidan et al. 2008; Bagherie-Lachidan et al. 2009; Kolosov et al. 2013).

Finally, the GI epithelium is made of several cell types, including goblet cells (for mucous production) and enterocytes. TJs between enterocytes influence the paracellular movement by altering the tightness of the cell junctions as in the gill. Enterocyte TJs have also shown regulation during environmental and dietary manipulation. Expression of barrier-forming claudins 3a and 3b mRNA transcripts were upregulated in the GI tract of the euryhaline *Tetraodon nigroviridis* acclimated in FW compared to those in SW (Bagherie-Lachidan et al. 2008; Bagherie-Lachidan et al. 2009). Additionally, starvation has also been shown to impact GI TJ expression. *C. auratus* reduced occludin mRNA expression when fasted for 1, 2 and 4 weeks (Chasiotis and Kelly 2008).

While still not fully understood, gill, integument and GI cells, along with the TJs that bind them, appear to form a complex, tightly regulated biological barrier tasked with adjusting to external conditions and minimizing the diffusive challenges faced by FW fish. However, this barrier is not capable of maintaining homeostasis all on its own necessitating mechanisms to transport ions from the surroundings, diet, and urine through transcellular routes across the gill, GI tract, and kidney respectively.

1.3.2 Transcellular movement

1.3.2.1 Branchial ion transport

FW branchial transport occurs in the different cells of the gill. While there is ongoing debate as to the involvement of PVC in transport, there is some evidence they play a part in sodium transport and acid-base balance (Wilson et al. 2000). In fact, the amiloride-sensitive epithelial Na^+ channel (ENaC) and vacuolar-type proton pump (V-ATPase) have both been localised to the apical membrane of PVCs in fresh-water reared *O. mykiss* as well as *Oreochromis mossambicus* (Wilson et al. 2000). However, the relatively low mitochondrial content and therefore metabolic potential to drive transport have been pointed to as likely limitations to any potential transport function in PVCs (Marshall 2002).

In contrast, MRCs likely carry out the bulk of branchial ion transport (Marshall 2002). Two subtypes of mitochondria-rich cells have been identified, dividing them into peanut lectin-insensitive (PNA^-) and peanut lectin-sensitive (PNA^+), with both representing ~10% of all gill cells (Galvez et al. 2002; Goss et al. 2001; Perry and Gilmour 2006). While similar ultrastructurally, both cell subtypes appear to be functionally distinct (reviewed by Marshall and Grosell 2005). Specifically, PNA^+ MRCs have been shown to exchange Cl^- from the water for intracellular HCO_3^- (Davis et al. 2002). This exchange is likely indirectly driven by a basolateral

V-type ATPase (Boisen et al. 2003). Upon entry into the cell, Cl^- exits across the basolateral membrane into the bloodstream via cystic fibrosis transmembrane conductance regulator (CFTR)-like anion channels (Marshall 2002). Alternatively, PNA^- MRCs play a role in Na^+ uptake driven by an apical V-type ATPase (Lin et al. 1994). The proton secretion by the H^+-ATPase establishes an electrical gradient, presumably allowing Na^+ to enter the cell via a Na^+ channel (Wilson et al. 2000). Alternatively, it has been suggested that Na^+ is absorbed via a Na^+/H^+ exchanger (NHE), which has been detected in a variety of teleosts (Choe et al. 2002; Claiborne et al. 1999; Edwards et al. 1999). Regardless of the molecular identity of the apical transporter(s), Na^+ is then secreted across the basolateral membrane via a Na^+, K^+-ATPase pump (NKA). Furthermore, HCO_3^- is transported out of the cell into the bloodstream via exchange with Cl^- which is then recycled out of the cell again via CFTR-like anion channels. Divalent cations such as calcium and magnesium may also be transported by the gill through dedicated transport pathways, likely present in both PNA^+ and PNA^- cells (Bijvelds et al. 1996; Marshall 2002; Marshall and Grosell 2005).

1.3.2.2 Gastrointestinal ion transport

The diverse teleost family includes herbivores, zooplanktivores, phytoplanktivores, detrivores, and carnivores that also vary in the strictness of their feeding strategy, with some species being highly specialized and confined to a certain diet, while others are omnivores. This variety is reflected in anatomical and other modifications of the alimentary canal to accommodate these different feeding strategies. While a primary function of the teleost gastrointestinal (GI) tract is nutrient absorption, it also doubles as a dynamic osmoregulatory organ (e.g. Bucking and Wood 2006a; Bucking and Wood 2006b; Marshall and Grosell 2005). For example, digestion is aided by secretions from the stomach (rich in low-pH activated enzymes and acids), pancreatic juice (rich in HCO_3^-, allowing the stomach acids being passed with the food to be neutralized) and bile

(secreted by the liver). As such, digestion requires an ion investment (Marshall and Grosell 2005). However, the GI tract is also an important site of ion absorption (from dietary loads presented by ingested meal), resulting in an intricate relationship between inorganic nutrient absorption and loss resulting from digestion and ionregulation. For example, a 3% body mass meal containing 50 mM Na^+ kg^{-1} food mass (Bucking and Wood 2006a), can provide a total of 150 µmol Na^+ kg^{-1} fish weight in a single meal (Grosell et al. 2000; Marshall and Grosell 2005), which is often digested for several hours – days depending on feeding frequency. In comparison, branchial Na^+ absorption rates in FW fish are around 200 µmol kg^{-1} hr^{-1} already exceeding total dietary ingestion. Therefore, the ion requirement for monovalent ion homeostasis, such as for sodium and chloride, are believed to be adequately addressed largely through branchial transport. In contrast, GI divalent ion transport may be comparatively more important for maintaining homeostasis (Bucking and Wood 2007).

1.3.2.3 Renal ion transport and urine formation

Despite the gill, skin, and GI tract working together to prevent water gain in FW, excess water infiltrates the body nonetheless via passive diffusion and/or during feeding (e.g. Bucking and Wood 2006). To aid in water elimination the kidney of FW fish produces copious amount of urine through high rates of glomerular filtration (Marshall and Grosell 2005). This is combined with active tubular reabsorption of ions to prevent ion losses from the filtrate (Marshall and Grosell 2005). The reabsorption of monovalent ions such as Na^+, K^+ and Cl^- into renal cells occurs primarily in the distal tubules of the kidney via basolateral NKA and an apical $Na^+/K^+/2Cl^-$ co-transporter (NKCC) (Braun et al. 2011; Dantzler 2003; Nishimura et al. 1983). While far less understood at the molecular level, there is evidence that divalent ions such as magnesium are also reabsorbed from the filtrate (e.g. Bucking et al. 2009).

1.4 Magnesium function and transport

Despite magnesium transport and regulation being relatively poorly understood, there is an established body of literature underlining the importance of magnesium for homeostasis. One of the most abundant ions in the cell, intracellular magnesium is largely compartmentalized or bound to proteins and nucleotides due to the wide ranging list of functions it carries out (reviewed by Bijvelds et al. 1998). For example, magnesium activates and modifies activity rates of a long list of enzymes (Bijvelds et al. 1998). Magnesium is also a required cofactor in phosphate group transfers, and plays a regulatory role in several ATP-dependent ion pumps (Hartzell and White 1989; Horie et al. 1987; Pusch et al. 1989). Magnesium has also been implicated as a secondary hormone messenger, with changes in intracellular magnesium impacting the hormonal output of cells (Rubin 1976). As a result of all of these varied and complicated roles, only around 10% of intracellular magnesium is found in the cytoplasm in a free ion state (Bijvelds et al. 1998).

The majority of the magnesium requirement in FW fish is believed to be supplied by their diet with 70-90% (depending on the fish and water conditions) of transport believed to take place in the GI tract (Bijvelds et al. 1998; Dabrowska et al. 1991; Shearer 1989). Dietary magnesium (0.12-1.3 g kg^{-1} diet) is essential for the development and survival of FW fish (Knox and Cowey 1981), although the exact concentration varies with species. For example, rainbow trout require 0.2 g kg^{-1} (Knox and Cowey 1981), while channel catfish require nearly 5 times as much at approximately 1 g kg^{-1} (Gatlin et al. 1982) for proper growth and survival, possibly reflecting differences in magnesium absorptive strategy and metabolic demands. The effects of a low-magnesium diet are slightly varied, and include higher mortality, reduced growth rate, and lower bone and muscle Mg^{2+} concentrations (Gatlin et al. 1982; Knox and Cowey 1981; Ogino and Chiou

1976; Ogino et al. 1978; Shim and Ng 1988). Excess magnesium can also be detrimental to fish growth however, as magnesium rich diets (above 745 mg kg^{-1}) decreased growth and survival rate, decreased activity for NKA, as well as superoxide dismutase (involved in superoxide partitioning; McCord and Fridovich 1969) activity in juvenile gibel carp (Han et al. 2012). As well, dietary magnesium requirements of FW fish are believed to inversely correlate with the environmental availability of magnesium (Shearer and Åsgård 1992) suggesting that dietary magnesium absorption is alterable to compensate for homeostatic needs. Fluxes of magnesium are variable along the GI tract of FW rainbow trout, with absorption in the stomach and secretion and absorption in the intestine (Bucking and Wood 2007). The predominant GI magnesium secretion correlated with a measured increase in water concentration, and was likely the result of bile, GI, and pancreatic secretions (Bucking and Wood 2006b) which are rich in Mg^{2+} binding enzymes. Finally, a single meal resulted in a significant increase in plasma concentration for magnesium at 8 hours post feeding, returning to normal at 12 hours (Bucking and Wood 2006b), further supporting the hypothesis of dietary magnesium absorption.

Branchial transport of magnesium is suspected in fish (Dabrowska et al. 1991; Shearer 1989) although evidence is mostly inferred as total magnesium deposition in the bodies of FW teleosts can exceed the total amount of magnesium available to them through diet alone (Dabrowska et al. 1991; Shearer 1989). So, it has long been reasoned that additional magnesium is taken in actively at the gills, although experimental evidence for active branchial uptake is scarce (Bijvelds et al. 1996; Bijvelds et al. 1997b; Flik et al. 1993; Hobe et al. 1984; Shearer and Åsgård 1992; Wendelaar Bonga et al. 1983). In studies that have identified branchial transport, it has been estimated to account for roughly 20%-30% of magnesium requirement in *O. mossambicus*, further increasing up to 50% in fish fed a magnesium deficient diet (Bijvelds et al. 1996; Bijvelds et al.

1997a; Flik et al. 1993). Ultimately, however branchial transport cannot maintain homeostasis alone, and GI absorption is also required (Bijvelds et al. 1998).

Teleost GI Mg^{2+} uptake is believed to occur through both a passive, paracellular pathway and an active, transcellular pathway, with the former accounting for the majority of transport (Behar 1974; Bijvelds et al. 1998; Schweigel and Martens 2000). Passive transport likely depends on GI TJ composition and claudin expressions which affect epithelial permeability (Kolosov et al. 2013). Assuming transcellular transport is similar to the mammalian model, absorption is likely accomplished by magnesium entry down its electrochemical gradient across the apical enterocyte membrane through a channel (suspected to be formed by transient receptor potential melastatin (TRPM) 6 and 7), after which it is extruded across the basolateral membrane and into the bloodstream, where it can be distributed throughout the body. This process has long been hypothesized to occur via a hypothetical Na^{+}/Mg^{2+} exchanger (NME) localized to the basolateral membrane, (Bijvelds et al. 1996; Bijvelds et al. 2001). Recently, the solute carrier 41a1 (SLC41a1) has been suggested as the putative NME in mammals (Kolisek et al. 2008; Kolisek et al. 2012; Wabakken et al. 2003) and fish (Islam et al. 2013). This exchange is believed to occur in an electroneutral fashion, transporting 1 Mg^{2+} ion out of the cell and 2 Na^{+} ions into the cells. This transport is driven by the large inward gradient of sodium maintained by basolateral NKA activity in enterocytes (Fleig et al. 2013). This mechanism is summarized in Figure 2.

After absorption of magnesium from the diet, and possibly to a lesser extent the water, the kidney appears to play a major role in magnesium homeostasis. While typically expected to reabsorb Mg^{2+} in order to recuperate diffusive losses, FW *O. mykiss* have been shown to "switch" renal function and secrete up to 27% of their dietary magnesium uptake over 48 hours (Bucking et al. 2010) through the urine. While there is currently no widely accepted molecular pathway for the

renal reabsorption and branchial uptake of magnesium, all three of the magnesium transporting proteins (TRPM6, TRPM7, SLC41a1) have been found in the gill and kidney of all tested teleosts, including *D. rerio*, *S. salar* and *Takifugu rubripes* (Arjona et al. 2013; Esbaugh et al. 2014; Islam et al. 2013) suggesting conserved magnesium transport pathways.

1.5 Objective

The primary objective of this thesis was to expand the current understanding of how magnesium is transported in several ionregulatory organs in the common goldfish, *C. auratus*. Firstly, molecular methodologies (qPCR, phylogenetic analysis) were used to examine the hypothesis that the GI, branchial and renal levels of SLC41a1 transcripts would respond in an inversely proportional manner to magnesium availability (i.e. dietary and environmental depravations of the ion would result in transcript upregulations) (Chapter 2).

Furthermore, potentiometric approaches (SIET, ISME) were used to study the hypothesis that different GI segments would exhibit differences in magnesium transport, and if those would match chyme concentrations and SLC41a1 transcript levels (Chapter 3). SIET was also used to observe magnesium transport kinetics at the 1st GI segment and test if they support the previously suggested transport model (i.e. if transport is carried out by a mixture of transcellular and paracellular mechanisms) (Chapter 3). Finally, SIET was used to test if magnesium flux can be inhibited by two pharmacological agents, ouabain (an NKA inhibitor) and cobalt(III)-hexaamine chloride (a magnesium channel blocker) at the 1st and 8th GI segments and gills.

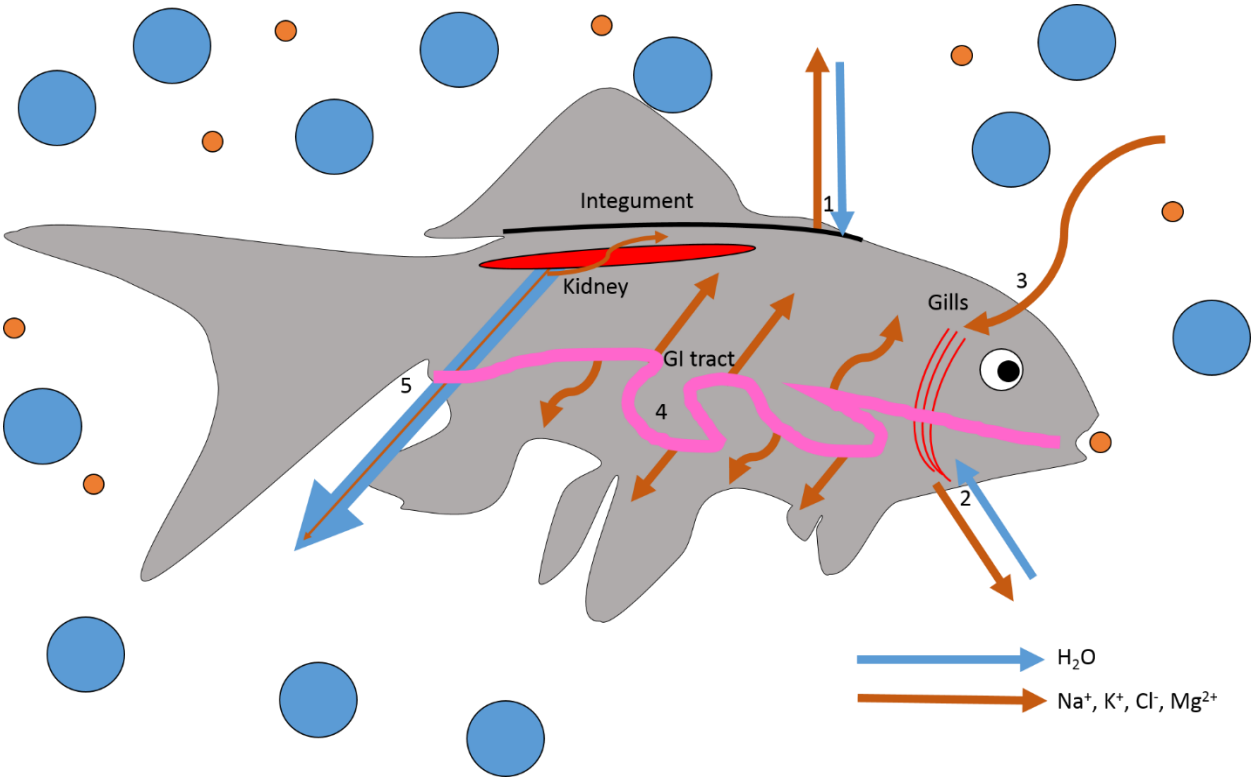

Figure 1: General osmoregulation in FW fish. Living in a hypoosmotic environment, fish are faced with a constant passive influx of water and efflux of ions across their integument (1) and gills (2). Homeostasis is maintained by ion absorption at the gill (3) and GI tract (4) and reabsorption at the kidney (5). Excess water is filtered and excreted as dilute urine via the kidney (5).

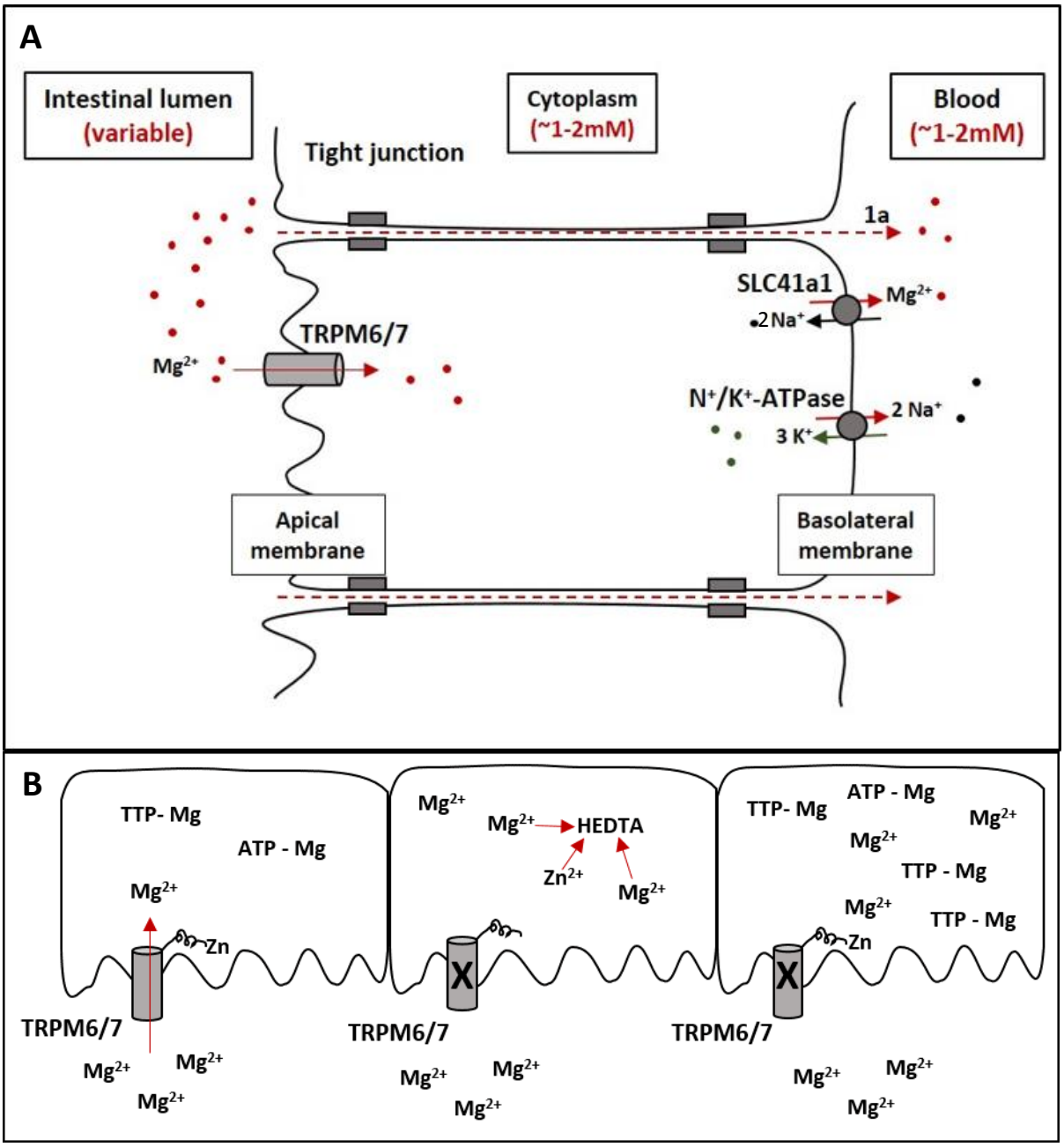

Figure 2: Proposed magnesium absorption mechanism. Magnesium ions can be passively absorbed across paracellular TJs from the lumen to the blood (A). Alternatively, magnesium is transported transcellularly, entering enterocytes via TRPM6/7 channel complexes (A, B). The channel complex is inhibited by high concentrations of intercellular Mg^{2+} (both nucleotide-bound and free) and HEDTA (likely due to an interaction with TRPM6/7's Zn^{2+}-binding motif) (B; adapted from Demeuse et al. 2006). Magnesium is then extruded basolaterally via the sodium-magnesium exchanger SLC41a1, likely driven by a large inward gradient of sodium maintained by NKA (A; adapted from Quamme 2008).

Chapter 2: Molecular characterization of SLC41a1 in C. auratus

Introduction

In order to be transported transcellularly across the ionregulatory epithelia of teleosts, such as the gill, kidney, and GI tract, magnesium must cross both the apical and basolateral cell membranes. The complex network of transporters facilitating this movement found on both membranes are constantly adjusted to the internal and external environment of the animal. Current mammalian research suggests transcellular magnesium transport is driven by an apical channel allowing for the ions to enter the cell down the electrochemical gradient, and a basolateral transporter, likely a sodium magnesium exchanger, that pumps magnesium actively against the concentration gradient out of the cell.

2.1 Apical entry into vertebrate cells is facilitated by TRPM6 and TRPM7

Apical cellular entry is believed to utilize a channel belonging to the TRPM family, specifically TRPM7 and/or TRPM6. TRPM7 is ubiquitously expressed both in diverse vertebrate classes (such as mammals and fish; (Arjona et al. 2013; Goytain and Quamme 2005; Islam et al. 2013; Schlingmann et al. 2007)), and within specific tissues examined. Initial studies suggested that TRPM7 was a non-selective channel (Runnels et al. 2001), indiscriminately transporting Mg^{2+}, Ca^{2+}, K^{+}, Na^{+}. However, recently the channel was shown to preferentially transport Mg^{2+} and Ca^{2+}, and to a lesser extent other divalent trace metals (such as Zn^{2+}, Ni^{2+}, Ba^{2+}, Co^{2+}, Mn^{2+}, Sr^{2+}, and Cd^{2+}; (Monteilh-Zoller et al. 2003; Nadler et al. 2001). Importantly, under physiologically representative conditions (i.e. a negative membrane potential), TRPM7 has been shown to transport Mg^{2+} and Ca^{2+} down their concentration gradient from the extracellular space into the cell (Nadler et al. 2001). Mutations in TRPM7 have been shown to retard growth and cause lethality in zebrafish embryos and was associated with lower levels of both calcium and

magnesium in hard tissues as well as deformities in skeletal formation (Elizondo et al. 2005; McNeill et al. 2007), once again highlighting the significant role magnesium plays in homeostasis.

Composed of 1,864 amino acids, TRPM7 contains a c-terminus kinase domain which has been hypothesized to play a role in phosphorylating and modulating the function of other TRPM7 units within the same channel complex, as well as a possible *cis* phosphorylation (wherein a subunit can phosphorylate itself) (Nadler et al. 2001; Runnels et al. 2001; Ryazanova et al. 2001). The protein has been localized to apical membranes in enterocytes and in distal convoluted tubules of rats (Nadler et al. 2001; Schlingmann et al. 2002) and was assumed to occupy the same location in *O. mykiss* (Esbaugh et al. 2014). Human embryonic kidney (HEK) 293 cells loaded with Mg.ATP and Mg.GTP were shown to inactivate the channel (Nadler et al. 2001; Schmitz et al. 2003). This inactivation was lost in the presence of (2-Hydroxyethyl)ethylenediaminetriacetic acid (HEDTA), a strong chelator of divalent ions (Kozak and Cahalan 2003). While initially interpreted as evidence that free Mg^{2+} inactivates TRPM7, this has been disputed as HEDTA also chelates intracellular Zn^{2+} (Figure 2B; Demeuse et al. 2006). This might compromise the molecular structure of the channel due to the presence of a Zn^{2+} binding domain, making the results inconclusive. Furthermore, the IC_{50} (concentration at which transport is reduced by 50%) of TRPM7 for Mg.ATP has been shown to depend on the intracellular concentration of unbound Mg^{2+} and *vice versa* (Demeuse et al. 2006). This suggests magnesium-bound nucleotides act synergistically with free magnesium to inactivate the channel, and was in fact observed with magnesium bound ATP, TTP, CTP, GTP and UTP, all of which inhibited TRPM7 more potently than free intracellular Mg^{2+} alone (Figure 2B; Demeuse et al. 2006; Schmitz et al. 2003).

A 2022 amino acid protein, TRPM6 was the second member of the TRP family implicated in magnesium transport, also containing a c-terminus kinase domain (Schlingmann et al. 2007).

As TRPM7, TRPM6 is believed to modulate the function of other TRPM6 units within a channel complex, as well as individual units self-phosphorylating (Schmitz et al. 2005). Uniquely, TRPM6 has also been suggested to modulate the function of TRPM7 units within a channel complex, while the reverse is likely not true (i.e. TRPM7 can't phosphorylate TRPM6). While currently not as well characterized, TRPM6 was shown to be similarly selective for Mg^{2+} and Ca^{2+} and showed consistent current-voltage relationships similar to TRPM7 (Voets et al. 2004). Overexpression of TRMP6 in different cell lines such as HEK-293 and Chinese hamster ovary kidney cells (CHOK) 1 also generated similar inward currents of divalent ions at negative cell membrane potentials (Li et al. 2006; Voets et al. 2004), again similar to TRPM7. This similarity in function possibly stems from the similarity in structure, as TRPM6 shares a high 80% similarity to TRPM7 between the 5^{th} and 6^{th} transmembrane domains which form the channel pore (Schlingmann et al. 2007).

Unlike TRPM7, TRPM6 is not universally expressed across tissue types, however the three primary ionregulatory organs in FW zebrafish (*Danio rerio*), namely the gills, GI tract and kidney, were all found to express TRPM6 mRNA transcripts (Arjona et al. 2013). Subcellularly, the channel localizes to apical membrane of distal-convoluted tubules in the kidney and brush-border membranes in the enterocytes of mice (Voets et al. 2004). Interestingly, functional TRPM6 (i.e. able to generate current-voltage relationships) has only been observed in cells also expressing TRPM7 (Chubanov et al. 2004; Chubanov et al. 2005; Schmitz et al. 2005). Simultaneous expression of TRPM6 and TRMP7 in HEK-293 cells resulted in incorporation of both proteins into channel complexes at the plasma membrane, readily detected by immunoblotting. These heteromultimers were further confirmed by co-immunoprecipitation and fluorescence resonance energy transfer (FRET) (Chubanov et al. 2004; Schmitz et al. 2005). Furthermore, mutations to the c-terminus kinase in TRPM6, but not TRPM7, have been correlated with hypomagnesemia and

secondary hypocalcaemia (HSH) in human patients (Chubanov et al. 2004; Schlingmann et al. 2002). Immunofluorescence studies have revealed that one such mutation (the TRPM6 S14L mutant) prevents TRPM6 from localizing to the plasma membrane and disrupts heterodimerization, which suggests the heterodimers are observed *in vivo* and are required for normal transepithelial transport of magnesium (Chubanov et al. 2004; Schlingmann et al. 2007).

Altogether, recent studies on TRPM6 and TRPM7 show that while structurally similar, both channels play an important and unique role in magnesium homeostasis. While TRPM6 is likely more important to transepithelial transport for its ability to heterodimerize with TRPM7 and kinase activation of the complex, TRPM7 is also essential for its facilitation of TRPM6 localization. TRPM7 is unique in its ubiquitous expression in vertebrate cells, and likely facilitates cellular magnesium homeostasis in additional, currently unknown ways.

While TRPM6 and TRPM7 fit the proposed transcellular magnesium pathway in that they can facilitate the ion traveling down an electrochemical gradient into the cell, this may not be the case in branchial cells. The FW environment does not provide an electrical or chemical gradient for the divalent ion to travel down, and thus may involve other transporters that remain to be studied. Nevertheless, both channels are found in the gill cells of FW fish.

2.2 SLC41a1 may facilitate basolateral extrusion

In contrast to apical entry, basolateral extrusion likely uses a transporter to move magnesium against the concentration gradient, from low intracellular concentrations to higher extracellular concentrations. The recently identified putative candidate is the SLC41A1 transporter. The 513 amino acid SLC41A1 was initially identified and characterised by Wabakken et al. (2003) in HEK-293 cells. Lacking a signal peptide (suggesting localization to the cellular membrane occurs via another mechanism, possibly via one of its transmembrane domains being

targeted by the secretory pathway), the protein is estimated to contain 10 transmembrane domains and has a 96 amino acid long N-terminal region oriented intracellularly (Wabakken et al. 2003). Two domains, D1 and D2, showed homology to consensus sequence Pfam01769 (Wabakken et al. 2003) which corresponds to an integral domain found in the prokaryotic Magnesium transporter E (MgtE) family of magnesium transporters. Indeed, D1, D2 and Pfam01769 were all homologous for the presumed functionally important motifs PX_6GN and $P(D/A)X_4PX_6D$, suggesting the SLC41 family is distantly homologous to the MgtE family (Wabakken et al. 2003). While there has been debate on the orientation of the C-terminus, recent experimental data suggests it is oriented intracellularly (Sponder et al. 2013). Like TRPM7, SLC41a1 has been discovered to be ubiquitously expressed in all vertebrate tissues tested in both terrestrial and aquatic vertebrates so far (Islam et al. 2013; Mandt et al. 2011).

Initial functional studies over-expressed human SLC41a1 (hSLC41a1) in *Xenopus* oocyte cells and measured the resulting flux under a variety of conditions using a two-electrode voltage-clamp (TEVC) approach (Goytain and Quamme 2005; Quamme 2010). These studies found that increasing the extracellular magnesium concentration of the bath (from 0.2 to 10mM) gave rise to a saturable inward current at hyperpolarized cell membrane potentials (>-150mV), reversible at around -20mV. These findings are consistent with SLC41a1 being either a constitutively active ion-channel or an electrogenic ion exchanger (Fleig et al. 2013). Interestingly, preparations excluding Na^+ from the bathing saline of the cells had no significant effect on the current (Goytain and Quamme 2005). This initially suggested SLC41a1 may not be a NME, due to the lack of Na^+ dependence for transport. Furthermore, expression of hSLC41a1 was clearly shown to increase intracellular Mg^{2+} concentrations in cells kept in magnesium-rich media (Kolisek et al. 2008; Mandt et al. 2011; Quamme 2010) suggesting channel-like characteristics.

However, an alternative explanation has been suggested for the TEVC studies. The TEVC approach is unable to account for the internal composition of the cell, and an exogenously introduced protein such as SLC41a1 could result in activation of unrelated endogenous Cl^- currents (Fleig et al. 2013). For example, Cl^- currents have been observed in *Xenopus* oocyte cells injected with different ions (e.g. Ca^{2+}) (Barish 1983; Dascal 2001; Miledi and Parker 1984). Therefore, experiments where Cl^- was removed from the bathing solution (carried out by Goytain and Quamme 2005) could not clarify if the measured inward current is solely due to the Mg^{2+} influx or a potential Cl^- efflux (Fleig et al. 2013). Furthermore, a similar experiment conducted in HEK-293 cells with overexpressed hSLC41a1 resulted in secondary activation of an endogenous ATP-sensitive Cl^- current, which was completely inhibited by the Cl^- channel blocker 4,4'-Diisothiocyanatostilbene-2,2'-disulfonic acid (DIDS) (Kolisek et al. 2008). As such, the TEVC experiments using a bathing solution without Na^+ or Cl^- were inconclusive in showing SLC41a1 to be a Na^+-independent channel.

Further transport anomalies exist in the literature. For example, homologous expression experiments suggest that magnesium is imported by cells expressing SLC41a1 kept in a magnesium-rich (10mM extracellular concentration, 0.5-1mM intracellular concentration), sodium-poor (0.5mM extracellular, 3mM intracellular) media (Kolisek et al. 2008; Lo et al. 2006) and that transport that was not saturable. This is in contrast to heterologous expression, supporting saturable transport into the cell along with reversibility depending on the transepithelial potential (Goytain and Quamme 2005; Quamme 2010). As well, expression of hSLC41a1 in *Salmonella* lacking traditional bacteria magnesium transporters, allowed these cells to survive in a low-magnesium environment (100μM Mg^{2+}) (Kolisek et al. 2008) suggesting the transporter was involved in magnesium uptake against a magnesium gradient. Finally, HEK-293 cells expressing

hSLC41a1 (containing 0.2mM Mg^{2+} and 12mM Na^{+}; resting potential -15mV) kept in physiological saline (1mM Mg^{2+} and 145mM Na^{+}) readily extrude Mg^{2+}, this time driven by the large inward Na^{+} gradient (Kolisek et al. 2012). Together, these findings make a case that under physiological conditions, SLC41a1 may be the hypothesized NME in vertebrates, while its function may depend directly on a large extracellular Na^{+} concentration to drive Mg^{2+} extrusion and indirectly on NKA activity to maintain the required gradient (Fleig et al. 2013). Further support is found in immunohistochemical studies using HEK-293 cells that showed hSLC41a1 localizes to the cell membrane (Kolisek et al. 2012). In order to facilitate cross epithelial absorption in ionregulatory tissues, the NME must localize to the basolateral side of GI cells in order for magnesium to be transported from the enterocytes' cytoplasm to the bloodstream (Bijvelds et al. 1998; Fleig et al. 2013). While it stands to reason GI transport in FW teleosts likely operates in a similar manner to mammals, there are currently no studies that have examined SLC41a1 localization in the piscine GI tract. Furthermore, there are no studies examining the gill either, an ionregulatory organ without a direct mammalian equivalent.

Currently, the only study that has examined SLC41a1 localization in teleosts was focused on the kidney of SW-acclimated euryhaline mefugu (*Takifugu obscurus*) (Islam et al. 2013). This study presented a unique mechanism for magnesium extrusion in the kidney proximal tubules, and proposed an secretory role for SLC41a1 which localizes primarily to apical membrane- associated vacuoles. This is in contradiction to the mammalian models that place SLC41a1 on the basolateral membrane and its role in secretion to the plasma. The authors hypothesized that the transporter amasses Mg^{2+} into these vacuoles, which exocytose the ion across its apical membrane and into the urine for secretion. Supporting this is evidence for vacuolar magnesium transport in winter flounder (*Pseudoleuronectes americanus*) kidneys, where radioisotope ^{28}Mg uptake was affected

by cytochalasin B (an actin filament inhibitor) (Renfro and Shustock 1985). However, SLC41a1 was not localized to any other fish tissue, nor was it examined in a FW fish which may use different transport pathways as renal magnesium reabsorption is displayed in contrast to secretion in SW.

Previous studies have investigated SLC41a1 expression and/or magnesium transport in light of elevated environmental magneiusm concentrations (e.g.seawater; Islam et al., 2013). However, other environmental factors such as temperature, may also impact magnesium transport as well. Temperature is known to increase metabolic rates, oxygen consumption (e.g. Schwarzbaum et al. 1992) and growth rate (e.g. Handeland et al. 2008). As magnesium is important for growth and development (e.g. Ogino et al. 1978; Shim and Ng 1988) temperature manipulations may impact magnesium transport however this is currently unknown. As well, water-bourne magnesium restrictions, as with ion-poor water (IPW) have not been investigated.

Due to the paucity of studies examining the molecular identity of the three magnesium transporters discussed in adult fish, currently restricted to Islam et al. (2013; pufferfish), Arjona et al. and Jansen et al. (2013 and 2016; zebrafish) and Esbaugh et al. (2014; trout), we attempted to identify the TRPM6, TRPM7, and SLC41a1 in a previously unstudied fish, *Carassius auratus* (goldfish). Furthermore, we attempted to study the transcriptional regulation of these transporters in three ionregulatory tissues of the goldfish (the gill, the kidney, and the GI tract) in response to a variety of environmental and dietary manipulations. To that end, the sequence for SLC41a1 was successfully cloned using homologous regions from previously sequenced fish species. While multiple, similar attempts were made to clone TRPM6 and TRPM7, these were unsuccessful. Thus, a series of phylogenetic analyses constructed with the known fish sequences are provided instead.

Firstly, the effect of water temperature on SLC41a1 mRNA transcript abundance was tested by sampling the three ionregulatory tissues in goldfish kept at 10, 15 and 20^{o}C for a month

using quantitative reverse transcription polymerase chain reaction (qPCR). Given the importance of magnesium for normal development in fish (e.g. Ogino et al. 1978; Shim and Ng 1988), combined with the known impact of temperature on development, it was predicted an increase in temperature would increase magnesium demand, and in turn, SLC41a1 transcript levels.

Additionally, SLC41a1 mRNA expression was measured in goldfish kept in regular, dechlorinated tap water (DTW) and ones kept in IPW for either 24 hours or 14 days, in order to discover how lowered environmental magnesium levels impact SLC41a1 mRNA abundance. It was predicted that fish faced with a more magnesium-deprived enrionvment and thus, increased ion loss, would counteract this via increased SLC41a1 expression in their ionregulatory organs.

Furthermore, I tested how SLC41a1 transcript levels respond to diets with different magnesium content, comparing fish fed FW *Mysis* shrimp (representing a low-magnesium diet), magnesium enriched *Mysis* shrimp (representing a regular magnesium-load diet), commercial food pellets (representing a regular magnesium-load diet similar in magnesium content to that of the enriched shrimp), and a commercial food diet with enriched magnesium content for 14 - 28 days. I hypothesized that due to its role in magnesium absorption, SLC41a1 transcript levels would be inversely proportional to dietary Mg^{2+} content.

Finally, the mRNA abundance of the transporter was tracked over a 24 hour food depravation period in fish fed either a Mg^{2+}-rich diet (enriched pellets) or a control diet (simple pellets). It was hypothesized SLC41a1 transcript levels would remain unchanged in all organs for both diets and would not be transcriptionally regulated over short-term intervals, as *C. auratus* have been observed to feed throughout the day, and it would stand to reason they maintain their magnesium transport mechanism while kept in stable conditions.

Materials and methods

3.1 General animal care

C. auratus (mass ~3 – 10 g; Big Al's, Toronto ON) were kept in large (~50L) solid plastic tanks with flow-through DTW and individual air lines. Water temperature and fish health was monitored daily, while water quality indicators (ammonia, nitrite and nitrate concentrations) were measured weekly. Feeding and temperature conditions varied with each experimental group, and are described in detail below.

3.2 Sequencing of C. auratus SLC41A1

Carassius auratus SLC41A1 primers were constructed using a homologous comparison of the gene in *Oreochromis niloticus* (ENSONIG00000003282), *Gadus morhua* (ENSGMOG00000004376), *Danio rerio* (XM_002663821), *Poecilia formosa* (ENSPFOG00000005128), *Astyanax mexicanus* (ENSAMXG00000003381), *Latimeria chalumnae* (ENSLACG00000001579), *Oryzias latipes* (ENSORLG00000012106), *Lepisosteus oculatus* (ENSLOCG00000011890), *Gasterosteus aculeatus* (ENSGACG00000010942), *Takifugu obscurus* (AB700626), *Takifugu rubripes* (AB700621), and *Tetraodon nigroviridis* (ENSTNIG00000007377). The sequences were obtained from Ensembl, a repository of annotated genome sequences, or from PubMed. Once the sequences were obtained, they were aligned using the online ClustalW2 algorithm (EMBL-EMBI, Hinxton, Cambridgeshire, UK) and areas of conservation were used to identify locations to design primers using the Primer3 software (http://primer3.ut.ee/). The primers used (Sigma-Aldrich Co, The Woodlands, Texas, USA) were re-suspended in RNAase- and DNAase-free molecular water at a concentration of 100µM and kept at -20^{o}C for long-term storage.

In order to test the designed primers, sample cDNA was synthesized from mRNA obtained from *C. auratus* gill, kidney, and GI tissues. To this end, fish were euthanized in DTW containing the muscle relaxant tricaine mesylate (MS-222) buffered to neutral pH (pH=7.5) using 1N NaOH. The gill basket was first removed and filaments excised from the supporting cartilage. A lateral incision was then made along the body wall to expose the GI tract which was removed in its entirety. Care was taken to ensure that no liver or other organ tissue was also collected. Finally, the entire kidney was collected by gently scrapping the renal tissue onto a spatula. All collected tissues were placed in aluminum packets and snap-frozen on dry ice using an aluminum press. Tissues were then stored at -80^{o}C until further processing for RNA extraction.

3.3 RNA isolation

The following protocol was used for all tissue samples obtained. Samples were homogenized with 0.5ml TRIzol reagent (Life Technologies Inc, Carlsbad, California, USA) per 100mg of tissue and put in sterile 1.5ml tubes (Axygen Inc, Union City, California, USA). 100 µl of chloroform (Fisher Scientific Co, Fair Lawn, New Jersey, USA) was then added to each sample per 0.5ml TRIzol used. Tubes were shaken and left to stand for 3 minutes at room temperature. Samples were then centrifuged at 12,000xg for 15 min at 4^{o}C. Following centrifugation, each sample separated into three separate layers: a red, chloroform-phenol phase (bottom), an interphase (middle) and a colourless, aqueous phase (top). The aqueous phase (containing the extracted RNA) was then pipetted out, taking care not to touch or disturb the other two phases, and added into new, sterile Eppendorf tubes.

3.4 RNA precipitation

0.25 ml of isopropanol (Fisher Scientific Co) was then added to the isolated aqueous phase per every 0.5ml of TRIzol used during the RNA isolation. After a 10 minute incubation at room

temperature, the aqueous phase was centrifuged at 12,000xg for 10 min at 4^{o}C, resulting in the formation of a gel pellet (containing the RNA). The pellet was isolated by pipetting out the remaining supernatant. The pellet was then washed with 0.25ml of 75% ethanol (GreenField Ethanol Inc, Brampton, Ontario, Canada). Upon a brief vortex, the tube was centrifuged at 7,500xg for 5 minutes at 4^{o}C. The wash was discarded, leaving behind the RNA pellet. The pellet was air dried for 10 minutes.

3.5 RNA resuspension

The RNA pellet was resuspended in RNAse free water and the concentration of RNA was measured spectrophotometrically with a BioTek Syngergy HT machine (BioTek Instruments Inc, Winooski, Vermont, USA). Quality was also checked (260:280 ratios). If an RNA 260:280 absorbance ratio fell above or below ~2, the sample was not used. Finally, the samples were stored at -80^{o}C until further use.

3.6 cDNA synthesis

First-strand complementary DNA was subsequently synthesized by reverse transcribing total RNA using an oligo(dT) primer and Superscript II Reverse Transcriptase (Invitrogen). Briefly the reaction conditions were as follows: 0.5µl Oligo(dT)15 (Roche Diagnostics, Indianapolis, Indiana, USA, at 500 µg/ml), 0.5µl dNTP Mix (Roche Diagnostics, at 10mM for each nucleotide), 250ng RNA (volume dependent on the particular sample concentration), 2µl of 5x First-Strand Buffer (Invitrogen), 1µl 0.1M DTT (Invitrogen), 0.25µl (50 units) of Superscript II Reverse Transcriptase (Invitrogen), and sterile, molecular grade water (volume dependent on sample RNA concentration). The reaction was run at 42^{o}C for 50 minutes, followed by a 15 minute inactivation at 70^{o}C in a Bio-Rad MyCycler (Bio-Rad Laboratories Ltd, Mississauga, Ontario, Canada). The synthesized cDNA was then kept in a -20^{o}C freezer until further use.

3.7 PCR amplification

In order to obtain sufficient quantity of SLC41A1 amplicon for sequencing, the sequence was amplified via PCR reactions carried out in a Bio-Rad MyCycler (Bio-Rad Laboratories Ltd, Mississauga, Ontario, Canada) with designed primers (Forward: AGGATAGAGATGAAGAAGGAGGG; Reverse: GAAACACAGAGCCAGGAAGC; Sigma-Aldrich Co). The PCR reaction consisted of 2 µl cDNA (equivalent to 1 µg), 2.5µl 10xPCR Buffer (Roche Diagnostics), 0.5 µl PCR Grade Nucleotide Mix (Roche Diagnostics), 2.5 µl of both primers, 0.2 µl FastStart Taq DNA polymerase (Roche Diagnostics), as well as 14.8 µl PCR-grade molecular water (Fisher Scientific Co), for a total volume of 25 µl. The PCR reaction conditions were as follows: an initial, one-time denaturation step 95^{o}C (2 minutes), followed by a repeated cycle of a 30 second 95^{o}C denaturation step, a 30 second 50-62^{o}C annealing step (exact temperature depends on the Tm of the primers being tested) and a 1-3 minute 72^{o}C elongation step (depending on the size of the expected product size; ~1 min per every 1,000 nucleotides), followed by a final elongation step at 72^{o}C for 7 minutes. After PCR amplification, reaction mixtures were run on a 1.5% agarose gel in Tris·HCl/acetic acid/EDTA buffer containing 0.5 ug/ml ethidium bromide. The UV image was acquired using a MiniBis Pro Imager (FroggaBio Scientific Solutions; Toronto, ON, CA).

3.8 Cloning

Briefly, cloning of the PCR amplicon for SLC41a1 was carried out with a QIAGEN PCR cloning kit. Ligation was performed using 4µl of purified PCR product, 1µl of pDrive Cloning Vector, and 5µl of Ligation Master Mix 2x. Subsequently, 2µl of the ligation mix were added to a tube of QIAGEN EZ competent cells, thawed on ice immediately prior to the transformation reaction. The tube was then heated in a 42^{o}C water bath for 30 seconds, after which it was

incubated on ice for 2 minutes. 250µl of room temperature SOC medium (20g/L Tryptone, 5g/L Yeast Extract, 4.8 g/L $MgSO_4$, 3.603 g/L Dextrose, 0.5g/L NaCl, 0.186g/L KCl) was then added to the tube, after which 100µl of the transformation mixture was plated onto an LB agar plate (5g/L NaCl, 5g/L Tryptone, 2.5g/L Yeast Extract, 7.5g/L Agar, additional dH2O up to 500ml). The plate was then incubated at room temperature until the mixture was absorbed into the agar, after which the plate was inverted and incubated at 37ºC for 18 hours. Resultant colonies were picked and sent to BioBasic (Markham, Ontario, Canada) for bidirectional sequencing using BigDye Terminator cycle sequencing. The obtained partial coding sequence has been submitted to Genbank (accession number KY203987).

3.9 SLC41a1 phylogenetic analysis

Using the above sequences obtained from mining Ensembl gene predictions and published sequence along with the newly obtained SLC41a1 sequence for *C. auratus*, both nucleic acid and amino acid sequences were aligned using ClustalW software within the MEGA 6 software. Subsequently, two phylogenetic trees (one for nucleic acid and one for amino acid sequences) were constructed using MEGA 6 software (Tamura et al. 2013) based on the maximum likelihood method with 500 bootstrap replicates. Maximum likelihood was picked over other methods, such as maximum parsimony and neighbourhood-joining due to its advantages in phylogenetic analysis. While the former minimizes branch length and thus fails to take into account possible instances of convergence and homoplasy and the latter utilizes a relatively simple clustering algorithm and does not make full use of the genetic sequences provided, maximum likelihood has become a widely accepted choice for phylogenetic analysis. However, the increased power of maximum likelihood comes at a higher time and computational cost.

3.10 TRPM6 and TRPM7 phylogenetic analysis

The above approach was used to design primers for TRPM6 and 7, with the intent to follow the same protocol to obtain novel sequences for *C. auratus*. The sequences used for TRPM6 were as follows: *Oreochromis niloticus (ENSONIG00000010763), Gadus morhua (ENSGMOG00000016504), Danio rerio (ENSDARG00000103454), Poecilia formosa (ENSPFOG00000015801), Astyanax mexicanus (ENSAMXG00000018877, ENSAMXG00000018882, ENSAMXG00000018893), Latimeria chalumnae (ENSLACG00000008829), Oryzias latipes (ENSORLG00000012478), Lepisosteus oculatus (ENSLOCG00000009721), Gasterosteus aculeatus (ENSGACG00000011569) and Takifugu rubripes (ENSTRUG00000001357) and Tetraodon nigroviridis (ENSTNIG00000004554).*

The sequences used for TRPM 7 were as follows: *Oreochromis niloticus (ENSONIG00000002611), Gadus morhua (ENSGMOG00000017502), Danio rerio (ENSDARG00000036232), Poecilia formosa (ENSPFOG00000016953), Astyanax mexicanus (ENSAMXG00000011104, ENSAMXG00000011081, ENSAMXG00000011092, ENSAMXG00000011087), Latimeria chalumnae (ENSLACG00000018358), Oryzias latipes (ENSORLG00000012746), Lepisosteus oculatus (ENSLOCG00000013042), Gasterosteus aculeatus (ENSGACG00000016500) and Takifugu rubripes (ENSTRUG00000006251) and Tetraodon nigroviridis (ENSTNIG00000010230).*

However, despite designing a multitude of primers (Table 1), attempting to optimize PCR conditions (running the primers at both higher and lower temperatures in order to, respectively, increase and decrease primer binding specificity) and using cDNA obtained from a variety of tissues, I failed to obtain a sequence for TRPM6 or 7. Phylogenetic analysis (MEGA 6) as

described above for SLC41a1 was conducted to provide a possible explanation for the difficulty I had amplifying a gene product.

Table 1: Attempted cloning primers for TRPM6 and TRPM7.

Gene	Primers	From
TRPM6	Forward 1: CTTTTGCAAGCGAGAATGTGT Reverse 1: GCTCTCCCTGTTCCCTCAA Forward 2: TGCAGAACGTCTCCTGTCC Reverse 2: GAGCAGCGCCATCTCTTG Forward 3: GACCTGTTTGTGTGGGCAG Reverse 3: GTCCCGAAACTAACCAGCAC Forward 4: GACACCCAACATTCAGGAGT Reverse 4: AACACACTTCTCCTCAAACTCA Forward 5: AAGTATGTTGGCGATGCTGT Reverse 5: CATAGTGTGAAACCAGAATTTGAC Forward 6: TTCACCTGTCTGCAAATGG Reverse 6: TGATGTAACGATAGCGGTTGTA Degenerate 1 Forward: GYTGAGRGARTGGCAGATGGA Degenerate 1 Reverse: GCTGAGAGAATGGCAGATGGA Degenerate 2 Forward: ATGGCCATGAARCTGPTYAC Degenerate 2 Reverse: ATGGCGATGAAGCTGCTGAC	Designed
TRPM7	Forward 1: AGAAATCCTGGATAGAAAGCACT Reverse 1: TCTTCTCCTTCTTGTCAGCCT Forward 2: GCACCGTTTCCTGACAATCA Reverse 2: CAGGAGTCGCACATACCAGA Forward 3: CCTCAAGAGTGGCTGGTCAT Reverse 3: TGGGGAAAAGAGGAGCCAAA Forward 4: TGTCCGACTTCCTGGCCAT Reverse 4: TCATTGATTGGCGGGACTCT Forward 5: TCACCAAGAGGGAATGTGTG Reverse 5: CTCCTCCAGCAGGTCCAC Forward 6: CTGATGAAGAGGCAGAAGATG Reverse 6: AGGAGGACATGCTGTTGTTG Forward 7: TAGAGGGGAGCCGGTGAC Reverse 7: CCAGCATGGTCTCCTCCAG Forward 8: CCCACAGATGCCTTCCAG Reverse 8: CCAGGCCCACATCAATCAA Forward 9: GATGGACAGGGTGGACTTTG Reverse 9: TGCACCGTTTCCTCACAATC Forward 10: CCTACAAGCAGTCTACCTCTTTG Reverse 10: TTGAACTTCCTGAACTCGCC Forward 11: AGCTCTACAACACGAAACAACC Reverse 11: CTGAACTCGCCGGTAATGCA Degenerate Forward 1: GCTGAAGAACTGGAGCAACTC Degenerate Reverse 1: GTACTCGTAIGTCCAGTGGC	Designed

3.11 Tissue expression

Using the obtained SLC41A1 sequence above, custom PCR primers were generated specific to the *C. auratus* sequence (Invitrogen; Table 2). These primers were used to generate a tissue mRNA expression profile analysis for the *C. auratus* SLC41a1 transcript using cDNA isolated and synthesized from the heart, gill, kidney, GI tract, brain, muscle, liver, and spleen. 18s, ubiquitously expressed in all tissues, was used as a control. The cDNA was synthesized as described above.

Table 2: qPCR primers used to quantify SLC41a1.

Gene – product size (bp)	**Primers**	**From; GenBank id**
SLC41a1 – 148 (gene of interest)	Forward: CATGTGAGCTGCAACTGTCC Reverse: GGAGAACGCCAGCCAAAG	Designed;
18s – 143 (control)	Forward: TCTCGATTCTGTGGGTGGT Reverse: CTCAATCTCGTGTGGCTGA	(from Perry et al. 2006); JF911800.1
B-actin – 156 (control)	Forward: GGCCTCCCTGTCTATCTTCC Reverse: TTGAGAGGTTTGGGTTGGTC	(from Tinoco et al. 2012); AB039726.2
EF-1 – 227 (control)	Forward: GATTGTTGCTGGTGGTGTTG Reverse: GCAGGGTTGTAGCCGATTT	(from Marlatt et al. 2008); AB056104.1
ARP – 186 (control)	Forward: CATCCAGCAGGTGTATGATAACGG Reverse: CTCACACCCTCCAGGAACCTC	(from Roesner et al. 2008); Authors did not submit obtained partial sequence to GenBank

3.12 qPCR

Quantitative polymerase chain reaction (qPCR) was used to quantify expression levels of SLC41a1 mRNA levels in *C. auratus* among the different treatments described below. 10 µl reactions were carried out in duplicates in a Roche Lightcycler 96, using the Power SYBR Green Life Technologies qPCR kit (Life Technologies Inc, Carlsbad, California, USA). Reactions

consisted of 5 µl Power SYBR Green Master 2x, 0.5 µl of both the forward and reverse primers (diluted to 10 µM), 2.5 µl PCR grade water and 1.5 µl cDNA. All primers were ran at an annealing temperature of 60^{o}C. The obtained threshold cycle (Ct) was averaged between the two duplicates and analysed. The primers for qPCR were designed from the cloned goldfish SLC41a1 sequence (Table 2) using Primer-3. 18S, B-actin, ARP and EF-1 expression was also measured with qPCR (using available primers, listed in Table 1) and used to normalize the SLC41a1 expression. All real-time primers were optimized with dilution curves to determine cDNA concentrations at which they would exhibit near 100% reaction efficiency. Melt curve analysis was obtained to ensure the formation of a single product. Sample reactions for each primer set were also run on a 1.5% agarose gel to confirm product size and subsequently sequenced (BioBasic, Markham, Ontario, Canada) to confirm product identity.

3.13 Dietary manipulations, diet preparation and feeding

All experiments involving dietary manipulation described in this thesis involved a similar diet preparation. Each feed (the composition of which is described in the methodology of the respective experiment) was mechanically crushed with a mortar and pestle and mixed with reverse-osmosis water. The resulting paste was then passed through a syringe onto an aluminum foil sheet and oven dried at 60^{o}C overnight. The dried food was then re-pelleted by crushing it into small bits with the mortar and pestle once more, upon which it was stored in a freezer (-20^{o}C) until needed.

Fish were provided with 5% of their body weight of their assigned diet at the same time of each day (at 10am) according to their assigned feeding schedule (with the exception of food-deprived treatments; once again, explained in the specific methodology for each experiment). After about 15 minutes, any uneaten food was scooped from the tank and disposed of.

3.13.1 Effect of time post feeding on SLC41A1 expression

Following acclimation to the laboratory, animals were placed on a feeding schedule where food was given at a set time each day in order to synchronize feeding associated behaviours and responses. Animals were fed Wardley commercial food pellets with a known magnesium content of 110 mM kg^{-1} (Bucking and Wood 2006b). After four weeks of this diet, animals were sacrificed and the gill, GI tract, and kidney were sampled 3hrs, 6hrs, 9hrs, 12hrs, and 24hrs following feeding (N=6). Feeding was then suspended for 7 days and a final group of fish were sampled as unfed fish (N=6). RNA extraction, cDNA synthesis, and qPCR were performed as described above.

3.13.2 Effect of a high magnesium diet on SLC41A1 expression

The above methodology was repeated with animals fed Wardley commercial food pellets that were reconstituted with an additional 110 mmols Mg^{2+} kg^{-1} (220mmol Mg^{2+} kg^{-1} total). This concentration was chosen, as it was estimated to double the existing magnesium concentration (Bucking and Wood 2006b).

All fish were kept at 20^{o}C throughout the experiment. After four weeks exposure to the high magnesium diet, the GI tract, kidney, and gill from 7 fish of each group were sampled 3hrs, 6hrs, 9 hrs, 12 hrs, and 24 hours following feeding (N=6). Feeding was again suspended for 7 days and a final group of fish were sampled as unfed fish (N=6). Once again, RNA extraction, cDNA synthesis, and qPCR were performed as described above.

3.13.3 Effect of a low magnesium diet on SLC41A1 expression

A second, similar experiment was carried out, this time testing the impact of low dietary magnesium. To this end, three diets were employed after the initial one week acclimation to the laboratory. First, a control diet of standard commercial food pellets was used as before. Second, a low magnesium diet consisting of FW Mysis shrimp was used, and finally, a magnesium enriched

Mysis shrimp diet (110mmol $MgCl_2$ kg^{-1} was added to shrimp) was used to mimic the magnesium content of commercial food pellets. All fish were kept at 20°C throughout the experiment. After two weeks of the specific diets, the gills, kidney, and GI tract from 7 fish from each group were sampled, and RNA extraction, cDNA synthesis, and qPCR were performed as described above. For this experiment and those going forward a single time point was chosen following feeding, as the time course analysis above indicated there was no change over several time-points following feeding.

3.14 Environmental manipulations

3.14.1 Effect of temperature on SLC41a1 expression

Two groups of *C. auratus* were kept in flow through water at each of 3 different temperatures, 10, 15 and 20°C for a total of 30 days. One group was fed daily, while a second was fed every other day with Wardley commercial food pellets. Once the experimental period was over, all fish were sacrificed as described earlier (6 hours post their final meal), and their gills, GI tracts and kidneys were sampled as previously described. RNA extraction, cDNA synthesis, and qPCR were performed as described above.

3.14.2 Effect of IPW exposure on SLC41a1 expression

In order to test how IPW exposure affects SLC41a1 mRNA transcript levels, 21 fish were acclimated at 20°C and fed Wardley commercial food pellets daily for a week. Then, 14 fish were moved to a second tank with flow through IPW. 7 of those fish were sampled after a 24 hours exposure, while the control and long-term exposure fish were sampled 13 days later (both fed 6 hours before sampling). Tissue collection, RNA extraction, cDNA synthesis, and qPCR were performed as previously described.

3.15 Determination of dietary magnesium concentration

Briefly, an ion-selective microelectrode filled with a selectophore specific for magnesium (magnesium ionophore II; Sigma-Aldrich Co), was used to estimate the magnesium concentration in diets used. Food was oven-dried (12 hours at 60^{o}C) and re-suspended in distilled water in serial dilutions (1 g ml^{-1}, 0.1 ml^{-1} and 0.01g ml^{-1}. All samples were then placed under mineral oil and the magnesium concentration was quantified using ion selective micro-electrodes (ISME; as described in Donini and O'Donnell 2005). The electrodes were calibrated using 0.5, 5, 10 and 100mM $MgCl_2$ solutions and the concentration was calculated using the following equation:

$a^h = a^c \times 10^{(\Delta V/S)}$,

where a^h is the ion concentration in the sample, a^c is the ion concentration in the calibration solution, ΔV is the voltage difference between the two and S is the slope measured in response to a 10 fold change in ion concentration (using the two calibration solutions most closely bracketing the sample being measured).

3.16 Statistics

The raw Ct values obtained for the mRNA transcript of each gene measured (SLC41a1, 18s, B-actin, ARP and EF-1) for each biological replicate of the temperature experiment were normalised via the normagene approach (explained in detail in Heckmann et al. 2011). A geometric average of the four different control genes (18s, B-actin, ARP and EF-1) was then taken for each sample to give the "control Ct" value, which was then used in the ΔΔCt calculation in order to compare the fold difference change between different treatments. Normagene was not used for the statistical analysis of other experiments (IPW exposure and dietary manipulation). Instead, the ΔΔCt calculation was applied to the gene of interest and a single control gene (ARP) whose transcript abundance did not change between experimental and control groups.

Data which failed normality or equal variance tests (such as the temperature experiment) was analyzed via Kruskal-Wallis One-Way ANOVA on ranks, followed by a Dunn's test for pairwise comparisons, as suggested by SigmaPlot 11. Otherwise, a parametric One-Way ANOVA followed by a Tukey test was used.

Results

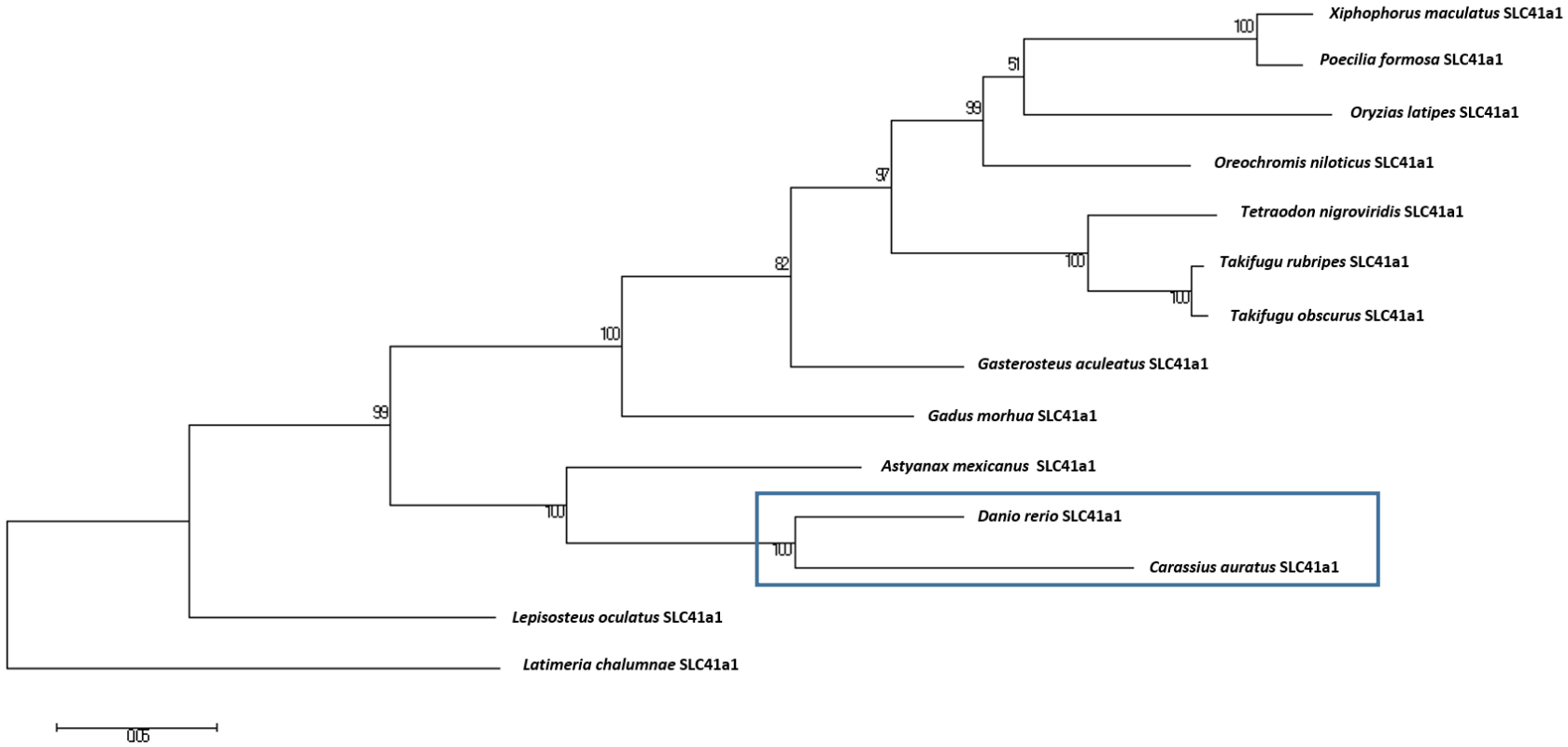

Figure 3: SLC41a1 nucleotide phylogeny. Phylogenetic tree constructed from published teleost SLC41a1 coding sequences along with my cloned sequence. The evolutionary history was inferred by using the Maximum Likelihood method based on the Tamura-Nei model (Tamura and Nei 1993). The tree with the highest log likelihood (-12290.1880) is shown. The percentage of trees in which the associated taxa clustered together is shown next to the branches. Initial tree(s) for the heuristic search were obtained automatically by applying Neighbor-Join and BioNJ algorithms to a matrix of pairwise distances estimated using the Maximum Composite Likelihood (MCL) approach, and then selecting the topology with superior log likelihood value. The tree is drawn to scale, with branch lengths measured in the number of substitutions per site. The analysis involved 14 nucleotide sequences. Codon positions included were 1st+2nd+3rd+Noncoding. There were a total of 2313 positions in the final dataset. Evolutionary analyses were conducted in MEGA6 (Tamura et al. 2013).

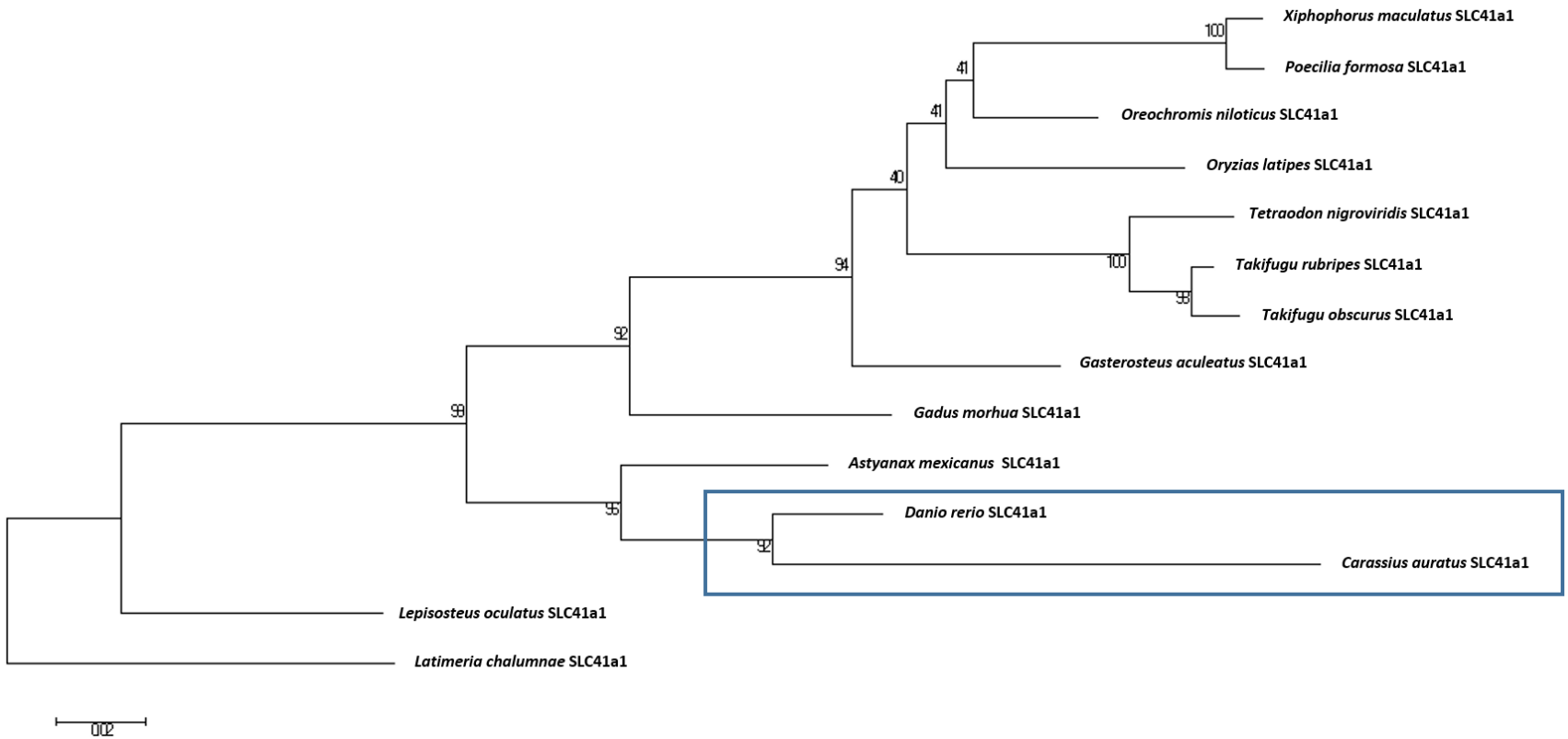

Figure 4: SLC41a1 amino acid phylogeny. Phylogenetic tree constructed from published teleost SLC41a1 coding sequences along with my cloned sequence, converted into amino acids. The evolutionary history was inferred by using the Maximum Likelihood method based on the JTT matrix-based model (Tamura and Nei 1993). The tree with the highest log likelihood (-4933.7624) is shown. The percentage of trees in which the associated taxa clustered together is shown next to the branches. Initial tree(s) for the heuristic search were obtained automatically by applying Neighbor-Join and BioNJ algorithms to a matrix of pairwise distances estimated using a JTT model, and then selecting the topology with superior log likelihood value. The tree is drawn to scale, with branch lengths measured in the number of substitutions per site. The analysis involved 14 amino acid sequences. The coding data was translated assuming a Standard genetic code Table. There were a total of 760 positions in the final dataset. Evolutionary analyses were conducted in MEGA6 (Tamura et al. 2013).

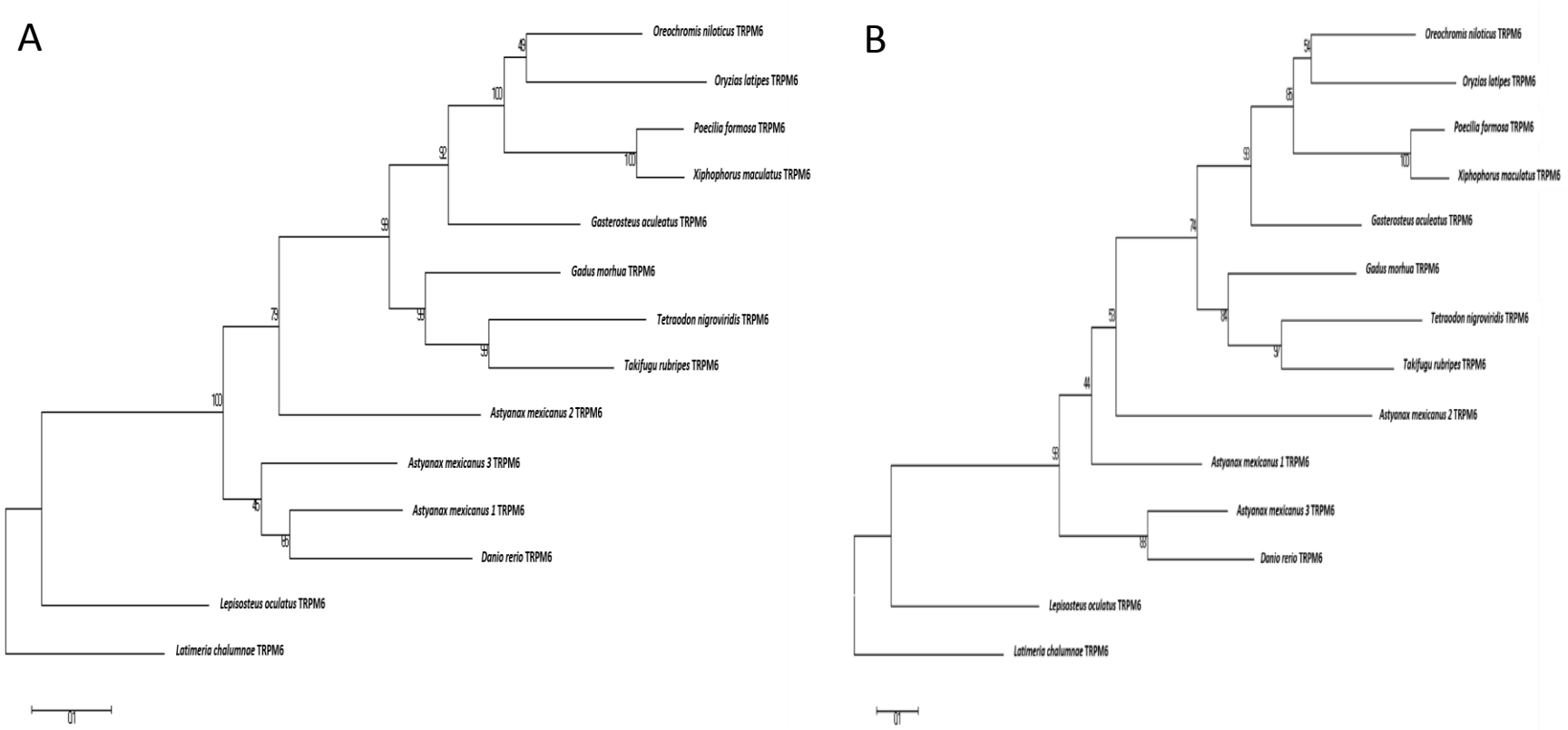

Figure 5: TRPM6 nucleotide (A) and amino acid (B) phylogeny **(with cavefish)**. The evolutionary history was inferred by using the Maximum Likelihood method based on the Tamura-Nei model (Tamura and Nei 1993). The tree with the highest log likelihood (-55960.8284 for A; -32166.8394 for B) is shown. The percentage of trees in which the associated taxa clustered together is shown next to the branches. Initial tree(s) for the heuristic search were obtained automatically by applying Neighbor-Join and BioNJ algorithms to a matrix of pairwise distances estimated using the Maximum Composite Likelihood (MCL) and JTT approach (A and B, respectively), and then selecting the topology with superior log likelihood value. The tree is drawn to scale, with branch lengths measured in the number of substitutions per site. The analysis involved 14 nucleotide sequences. The total positions in the final dataset were 6214 and 1790 (A and B, respectively). Evolutionary analyses were conducted in MEGA6 (Tamura et al. 2013).

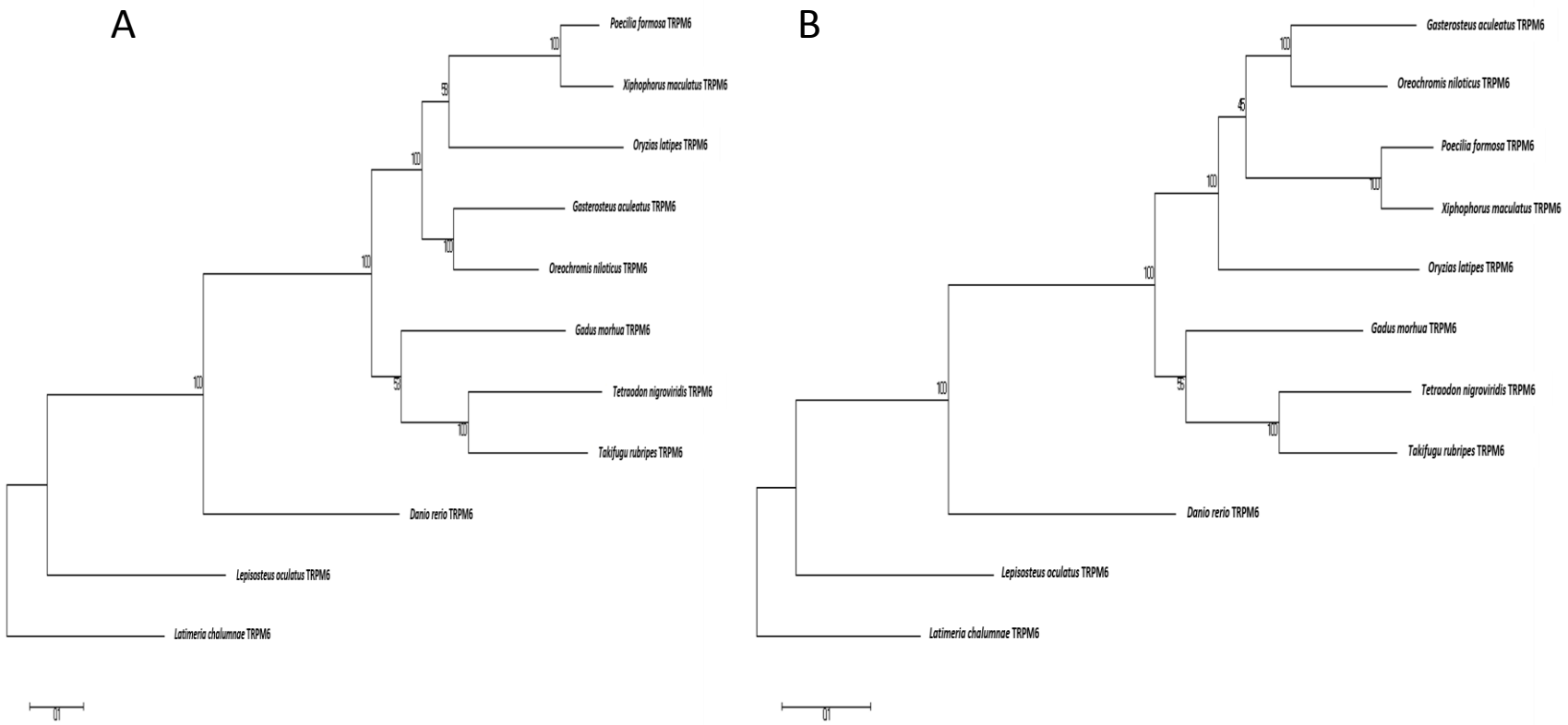

Figure 6: TRPM6 nucleotide (A) and amino acid (B) phylogeny **(without cavefish)**. The evolutionary history was inferred by using the Maximum Likelihood method based on the Tamura-Nei model (Tamura and Nei 1993). The tree with the highest log likelihood (-52974.3485 for A; -29881.0647 for B) is shown. The percentage of trees in which the associated taxa clustered together is shown next to the branches. Initial tree(s) for the heuristic search were obtained automatically by applying Neighbor-Join and BioNJ algorithms to a matrix of pairwise distances estimated using the Maximum Composite Likelihood (MCL) and JTT approach (A and B, respectively), and then selecting the topology with superior log likelihood value. The tree is drawn to scale, with branch lengths measured in the number of substitutions per site. The analysis involved 11 nucleotide sequences. The total positions in the final dataset were 6229 and 1892 (A and B, respectively). Evolutionary analyses were conducted in MEGA6 (Tamura et al. 2013).

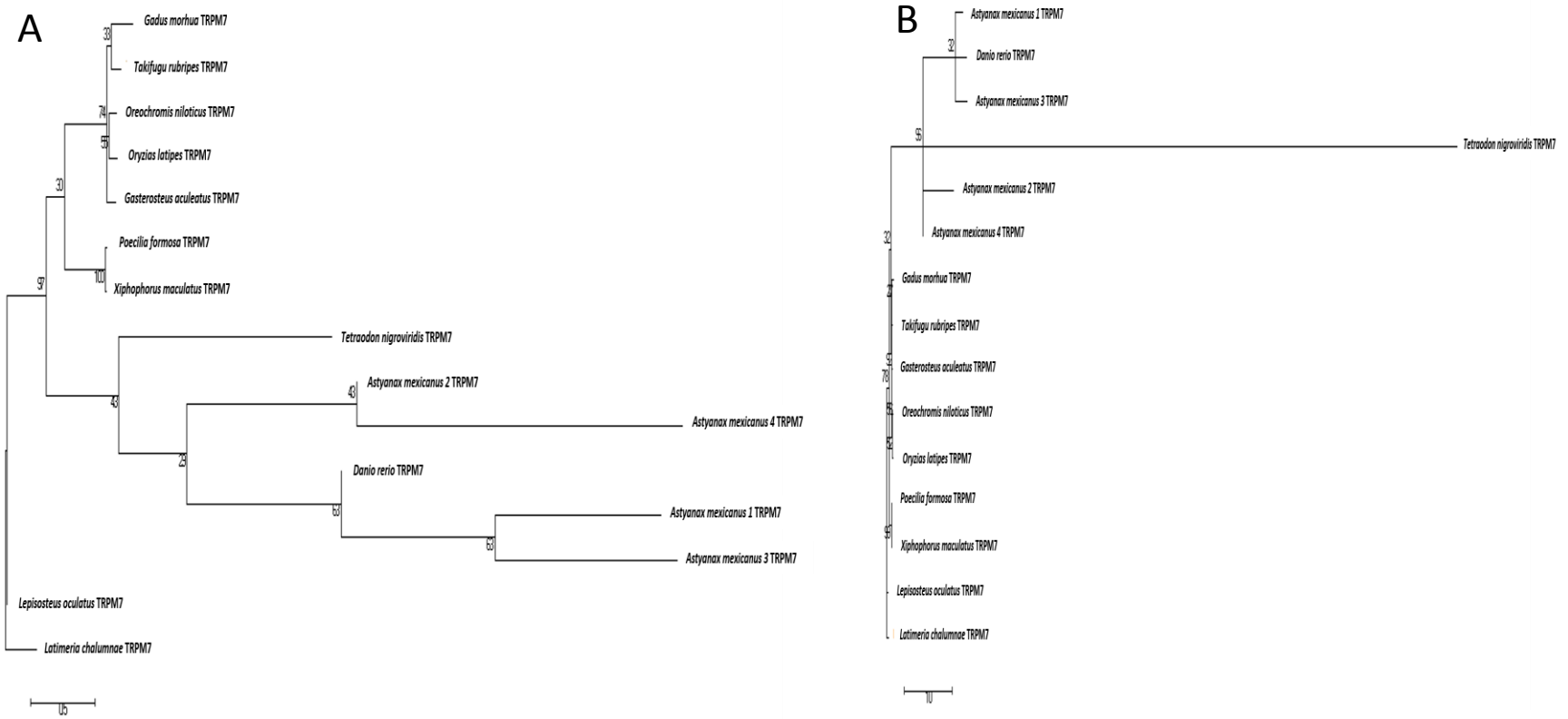

Figure 7: TRPM7 nucleotide (A) and amino acid (B) phylogeny **(with cavefish)**. The evolutionary history was inferred by using the Maximum Likelihood method based on the Tamura-Nei model (Tamura and Nei 1993). The tree with the highest log likelihood (-6895.6198 for A; -3630.4820 for B) is shown. The percentage of trees in which the associated taxa clustered together is shown next to the branches. Initial tree(s) for the heuristic search were obtained automatically by applying Neighbor-Join and BioNJ algorithms to a matrix of pairwise distances estimated using the Maximum Composite Likelihood (MCL) and JTT approach (A and B, respectively), and then selecting the topology with superior log likelihood value. The tree is drawn to scale, with branch lengths measured in the number of substitutions per site. The analysis involved 15 nucleotide sequences. The total positions in the final dataset were 493 and 121 (A and B, respectively). Evolutionary analyses were conducted in MEGA6 (Tamura et al. 2013)

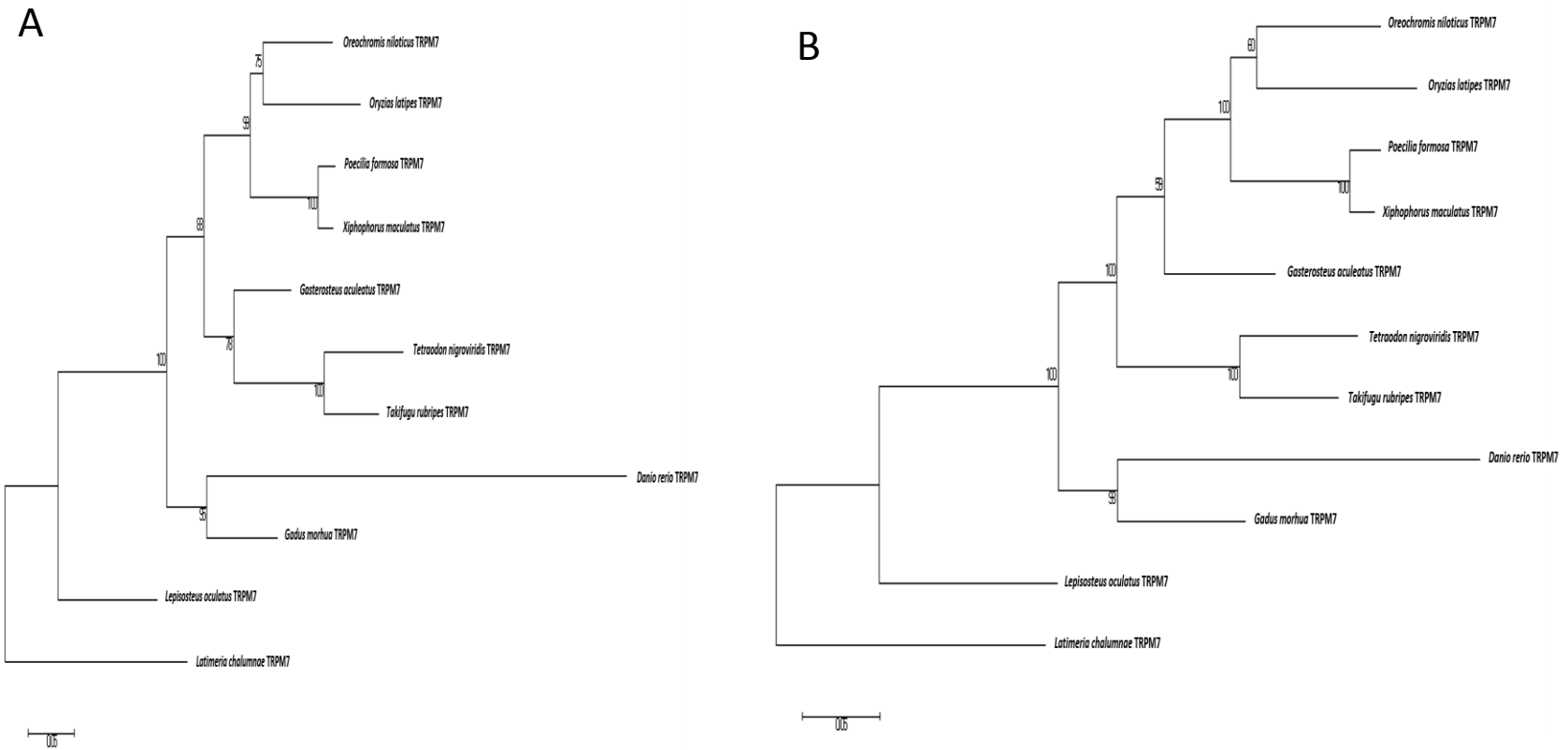

Figure 8: TRPM7 nucleotide (A) and amino acid (B) phylogeny **(without cavefish)**. The evolutionary history was inferred by using the Maximum Likelihood method based on the Tamura-Nei model (Tamura and Nei 1993). The tree with the highest log likelihood (-36819.2273 for A; -18534.9645 for B) is shown. The percentage of trees in which the associated taxa clustered together is shown next to the branches. Initial tree(s) for the heuristic search were obtained automatically by applying Neighbor-Join and BioNJ algorithms to a matrix of pairwise distances estimated using the Maximum Composite Likelihood (MCL) and JTT approach (A and B, respectively), and then selecting the topology with superior log likelihood value. The tree is drawn to scale, with branch lengths measured in the number of substitutions per site. The analysis involved 11 nucleotide sequences. The total positions in the final dataset were 6155and 1815 (A and B, respectively). Evolutionary analyses were conducted in MEGA6 (Tamura et al. 2013).

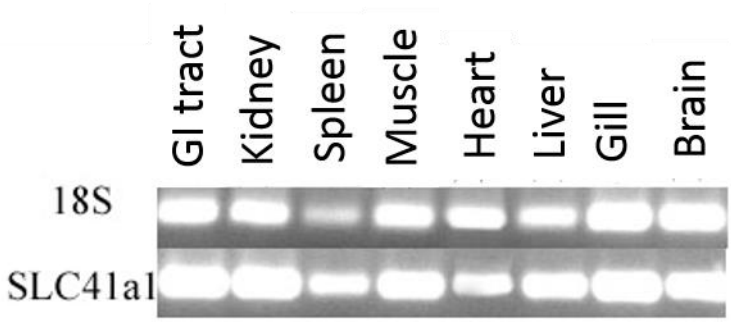

Figure 9: SLC41a1 tissue distribution. Tissue distribution of the SLC41a1 mRNA transcript (1531 bp) in the common goldfish (*C. auratus*) displayed on an ethidium bromide containing 1.5% agarose gel. Transcripts were detected in the GI tract, kidney, spleen, muscles, heart, liver, gill and brain. and ran on a 1.5% agarose gel via electrophoresis.

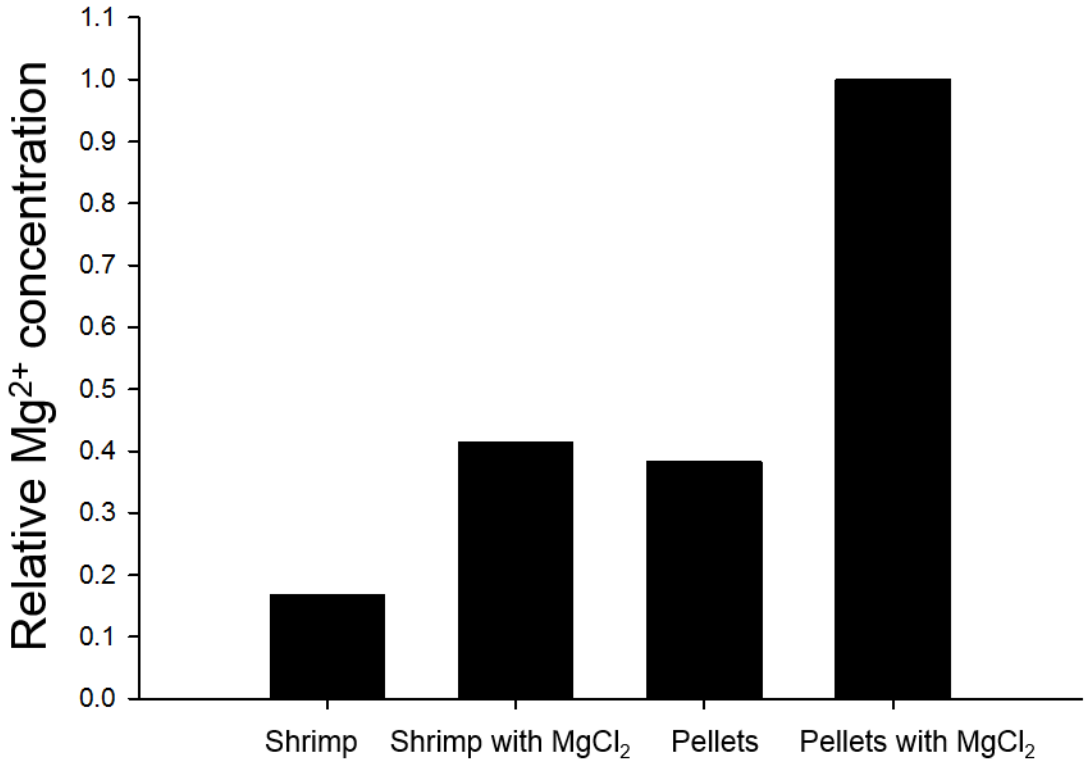

Figure 10: Relative dietary Mg^{2+} concentration. Mg^{2+} concentration in each of the diets used for the feeding experiments, as measured with ISME and normalized to the magnesium enriched pellet diet.

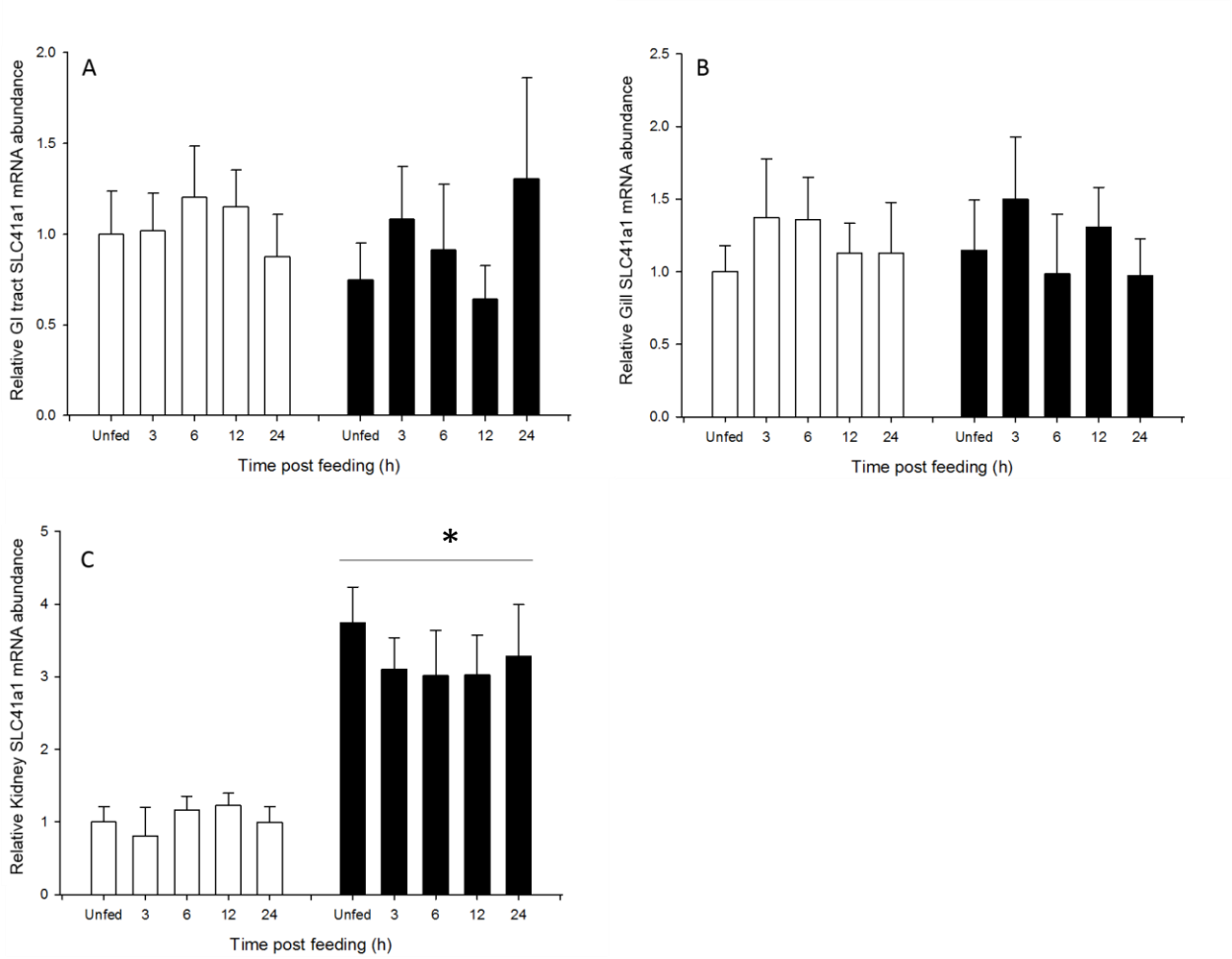

Figure 11: Effect of high Mg^{2+} diet and time post feeding on SLC41a1 expression. The GI tract (A), gill (B) and kidney (C) of *C. auratus* fed a control, commercial pellet diet (white bars) and a magnesium enriched commercial pellet diet (black bars) were sampled. Ct values obtained from each treatment with qPCR were compared using the ΔΔCt method, using the unfed time-point for the control diet as a reference. ANOVA on ranks followed by pairwise Holm-Sidak comparisons tests (n=7) were used to determine significant difference between groups (denoted by *).

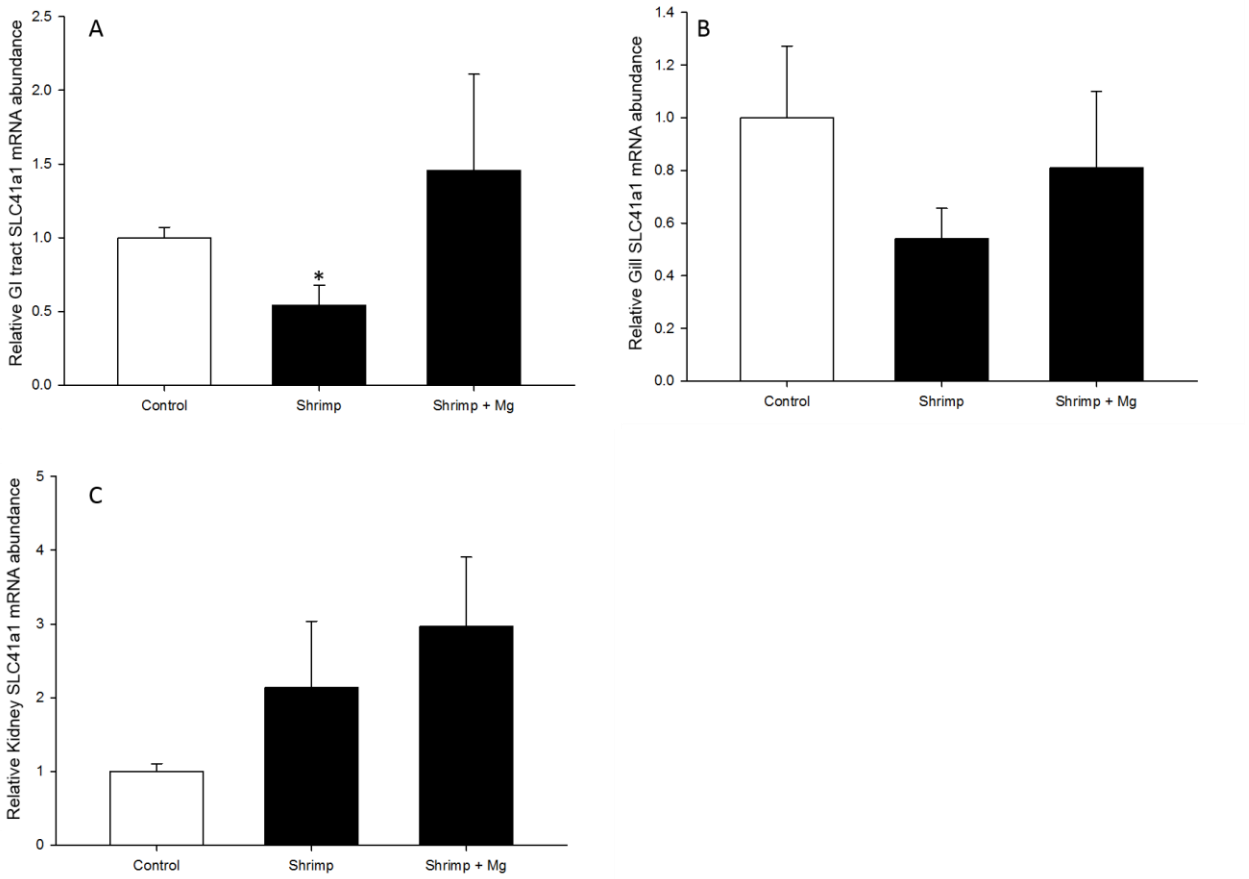

Figure 12: Effect of diet on SLC41a1 expression. SLC41a1 mRNA transcript expression was measured in the GI tract (A), gill (B) and kidney (C) in *C. auratus*. Fish were kept in regular, dechlorinated water, and were fed either a control pellet diet, a low-magnesium shrimp diet, or a regular-magnesium shrimp diet. Ct values obtained from each treatment with qPCR were compared using the ΔΔCt method, using the commercial pellet diet as control. Data is presented as average relative expression (normalized to the control diet) A one-way ANOVA followed by a Tukey test was used to compare the individual treatments (n=6-7). * indicates significant difference from control ($p<0.05$).

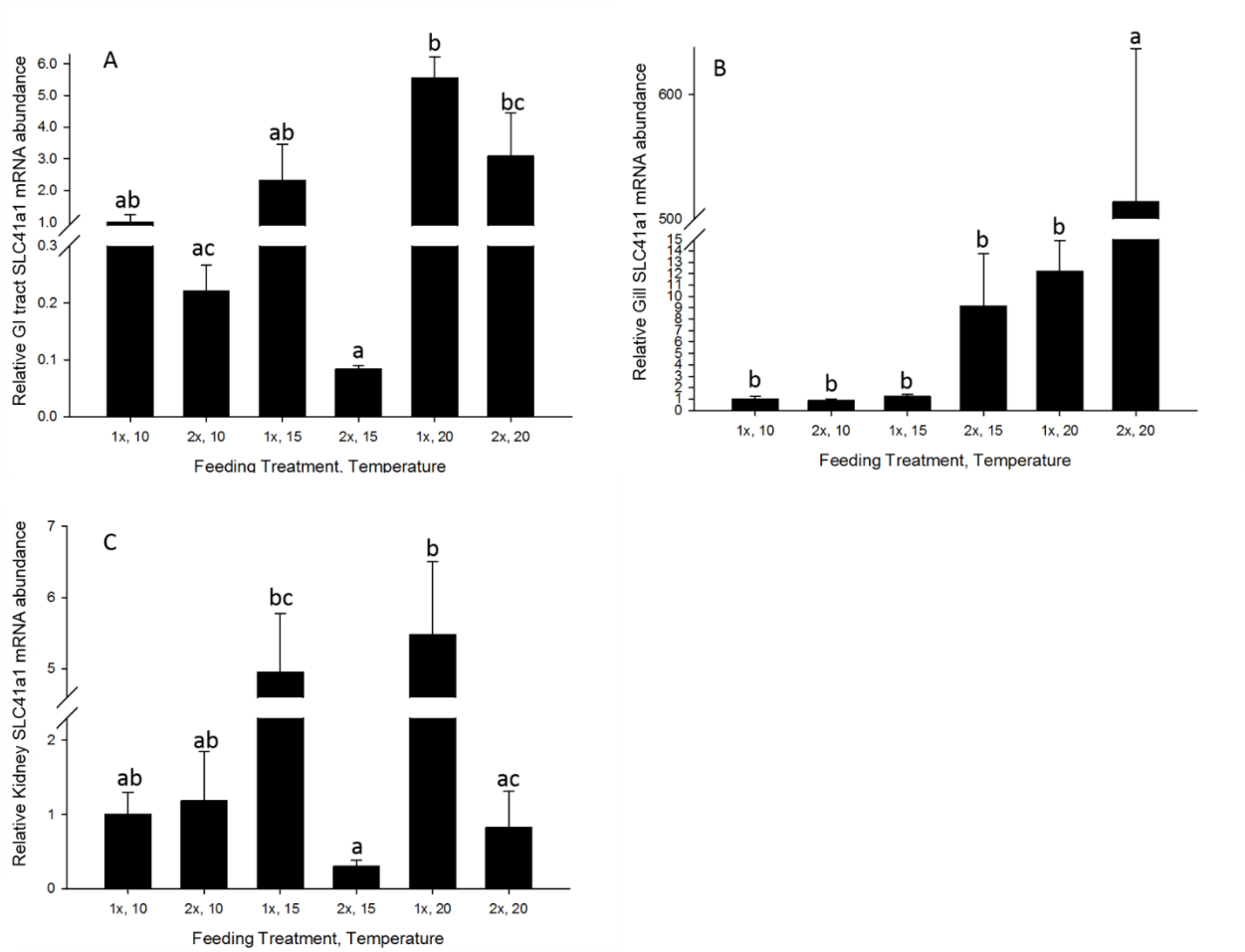

Figure 13: Effect of feeding regime and temperature on SLC41a1 expression. SLC41a1 mRNA transcript expression was measured in the GI tract (A), gill (B) and kidney (C). Fish were either fed daily (1x) or every other day (2x) and kept at either 10, 15, or 20°C over a 30 day period. Expression was assessed with qPCR, and normalised with the geometric average of the expression of four housekeeping genes: β-actin, ef-1 α, ARP and 18s (with the only exception being the kidney, using only ARP). Prior to calculating gene expression using the ΔΔCt method, all obtained Ct for the gene of interest and control genes were ran through the normagene algorithm. Data is expressed as mean fold difference ± s.e.m. relative to the daily 1x, 10°C treatment; (ANOVA on ranks followed by pairwise Dunn's comparisons test; n=4-7). Different letters denote significant difference ($p<0.05$).

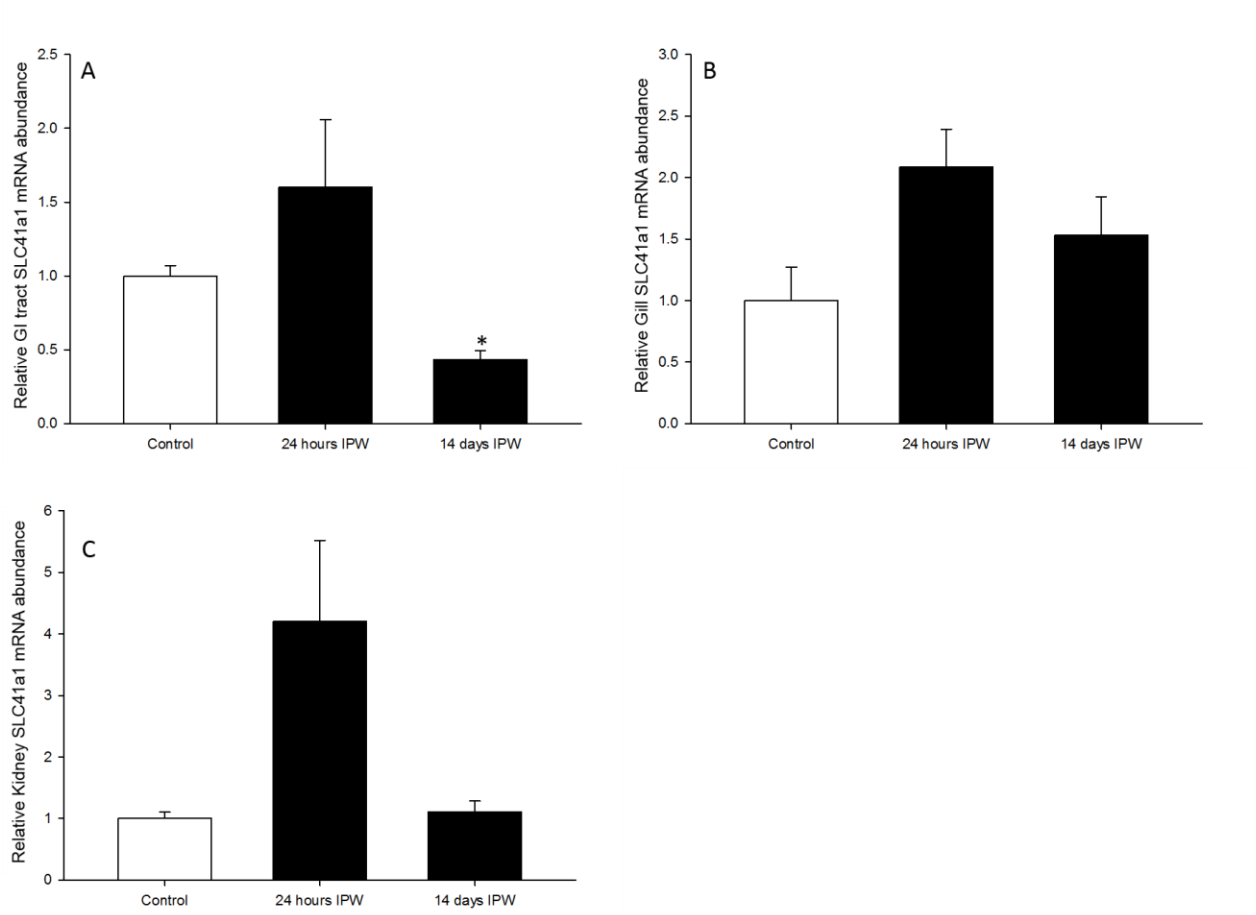

Figure 14: Effect of IPW on SLC41a1 expression. SLC41a1 mRNA transcript expression was measured in the GI tract (A), gill (B) and kidney (C) of *C. auratus* kept in regular, dechlorinated water for 2 weeks, and were then either sampled, or exposed to IPW for 24hours, or 14 days. Ct values obtained from each treatment with qPCR were compared using the ΔΔCt method, using the fresh-water only treatment as control. A one-way ANOVA followed by a Tukey test was used to compare the individual treatments (n=6-7). Different letters indicate significance ($p<0.05$).

4.1 Phylogenetic analysis of SLC41a1 and available TRPM6 and TRPM7 sequences

Cloning SLC41a1 resulted in a nearly complete partial sequence of ~1500 nucleotides (See Appendix Figures 28 and 29 for nucleotide and amino acid sequence alignment with known fish sequences). The obtained sequence was used in a series of phylogenetic analysis using other SLC41a1 sequences (available off genebank and Ensembl) in order to confirm if it corresponded to SLC41a1. Using a boot-strapped maximum likelihood analysis directly on the nucleotide sequences, *C. auratus* clustered most closely with the *D. rerio* (in 100% of constructed trees; Figure 3). The two further grouped with *A. mexicanus*, once again in 100% of trees, with *C. auratus* having a longer branch length indicating a slightly higher number of site substitutions. Converting the sequences to amino acids, revealed the same trend in groupings and branch lengths (Figure 4), although support dropped from 100% to 92-96%. Still, the phylogenies support the obtained sequence being SLC41a1, as *C. auratus* and *D. rerio* are both relatively closely related, and both belong to the *Cyprinidae* family. Along with *A. mexicanus*, the three fish belong to the superorder *Ostariophysi*. Furthermore, three members of the *Tetraodontidae* subfamily, *T. obscurus*, *T. rubripes* and *T. nigrovirids*, all clustered together for both the nucleic acid and amino acid trees indicating correct construction of the trees (Figures 3 and 4).

Finally, a phylogenetic tree was generated using the described methods but incorporating two SLC41 isoforms (SLC41a2 and SLC41a3). The obtained SLC41a1 *C. auratus* sequence clustered with SLC41a1, not the other two isoforms (Appendix Figure 27).

Given that *A. mexicanus* were the only fish species to have multiple sequences listed for both TRPM6 and TRPM7, phylogenetic analysis was carried both with and without them. Nucleotide alignment of the TRPM6 genes showed zebrafish clustering most closely with cavefish sequence 1 (Figure 5A) while *D. rerio* clustered with *A. mexicanus* sequence 3 for amino acids

(Figure 5B). The bootstrap analysis showed these groups clustering in 86 and 88% of all constructed trees with nucleotide and amino acid sequences, respectively. Cavefish sequence 2 branches off later, not pairing with any other sequence (Figures 5A and B). Removing the 3 partial cavefish sequences from the phylogeny results in the zebrafish sequence branching off on its own from the remainder of the teleost sequences in 100% of the trees constructed for both the nucleotide and amino acid sequences (Figures 6A and B). *T. nigroviridis* and *T. rubripes* formed a high probability clade in both nucleotide and amino acid sequences, regardless of the presence or absence of the *A. mexicanus* sequence (Figures 5 and 6).

D. rerio once against clusters with *A. mexicanus* for TRPM7 analysis of both nucleotide and amino acid sequences (in 63 and 32% of all trees generated, respectively, with *A. mexicanus* sequences 1 and 3; Figures 7A and B). The other (2^{nd} and 4^{th}) *A. mexicanus* sequences cluster together as well as with the *D. rerio* - *A. mexicanus* 1 and 3 cluster. *T. nigroviridis* also clustered with *A. mexicanus* and *D. rerio* in the amino acid analysis, however, displayed a long branch length (Figure 7B). Phylogenies excluding the multiple *A. mexicanus* sequences exhibit *D. rerio* having the longest branch length, clustering with *G. morhua* (Figures 8A and B). This is indicative of the zebrafish having the largest number of site substitutions of the analyzed TRPM7 sequences.

4.2 Tissue expression

SLC41a1 mRNA transcripts were detected in all of the examined tissues, namely heart, liver, brain, spleen, muscle, GI tract, gill, and kidney (Figure 9).

4.3 Diet preparation

The shrimp diet was measured to have the lowest relative Mg^{2+} content at 17% of the concentration detected in the highest diet, the $MgCl_2$ enriched pellet diet (Figure 10). Both the

$MgCl_2$ enriched shrimp and regular pellet diets were similar in Mg^{2+} content, at 41% and 38% of the concentration measured in enriched pellets, respectively (Figure 10).

4.4 Effect of time post feeding on SLC41a1 expression

There was no significant difference in SLC41a1 transcript expression in the GI tract and gill of *C. auratus* fed the control pellet diet compared to fish fed a magnesium-enriched pellet diet at all time points (Figures 11A and B). While expression varied from 1±0.3 (control; regular diet, unfed) to 0.7±0.2 (magnesium rich diet, 12 hours post feeding) in the GI tract and 1±0.2 (control; regular diet, unfed) to 1.5±0.5 (magnesium enriched diet, 3 hours post feeding) in the gill, none of the pairwise comparisons showed significant difference over the course of digesting a meal or from fasted levels. As such, enriched magnesium diet (post 4 weeks), feeding (up to 24 hours post-meal ingestion), and fasting (up to 7 days) does not seem to impact SLC41a1 expression in both organs.

The kidney, alternatively, showed ~3 fold increased expression in fish fed magnesium-enriched pellets at all time points relative to all feeding and fasting time points in fish fed the control, commercial pellet diet (Figure 11C). Within fish on either diet, however, there was no variation at the different feeding time points (Figure 11C). As such, SLC41a1 appears to upregulate in the kidney in response to increased dietary magnesium (post 4 weeks), however, feeding (up to 24 hrs post-meal ingestion) and fasting (up to 7 days) does not seem to affect transcript levels.

4.5 Effect of different diets on SLC41a1 expression

The shrimp and magnesium-enriched shrimp diets both had no significant impact on the SLC41a1 mRNA expression in the gill and kidney relative to the control commercial pellet diet (Figures 12B and C). The kidney expression varied from 1.00±0.09 for fish fed the control diet, 2.13±0.89 for fish fed shrimp and 2.96±0.94 for fish fed the magnesium enriched shrimp however

these were not statistically different (Figure 12C). Similarly, the gill expression varied from 1.00±0.27 in the control diet to 0.54±0.11 and 0.80±0.29 in fish fed shrimp and magnesium-enriched shrimp, respectively again without significance (Figure 12B). Alternatively, the GI tract showed a significant decrease in fish fed shrimp (0.54±0.39) relative to the control (1.00±0.07). However, there was no difference between the control diet and the magnesium-enriched shrimp (1.45±0.65) showing recovery of expression with magnesium addition to the shrimp diet (Figure 12A). These results were in contradiction with the magnesium-enriched pellet diets where the kidney responded to dietary manipulation (Figure 11C) and the gill and GI tract didn't (Figures 11A and B).

4.6 Effect of temperature on SLC41a1 expression

Temperature did not impact gill SLC41a1 mRNA expression in a consistent manner, with only a single group being significantly upregulated, fish fed every 48 hours kept at 20^{o}C (Figure 13B). This staggering upregulation (~500 fold) is likely incorrect, as upon closer inspection of the data control gene values were observed to be impacted for this group. SLC41a1 was upregulated in the GI tract for daily fed fish kept at 20^{o}C (5.5±0.66 fold increase), and to a lesser extent fish fed every 48 hours kept at 20^{o}C (3±1.37) relative to fish fed every 48 hours kept at 15^{o}C (Figure 13A). Kidney expression was increased in daily fed fish kept at 15 and 20^{o}C (4.9±0.84 and 5.4±1.01 fold increase, respectively) relative to fish fed every other day kept at those temperatures (Figure 13C).

4.7 Effect of IPW exposure on SLC41a1 expression

All 3 tissues sampled followed the trend of (non-significantly) increasing relative expression at 24hrs IPW exposure associated with a larger variability (Figures 14A, B and C) followed by values returning to near control values for the gill and kidney at 14 days IPW exposure

(Figures 14B and C). The GI tract was the only tissue to display a significant transcriptional change and showed a significant relative reduction (down to 0.43±0.06) at 14 days of IPW exposure (Figure 14A).

Discussion

5.1 Phylogenetic analysis

Given the clustering of the obtained SLC41a1 sequence with closely related species such as *D. rerio* and *A. mexicanus* (Figures 3 and 4), as well as the obtained sequence clustering with other SLC41a1 sequences, rather than SLC41a2 or SLC41a3 sequences (Figure 28) and it containing the two SLC41a1 conserved domains, D1 and D2 (highlited in Figure 30) we can assume that the obtained sequence is in fact, the *C. auratus* SLC41a1 coding sequence. Furthermore, the tissue distribution of SLC41a1 transcripts across all studied tissues (Figure 9) supports observations in literature that the protein is universally expressed across all tissues in both mammals and teleosts (Islam et al. 2013; Mandt et al. 2011).

Unfortunately, neither TRPM6 nor TRPM7 were successfully cloned and sequenced. Despite using the same methodology as SLC41a1, and designing a variety of primers (Table 1), no product near the expected size for any of the primer combinations was obtained. Instead, phylogenetic analysis was carried out on the available sequences from other fish species, in order to possibly understand why cloning was unsuccessful. Exclusion of cavefish from analysis resulted in *D. rerio* not clustering with any other sequence for TRPM6, as well as a relatively long branch length (representative of substitutions per site) suggesting zebrafish are very different from all other species (Figures 6A and B). It stands to reason that *C. auratus* would follow that trend, and have a very different sequence form the other non-cyprinid species, as it is closely related to *D. rerio*. TRPM7 analysis including the cavefish sequences resulted in the familiar *A. mexicanus – D. rerio* cluster, however, it also included *T. nigroviridis* for both the nucleotide (Figure 7A) and amino acid analysis (Figure 7B). The amino acid was especially perplexing, as it showed *T. obscurus* to have an exceptionally long branch length, indicating a large number of site differences

with other sequences, implying it is very different from the other teleosts. Excluding the cavefish sequences resulted in *D. rerio* clustering with *G. morhua*, once again resulting in a very long branch length for zebrafish, supporting zebrafish (and possibly *C. auratus* sequence) being markedly different from other teleost fish and the use of consensus sequences difficult (Figures 8A and B).

The presented phylogenetic analysis may provide an explanation as to the failure of the cloning attempts. As with SLC41a1, zebrafish were used as the primary sequence off which primers were designed, preferentially using conserved sites between all fish species. However, given the presence of a multitude of partial cavefish sequences (the second most closely related fish species used) available for both proteins, as well as the evident differences of *D. rerio* with the remainder of the sequences (resulting in no close clusters in analysis excluding *A. mexicanus* for TRPM6 and very long branch length for TRPM7), it is possible this strategy was not successful, as cyprinid sequences appear to be very different from the remainder of the fish. This could possibly be due to a shared mutation which sets cyprinid TRPM6 and TRPM7 genes apart from other teleosts, or the available sequences are simply faulty due to sequencing errors or mislabelling. As such, an alternative approach might be to focus only on the cyprinid sequences when designing primers for the two channels, or (in the case of sequencing errors in the cyprinid sequences) exclude them from the primer-designing process.

5.2 SLC41a1, TRPM6 and TRPM7, and their role in Mg^{2+} transport in the GI tract, kidney, and gill

While the mammalian, FW, and SW teleost kidneys all carry out different strategies in terms of ion and osmoregulation, they all express the suspected molecular hallmarks of vertebrate magnesium transport (i.e. TRPM6, TRPM7 and SLC41a1). As such, a contrast of the three

different strategies may present us with a better understanding of the proteins carrying out magnesium transport in vertebrate tissues.

The mammalian kidney is tasked with water conservation and salt reabsorption. Magnesium is initially filtered at the glomerulus, and then passed along the tubular system, where the majority of it is re-absorbed (Quamme and de Rouffignac 2000; Schlingmann et al. 2007). Firstly, the proximal convoluted tubule is believed to reabsorb about 10-15% of Mg^{2+} from the glomerular filtrate, primarily relying on passive, paracellular transport (Le Grimellec et al. 1973; Morel et al. 1969). The loop of Henle exhibits a similar trend, absorbing up to 60% of Mg^{2+} filtered into the tubular system and transport is believed to be primarily passive, and paracellular in nature (de Rouffignac and Quamme 1994). Finally, the distal convoluted tubule also reabsorbs Mg^{2+} (10-15% of the glomerular filtrate and 30-50% of Mg^{2+} delivered by the loop of Henle), however, transport in this section is thought to be active and transcellular (de Rouffignac et al. 1983; Quamme et al. 1980) as the distal convoluted tubule has very high epithelial resistance and a large electrochemical potential to overcome, (Quamme and de Rouffignac 2000). Entry is believed to be through a channel complex (possibly TRPM6/TRPM7) down an electrochemical gradient (Schlingmann et al. 2007). Once inside the cell, Mg^{2+} is believed to be transported across the basolateral membrane via an electroneutral NME, potentially SLC41a1 (Schlingmann et al. 2007).

In contrast, teleosts are aquatic vertebrates, and face very different ion and osmoregulatory challenges depending on the osmotic pressure of their environment (reviewed in Beyenbach 2000). FW fish face constant water intake and ion loss to their hypoosmotic environment (~1-20mOsm/kg), and must therefore produce large volumes of dilute urine, reabsorbing most of the ions secreted by the glomerulus (Beyenbach 2000). Conversely, SW teleosts must excrete the constant ion load they absorb from the hyperosmotic environment (~1000mOsm/kg) (Beyenbach

2000). Significant breakthroughs have been made in the last few years in regards to renal function in SW fish, with increasing support for the currently accepted mechanism as follows (first proposed by Hickman and Trump 1969). SW excretion in the tubular system is associated with a two-step mechanism. Firstly, Mg^{2+} must cross the basolateral membrane, going down its electrochemical gradient, possibly through an unknown channel. Mg^{2+} must then be secreted from the cell into the lumen, going against a very large electrochemical gradient (~100mV) and must therefore be carried out by an active transporter (Beyenbach 2000). Vesicular transport has been proposed as a vehicle for this apical secretion (Chandra et al. 1997; Hentschel and Zierold 1994; Renfro and Shustock 1985), and is supported by the presence of Mg^{2+} rich vesicles expressing SLC41a1 found near the apical membrane of tubular cells (Islam et al. 2013). This is directly opposite to the transport direction in the mammalian kidney, and the presence of a unique transport pathway is to be expected.

FW stenohaline fish, such as *C. auratus*, are poorly understood amongst vertebrates in terms of magnesium renal handling. Similarities between FW fish and mammalian renal handling strategy (i.e. reabsorption) suggest similarities in the mechanism for tubular reabsorption of Mg^{2+}, implying TRPM6/7 expression at the apical membrane, and NME (possibly SLC41a1) expression at the basolateral membrane. Indeed the detection of TRPM6/7 and SLC41a1 in the renal tissue of freshwater fish (Fig. 9; Arjona et al. 2013; Esbaugh et al. 2014) suggest a conserved transport pathway with mammals. However, while mammalian reabsorption is largely passive and paracellular, such a strategy results in higher water reabsorption. Thus, it has been proposed that FW kidney Mg^{2+} reabsorption must rely more on active transport (Bijvelds et al. 1996), and thus may have higher levels of transporter expression although this remains to be investigated. Regardless, the direction of magnesium transport is again opposite to that observed in SW teleost

fish. The presence of the identical transporters (TRPM6/7, SLC41a1) in SW fish kidneys (Esbaugh et al. 2014; Islam et al. 2013) is thus perplexing.

Euryhaline species such as *O. mykiss* have been used to study teleost kidney function, due to their ability to survive different salinities. Comparisons between their physiology when reared in FW and SW can therefore glean insight into the differences in renal strategy required for teleost survival in either environment. Renal plasma membrane preparations made from *Oreochromis mossambicus* acclimated to SW and FW transported Mg^{2+} in a similar manner to *in vivo* observations in SW reared *Pseudopleuronectes americanus* (Cliff and Beyenbach 1992; Renfro and Shustock 1985). Thus it has been postulated that euryhaline species maintain mechanisms for ion excretion even when kept in FW, in order to be able to handle sudden influx of ions if they re-enter saline environments (Beyenbach 2000; Bijvelds et al. 1998). Interestingly, nephrons identified in the FW rainbow trout are not all filtering and thus contributing to alleviating the excess water load gained in freshwater (Brown et al. 1980). A large proportion are perfused but are not filtering water and producing copious dilute urine. Perhaps these nephrons are involved with secretory processes (Cliff and Beyenbach, 1992) that enable a dynamic management of whole body magnesium; secreting when excessive dietary magnesium is ingested as has been observed in *in vivo* kidney observations (Bucking et al. 2010). Perhaps it is these nephrons that express SLC41a1, allowing secretion in a similar manner to SW fish (Islam et al. 2013).

Similarly, both mammalian and FW teleost GI tracts must absorb substantial dietary Mg^{2+} load to meet homeostatic demand. Exhibiting a curvilinear relationship between luminal Mg^{2+} concentration and rate of transport, absorption is believed to be a mixture of passive diffusion and facilitated active transport (Bijvelds et al. 1996; Karbach and Feldmeier 1991; Shearer and Åsgård 1992). The suggested model of GI absorption in mammals shares similarities with the proposed

tubular reabsorption model in mammals, as it includes Mg^{2+} entering the cell (enterocyte) down its electrochemical gradient via a channel (now believed to be a TRPM6 and TRPM7 complex) and basolateral extrusion via an electroneutral NME (possibly SLC41a1) (Schlingmann et al. 2007). Given the presence of orthologues of all three transporters in the teleost GI tract, it stands to reason FW enterocytes will utilize a similar mechanism (Figure 2A). In comparison, SW teleosts must ingest SW to combat water loss. Absorbing 60-85% of ingested water along the GI tract, Mg^{2+} can reach concentrations of 100mM in the rectum (double the SW concentration of 50mM) as it is mostly excluded from transport. Ultimately, there is roughly a 10% net absorption of Mg^{2+} entering the GI tract (Beyenbach 2000). Despite this, as with mammalian and FW fish GI tracts, TRPM6, TRPM7 and SLC41a1 mRNA transcripts are all detected in the GI tract of SW animals, suggesting magnesium homeostasis is regulated by the same cellular transporters (and possibly similar mechanism) in the marine GI tract despite dissimilar absorption needs (Arjona et al. 2013; Esbaugh et al. 2014; Islam et al. 2013; Low et al. 2011).

Finally, as described in the introduction, there is evidence for FW branchial uptake of Mg^{2+} from the environment (primarily that body deposition exceeds dietary availability of the ion). Given the lack of electrochemical gradient for passive entry from FW into the gills, Mg^{2+} absorption must be active (Bijvelds et al. 1998) while paracellular permeability is very low, and as a result, diffusive losses at the gill are minimal, as evidenced by *O. mykiss* excreting the majority of Mg^{2+} injected into them renally (Oikari and Rankin 1985). While the three magnesium transporters are all present at the gill, their function has not been well studied. Assuming a similar function as proposed in the mammalian kidney, Mg^{2+} would have to enter branchial cells via TRPM6/7 and cross the basolateral membrane via SLC41a1. Our study confirmed SLC expression in the gill of FW fish (Figure 9), previously observed in FW-acclimated pufferfish, suggesting

potential role in magnesium transport (Islam et al. 2013). However, expression of SLC41a1 was also detected in the gill of SW pufferfish, and transcriptional levels appear unresponsive to environment levels of magnesium as in our study (Figure 14B).

Given the extensive expression of the three magnesium transporters, their function must be paramount to magnesium homeostasis in vertebrates. The understanding of their specific roles therefore would yield a better understanding of how the divalent ion is maintained.

5.3 Dietary manipulation and feeding schedule

SLC41a1 mRNA transcript expression was hypothesized to increase in treatments where Mg^{2+} availability was decreased, similar to observed trends in SLC41a1 regulation in mice kidney and colon and TRPM6 regulation in the zebrafish gill, kidney and GI tract (Goytain and Quamme 2005; Arjona et al. 2013). Namely, *C. auratus* faced with dietary magnesium restriction were expected to upregulate SLC41a1 in their GI tract, gill and kidney relative to the fish fed the control diet or the Mg^{2+}-enriched low magnesium diet. However, a reduction in dietary magnesium (shrimp diet) caused a significant reduction in GI SLC41a1 transcripts relative to control (Figure 12A). Magnesium enriched shrimp recovered transcript levels, implying Mg^{2+} availability was a driving factor of this expression change. This trend was not observed in the gill or kidney, however. The observed GI trend was opposite that of TRPM6 in zebrafish, wherein the channel was upregulated in the GI tract when dietary magnesium was reduced, while the gill and kidney were similarly not affected (Arjona et al. 2013).

In contrast, since excess accumulation of Mg^{2+} is detrimental to teleost development, it was hypothesized *C. auratus* would attempt to minimize renal reabsorption, and active uptake of the ion from their diet and environment by downregulating mRNA transcript levels when faced with elevated dietary magnesium levels. The failure of the $MgCl_2$ enriched commercial pellet diet to

elicit a change in SLC41a1 transcript expression over 4 weeks of feeding relative to the control diet in the gill and GI tract, suggests that the exchanger's mRNA abundance is stable in *C. auratus* presented with sufficient dietary Mg^{2+} (Figures 11A and B). The presented GI and branchial results agree with TRPM6 mRNA expression in the same organs of *D. rerio* fed a 10 fold enriched magnesium diet (relative to control) for 2 weeks, where no changes were observed (Arjona et al. 2013). However, the kidney findings go directly against the trend of TRPM6, in that the channel was downregulated in magnesium-enriched diets in zebrafish, while we observed a ~3fold increase in expression for the high Mg^{2+} diet. This response was not expected under the assumption that SLC41a1 is part of the renal reabsorption pathway, and as such, would either be downregulated or remain stably expressed when fish are presented with excess magnesium, and might suggest that SLC41a1 may not be a part of that pathway. Taken together, SLC41a1 appears to behave opposite TRPM6, as part of an excretory mechanism under dietary manipulation. Specifically, in the kidney, it behaved in a similar manner to the excretory mechanism described for SW reared mefugu, namely, it increased when faced with a higher magnesium load, possibly hinting at an excretory role (Islam et al. 2013). As well, it decreased with decreasing dietary magnesium in the GI tract. If the transporter were secretory, this would be paramount in minimizing magnesium loss to the lumen.

Interestingly, isolated mammalian distal tubule cells have been shown to rapidly (within 1-2 hours) respond to changes in the Mg^{2+} content of their growth media and can rapidly increase or decrease transport accordingly (Dai and Quamme 1991; Dai et al. 1997). Similarly, FW *O. mykiss* rapidly upregulate kidney secretion for the ion in response to magnesium loading (Oikari and Rankin 1985). These short-term rapid changes in transport are too fast to be maintained by transcriptional regulation, and are likely a product of magnesium transporter sensitivity to cellular

concentration. A lack of response of SLC41a1 over the course of digesting a meal for 24hrs suggests that any changes in magnesium absorption over this short time frame (as seen in FW rainbow trout; Bucking et al. 2010) was not influenced through transcriptional regulation (Figures 11A, B and C) but perhaps through post-transcriptional regulation.

5.4 Environmental Changes

Higher temperature is associated with increased metabolic activity (Beamish 1964) and growth, and Mg^{2+} regulates a variety of enzymatic reactions and is required for bone and scale development. Thus, it was hypothesized that as water temperature increased, so would the demand for Mg^{2+}, resulting in increased mRNA transcripts in the ionregulatory organs. While the general trend of SLC41a1 expression was an increase in the GI tract and kidney with temperature, this increase was seemingly lost in fish fed every 2 days (and hence faced with a dietary magnesium restriction; Figures 13A and C). Taken together, these results might point to dietary availability rather than temperature being the driving factor in transcript regulation. This trend is consistent with SLC41a1 being part of a secretory mechanism in the GI tract and kidney, as a reduction in such a mechanism (and the expression of the proteins carrying it out) should result in increased net magnesium absorption to compensate for reduced dietary availability.

Finally, it was hypothesized SLC41a1 transcript level in the gill, GI tract and kidney would increase in fish exposed to IPW for 24 hours, maximizing Mg^{2+} absorption in order to combat the increased ion loss caused by being abruptly transferred to a more hypoosmotic environment. Upon a 2 week exposure, alternatively, expression was expected to go back to near control values, as TJs would be tightened over time, minimizing ion loss (Chasiotis et al. 2009; Kwong et al. 2013). While 24 hour exposure to IPW did not cause a significant change in any of the ion regulatory organs, the general trend observed was an increase in relative abundance at 24 hours of IPW

exposure (Figures 14A, B and C). A lack of response at 24hrs however agrees with the lack of a significant response at 24 hours following feeding (Figure 11A, B and C). Following 2 weeks in IPW, expression was significantly lowered in the GI tract, and returned back to control levels in the gill and kidney. Such downregulation in the GI tract might once again be consistent with SLC41a1 playing a secretory role, as reduction in secretion would be useful in a hypoosmotic environment such as IPW to maximize dietary assimilation of magnesium.

5.5 Hypothesis for SLC41a1 function

Despite the large strides made towards better understanding vertebrate Mg^{2+} transport mechanisms, a large part of which has been work towards characterising SLC41a1, TRPM6 and TRPM7, many questions remain unanswered. One of the main goals of this thesis was to identify key suspected transporters in a stenohaline FW fish and address some of the gaps in our knowledge of how the proteins are regulated when fish are faced with internal (dietary manipulation) and external (temperature and IPW exposure) challenges to their homeostasis. Given the evidence for SLC41a1 having NME function, it was hypothesized that SLC41a1 would fulfil the role of basolateral membrane exchanger in the proposed renal, branchial, and GI absorption mechanisms (similar to the mechanism illustrated in Figure 2A).

Alternatively, SLC41a1 has been suggested to facilitate apical cellular secretion, as observed in the pufferfish kidney (Islam et al. 2013). Interestingly, studies on human SLC41a1 expressed in M7-KO DT-40 cells revealed that the protein localizes to the cell surface, and is continuously internalised by endosomal formation (Mandt et al. 2011). Furthermore, isolated plasma membranes from either the basolateral domain or the apical domain of hepatocytes suggests at least three distinct transporters involved in magnesium transport (Cefaratti et al. 2000). The first was a basolateral Na^{+}-dependent, bidirectional transporter, while the apical membrane

contained two; one that was similar to the basolateral transporter with the exception that it was unidirectional for extrusion and inhibited by amiloride, and a second that was a novel unidirectional Ca^{2+}/Mg^{2+} exchanger (Cefaratti et al. 2000). The amilioride sensitive apical transporter was hypothesized to be SLC41a1, which is in contrast with its role in basolateral magnesium extrusion.

Given the wide range of cellular functions regulated by cytoplasmic magnesium, it stands to reason the vertebrate cell must have a mechanism maintain intracellular magnesium within tight margins and thus may express multiple magnesium transport pathways. The presented findings point to SLC41a1 participating in an apically-associated secretory mechanism, rather than the proposed mammalian absorptive mechanism (summarized in Figure 15). As such, while SLC41a1 may indeed possess NME activity, it may not facilitate basolateral extrusion (carried out by another magnesium transporter), but rather, apical secretion. This hypothesis warrants further studies, which must address the cellular localization of the protein in the different cells of FW fish. Furthermore, it must be uncovered whether or not this apical secretory mechanism relies on the presence of magnesium-concentrating vesicles as the ones proposed in the SW kidney.

Finally, I further propose that SLC41a1 may be a part of a constitutive magnesium regulatory pathway, one that is not regulated in response to immediate changes in magnesium homeostasis, but one that is regulated over long time frames. Along with SLC41a1's ubiquitous expression (even in tissues not known for ion balance regulation), altogether I propose that this suggests that SLC41a1 is a part of a cellular homeostatic pathway that is regulated over long time frames, tasked with maintaining cellular Mg^{2+} levels within a specific intracellular range.

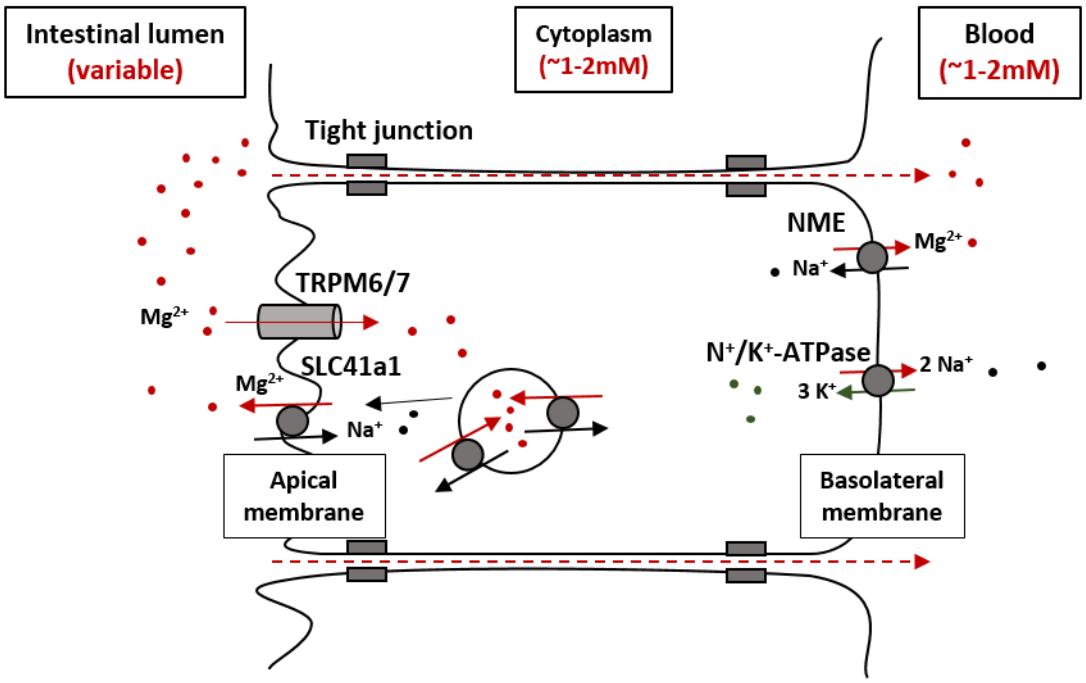

Figure 15: Revised SLC41a1 mechanism. Magnesium is primarily absorbed paracellularly across TJ between enterocytes in FW fish. Transcellular active transport allows for a smaller amount of absorption, with Mg^{2+} entering via TRPM6/7 complexes and being basolaterally extruded via a NME. Finally, excess cellular magnesium is compartmentalized in vesicles by SLC41a1 and transported back into the lumen.

Chapter 3: Potentiometric study of magnesium transport in C. auratus

Introduction

6.1 SIET as a tool for measuring ion transport

The Scanning Ion-selective Electrode Technique (SIET) has been used to calculate the flux of specific ions across tissues kept in an aqueous bath (e.g. Del Duca et al. 2011; Donini and Donnell 2005; Nguyen and Donini 2010). Selective electrodes (manufactured to detect specific ions) and reference electrodes are used to detect changes in ion concentrations in the fluid surrounding the tissue. More specifically, the selective electrode detects the ion concentration as a voltage measurement both near the tissue, and removed from the tissue. Together this gives rise to a flux measurement representative of the magnitude and direction of transport. As such, SIET offers a powerful tool for studying ion transport. It has been extensively used for characterizing $NH4^+$, Na^+, Cl^-, K^+ and H^+ transport across tissues in several insects, including the anal papillae in the common mosquito (*Aedes aegypti*) and the midge (*Chironomous riparius*), (Del Duca et al. 2011; Donini and Donnell 2005). These studies have examined zonation of transport along an organ structure such as the anal papilla on a microscopic scale, and have been used to characterize transport through the application of specific inhibitors (e.g. methazolamide on H^+ and Cl^-) (Nguyen and Donini 2010). SIET has also been successfully used to investigate $NH4^+$, H^+ and Na^+ transport across different areas of the skin in larval *D. rerio*,(Aires et al. 2014; Lin et al. 2006; Shih et al. 2008).

SIET potentially offers a novel technique to study transport across the teleost GI tract and gill. In particular, SIET offers advantages examining transport on fine scales and possibly, using specific ion selective electrodes, for ions that are difficult to study using traditional approached in fish physiology, such as magnesium.

The GI tract of fish and mammals displays extensive zonation in areas such as morphology, function, enzyme activity, and transporter expression. However, despite being the proposed site for both dietary magnesium and calcium absorption, the GI tract has been relatively understudied in terms of region specificity. Mammalian studies have suggested both ions are continuously transported across the entire length of the GI tract, however the distal GI tract (colon and rectum) are the regions with highest activity (Hardwick et al. 1991). Conversely, the stomach appears to display the highest rate of ion absorption in the FW *O. mykiss* (Bucking and Wood 2007). The anterior intestine was implicated in excretion for many ions, likely due to secretions by complimentary organs, while the mid and posterior intestine displayed a variable flux (Bucking and Wood 2007). pH was also observed to differ along the GI tract, with the stomach providing an acidic environment (decreasing in pH immediately post feeding), while all the sections of the intestine were more alkaline (generally increasing pH post feeding) (Bucking and Wood 2009). The differences in acidity must impact ion transport, as they affect how the rate at which ions are dissolved in the fluid phase of chyme (and are therefore available for transport) (Bucking and Wood 2009). TJ composition along the length of the GI tract also varies in a region-specific manner. *O. mykiss* has been particularly well studied, showing differences for a multitude of TJ genes (Kolosov et al. 2014). Claudin 12, implicated in controlling paracellular magnesium transport, is of particular interest, as expression increases along the alimentary canal (lowest in the esophagus and highest in the posterior GI tract) (Kolosov et al. 2014).

Finally, the three magnesium transporters discussed in the molecular introduction, namely, SLC41a1, TRPM6 and TRPM7, are expressed differently along the GI tract in mammals. While TRPM7 was expressed equally along the entire length of the GI tract in both humans and mice, TRPM6 was expressed more highly in the latter regions of the GI tract (Lameris et al. 2015)

corresponding to increased levels of absorption (Hardwick et al. 1991). The general trend of increased mRNA expression further down the alimentary canal was also observed for SLC41a1 (de Baaij et al. 2016; Goytain and Quamme 2005). To the best of my knowledge, there are no papers published on the spatial zonation of the different magnesium transporters in the GI tract of any fish species.

While previously used to measure transport rates (Bijvelds et al. 1996; Bijvelds et al. 1997a; Bijvelds et al. 2001) magnesium radioisotopes are not ideal, as they either have very short half-lives (11.9 seconds and 9.8 minutes for Mg^{23} and Mg^{27}, respectively) or are cost-prohibitive (Mg^{28}) (Beyenbach 2000). While magnesium levels can also be measured using atomic absorption spectrometry on different samples (plasma, chyme, urine, tissues, etc.) to calculate transport rates across different tissues (Edmonds et al. 1991; Grant et al. 1969) such studies are also cost prohibitive, require the use of passive marker in order to control for absorption (Bucking and Wood 2006b; Bucking and Wood 2007; Bucking and Wood 2009), and are time intensive for sample preparation. Given the difficulty to directly measure magnesium transport, the scanning ion-selective electrode technique (SIET) could provide a useful alternative to these methods in piscine physiology. Moreover, not only can it offer opportunities to study ions that are otherwise overlooked for technical reasons, it also offers a chance to study ion transport on a small scale, examining small tissues as well as zonation along micro-axes.

6.2 Hypothesis

Given the evidence for specialization of different segments of the teleost GI tract and previously observed concentrations along the GI tract (Bucking and Wood 2007), it can be hypothesized that magnesium is transported differentially along the GI tract. To this end, a protocol was established to use SIET to measure magnesium fluxes along the serosal (plasma side) and

mucosal (lumen side) of the GI tract from both fed and fasted *C. auratus*. During the development of this technique, transport of magnesium at the gill was also investigated for comparison. Given the assumption that magnesium transport consists of both passive and active transport (Schweigel and Martens 2000), it was assumed magnesium flux would be higher closer to the esophagus, as dietary magnesium would be depleted along the GI tract in fed fish (Bucking and Wood 2007). Furthermore, previous research suggests magnesium uptake by the gill, hence absorptive fluxes were predicted for the gill. Unfortunately, the ionophore used to measure Mg^{2+} (magnesium ionophore II) is also selective for H^+ and Ca^{2+}. To remedy this, H^+ flux was measured along with corresponding Ca^{2+} fluxes. Furthermore, qPCR was used to estimate mRNA transcript levels for SLC41a1 in each GI tract segment, in order to observe if expression of the transporter correlates with the observed magnesium fluxes.

I hypothesized higher fluxes would correlate with higher SLC41a1 expression, as it would be indicative of higher active transport rates. SIET was also used to assess the effects of cobalt(III)-hexaammine chloride (Co3Hex) and ouabain on magnesium, calcium and proton fluxes in the 1st and 8th GI segments, as well as gill. Co3Hex has been reported to act as a magnesium channel inhibitor due to the radius of the molecule (244pm) closely mimicking that of the first hydration shell of Mg^{2+} (250pm). As such, it was hypothesized that it would result in a reduction in magnesium flux in the GI tract and gill, via inhibition of TRPM6/7 and any other channels through which magnesium is taken up by the tissues. Conversely, it was hypothesized to not have any impact on calcium or proton transport as it has not been shown to impact either transporter. Finally, ouabain inhibits NKA activity, and can therefore disrupt sodium gradients. It was therefore hypothesized that it would inhibit transport for calcium and magnesium due to the proposed epithelial extrusion of the ions via NCX1 (a sodium calcium exchanger) and NME (a sodium

magnesium exchanger, possibly carried out by SLC41a1). Reduction of transport for both ions was also expected in the gill (Bijvelds et al. 1998; Hwang et al. 2011). Ouabain was expected to also reduce proton fluxes across all tissues tested as it would interfere with NHE found in the gill and GI tract (Choe et al. 2002; Claiborne et al. 1999; Edwards et al. 1999). Remaining proton fluxes would likely be due to H^+-ATPase activity which is not impacted by ouabain.

Materials and methods

7.1 Animal care, dissections and tissue preparations

C. auratus used were kept in large dechlorinated flow-through tanks at 20^{o}C. They were supplied with constant aeration, and water quality analysis was performed daily. Fed animals were given food 3 hours prior to dissection. All fasted animals were food-deprived for 7-10 days before experimentation.

All tissue incubations and SIET readings were carried out using Cortland's saline (123mM NaCl, 5mM KCl, 1mM $CaCl_2$, 1.9mM $MgSO_4$, 11.9mM $NaHCO_3$, 2.9mM NaH_2PO_4, 5.5m Glucose). 3.8mM MS-222 (Western Chemical Inc, Ferndale, WA USA) was added immediately prior to use in order to minimize muscle contractions of the GI tract and allow for accurate readings. 10mM of 4-(2-hydroxyethyl)-1-piperazineethanesulfonic acid (HEPES) was added to saline used to measure proton (H^+) fluxes for more stable readings. Finally, all saline used was pH balanced to 7.4 with 1N NaOH. All reagents (except MS-222) were purchased from Fisher Scientific Co. Stock saline (lacking MS-222 and HEPES) was kept at ~4^{o}C to minimize microbial growth in the saline. For all treatments, fish were sacrificed through immersion in buffered (pH=7.5; 1 N NaOH) MS-222. Once euthanized, the entire GI tract or gill basket was removed and placed into ice-cold Cortland saline and kept on ice until use.

To determine zonation of transport along the GI tract, the entire GIT was sectioned into 8 identical length segments from anterior-most (1) to posterior-most (8). To perform everted GI readings, the 1st section was sampled and tied to a plastic pipette tip melted onto a thin metal string (working very similar to a glass rod). The segment could then be everted and was subsequently checked under a dissection microscope for tears and damage before use.

Immediately before measurements, the GIT section under observation was pinned using metal insect pins on either side of the tissue into an agar dish and immersed in Cortland saline. 3.8mM MS-222 was added to the Cortland bath in order to minimize muscle contractions of the GI tract and allow for accurate readings. When preparing fasted GI tissues, the individual sections were filled with Cortland saline using a syringe (matching the composition of the serosal bath), after which they were tied at both ends creating a sac. The ends of each section of GI tract from fed animals were tied as to minimize the leak of luminal contents into the bath. In the case of studying zonation, chyme was left within the lumen of the tract. For all other studies involving fed tissues, the chyme was rinsed from the luminal tissue using Cortland. In both cases, SIET readings were taken near the serosal side of the tissues in these preparations. During everted SIET measurements, the serosal side (the inside lining in the case of everted GI preps) was filled with Cortland in a similar manner to fasted sections described above, matching the bath and readings were taken on the mucosal side (on the outside). Any GI tissues not immediately used for measurements were maintained in ice-cold Cortland saline for a maximum of 3 hours, after which they were discarded.

Gill readings were taken by pinning gill arches in agar dishes and covering them in either simple dechlorinated FW, or FW containing 0.1mM ouabain, 0.1mM Co3Hex or both drugs. Readings were taken at the tip of the gill filaments. Tissues were discarded after a maximum of 10 minutes, or in case the tissue began changing colour.

7.2 Scanning ion-selective electrode technique (SIET)

The SIET technique measures the voltage difference between a selective microelectrode and a reference electrode (forming a complete circuit) in a saline bath. While the reference electrode remains immobile in the bulk of the bathing solution, the selective electrode is mounted

on a platform controlled by a 3D micro-stepper motor manipulator (CMC-4; Applicable Electronics, Forestdale, MA). This allows for the microelectrode to sample in a customizable manner, as programmed by the automated scanning electrode technique software (ASET; Sciencewares, East Falmouth, MA, USA). Ultimately, voltage gradients (in μV) are measured between the surface and away from the tissue being studied, which are ultimately used to calculate the ion flux (covered in more detail under the calculations section). Both the selective and reference electrodes are connected to a headstage (by an Ag/AgCl wire holder for the former and Ag/AgCl half-cell for the latter; WPI, Sarasota, FL), which is in turn connected to an ion polarographic amplifier (IPA-2; Applicable Electronics, Forestdale, MA) and outputs data via the ASET software. The technique is covered more extensively by Ngyuen and Donini 2010 and Rheault and O'Donnell 2001.

7.3 Construction and salinization of electrodes

Glass capillaries (model TW150-4; WPI, Sarasota, FL) were pulled on a P-97 Flaming-Brown horizontal micropipette puller (Sutter Instruments, Novato, CA) to a tip diameter of 5–8μm as described in Ngyuen and Donini 2010. First, the microelectrodes were heated to 350^{o}C on a hot plate for 15 minutes. The microelectrodes were then vapour salinized by covering them with a borosilicate dish containing N,N-dimethyltrimethylsilylamine (Fluka, Buchs, Switzerland; ~1μl per electrode) and keeping them at 350^{o}C for an hour. Microelectrodes were then cooled and stored until further use, re-salinizing them every two weeks.

All reference electrodes used for this study were provided by Dr. Andrew Donini. The procedure used to make them is outlined in Nguyen and Donini 2010. Briefly, a borosilicate glass microcapillary (model TW150-4; WPI) was heated at one end to form a 45^{o} bend and filled with 3M KCl solution containing 3% agar.

7.4 Assembly of ion-selective microelectrodes for Mg^{2+}, Ca^{2+} and protons H^{+}

Ion-selective microelectrodes (ISMEs) were constructed in the manner described by Nguyen and Donini 2010 (originally adapted from Smith et al. 1999). Salinized microelectrodes were assembled by adding the appropriate backfill (See below) through a melted-tip syringe via the blunt end of the glass. Air pressure was applied after the backfill was added to ensure lack of air pockets and gaps in the microelectrode. Finally, a second melted tip syringe was used to add the appropriate ionophore (See below) by forming a small bubble and front-filling the microelectrode for a total of 100-150nm column length. Finally, the magnesium and calcium selective microelectrodes were briefly dipped in tetrahydrofuran-dissolved polyvinyl chloride (Fluka, Buchs, Switzerland) as described by Rheault and O'Donnell 2004.

Magnesium-selective electrodes contained Magnesium II ionophore cocktail (Fluka Chemical Co., Ronkonkoma, NY, USA) and were backfilled with 100mM $MgCl_2$. Magnesium microelectrodes were then calibrated using 1mM and 10mM $MgCl_2$ solutions, obtaining an average slope of 29.741 ± 0.254 (average ± s.e.m.; n=26).

Calcium-selective microelectrodes contained Calcium II ionophore cocktail (Fluka Chemical Co., Ronkonkoma, NY, USA) and had a 100mM $CaCl_2$ backfill. The calibration solutions used were 1 and 10mM $CaCl_2$ solutions, giving an average slope of 31±1.2 (n=25).

Finally, the proton microelectrodes contained H^{+} Ionophore I Cocktail B with a 100mM NaCl/100 mM sodium citrate backfill (buffered to pH 6.0). These microelectrodes were not dipped in PVC (it would interfere and prevent near-Nernstian slope from being achieved) and were

calibrated using pH7 and pH10 calibration solutions (Sartorius Stedim North America Inc., Bohemia, NY, USA) giving a slope of 52.862 ± 0.421 (n=15).

7.5 Effects of cobalt(III)-hexaammine chloride and ouabain on the SIET measured Mg^{2+}, Ca^{2+} and H^{+} fluxes at the serosal and mucosal sides of the 1st and 8th GI segments, as well as at the gill

Co3Hex has been reported to act as a magnesium channel inhibitor due to the radius of the molecule (244pm) closely mimicking that of the first hydration shell of Mg^{2+} (250pm). As such, it was introduced in Cortland's saline at a 10^{-4}M concentration at the mucosal and serosal sides of the 1st GI segment and fresh water for the gill in order to test how it would impact SIET readings for Mg^{2+}, Ca^{2+} and H^{+} fluxes.

Similarly, ouabain has been extensively used as an inhibitor of active transport, due to its effect on NKA activity. The currently accepted molecular mechanism for GI basolateral extrusion of magnesium has linked Mg^{2+} and Na^{+} transport via SLC41a1. As such the effects of 10^{-4}M ouabain (Shuttleworth et al. 1978) were also tested at the same tissues as Co3Hex. Finally, potential synergistic effects of the 2 chemicals were tested by repeating the experiment with both present in the saline or water.

7.6 Concentration gradient and flux calculations

The voltage gradient ASET readings obtained were converted into ion concentration gradients with the following formula (described in Donini and Donnell 2005 and Rheault and O'Donnell 2004):

$$_{\Delta}C = C_B \times 10^{(\Delta V/S)} - C_B,$$

where $_{\Delta}C$ is the concentration gradient between the "at" and "away" points (recorded in µmol $l^{-1}cm^{-3}$), C_B is the background ion concentration (recorded in µmol l^{-1}), $_{\Delta}V$ is the voltage gradient (µV) and S is the slope of the electrode over a 10 fold difference in ion concentration. For all

experiments in this thesis, the "at" point was ~5-10µm away from the surface of the epithelium being recorded, while the "away" reading was ~200µm outward (into the bath).

Positive values measured at the serosal surface and negative values measured at the mucosal surface of GI preps indicate transepithelial movement of ions indicative of GI absorption (i.e. ions are taken from the lumen/mucosa and transported across to the bloodstream/serosa). Negative values measured at the gill surface indicate ions being taken up by the gill from the bath. The opposite relationship is also true.

This formula works under the assumption that the ion activity coefficient is the same in both the calibration solution and the experimental solutions. The obtained slope (S) from the calibration solutions should be near-Nernstian. In the case of a 10 fold concentration change it should have an approximate slope of 29 for divalent ions (like Mg^{2+} and Ca^{2+}) and 58 for monovalent ions (like H^{+}).

Ultimately, $_{\Delta}C$ can be converted into flux using Fick's law of diffusion:

$J_I = D_I (_{\Delta}C) / _{\Delta}X,$

where J_I is the net flux (measured in pmol cm^{-2} hr^{-1}), D_I is the diffusion coefficient of the measured ion ($1.19x10^{-5}$ cm^2 s^{-1} for Ca^{2+}; $7.1x10^{-6}$ cm^2 s^{-1} for Mg^{2+}; $9.4x10^{-5}$ cm^2 s^{-1} for H^{+}) and $_{\Delta}X$ is the distance between the two points measured in cm.

Any measurements taken in HEPES-containging saline were adjusted appropriately for the change in buffering capacity (as described in Donini and O'Donnell 2005) with the following equation:

$J_I = [(D_H+D_I)B_H] X (_{\Delta}C/_{\Delta}X),$

where D_H is the diffusion coefficient of HEPES ($6.2x10^{-6}$ cm^2 s^{-1}) and B_H is the buffering capacity of HEPES obtained as

$B_H = (C_H/C_B) \times [F/(1+F)^2]$,

where C_H is the HEPES concentration (mol^{-1}) and F is calculated from

$F=\log_{10}(pK_{aH}) / CB$,

where $\log_{10}pK_{aH}$ is the dissociation constant of HEPES.

7.7 Chyme magnesium concentration

ISMEs were used to estimate the magnesium concentration in chyme obtained from different segments along the GI tract (anterior, mid and posterior third). Chyme was collected and pooled from 5 different fish, oven-dried (12 hours at 60^{o}C) and re-suspended in distilled water (1 g ml^{-1}). Chyme samples were measured using the same methodology explained in the previous chapter.

7.8 Gastrointestinal zonation of SLC41a1

In order to test the relative abundance of SLC41a1 mRNA transcripts along the *C. auratus* GI tract, fish were kept at 20^{o}C and fed daily for 2 weeks. Subsequently, they were dissected under a microscope, with their GI tract being separated into 8 equal length segments starting at the esophagus and finishing at the rectum. RNA extraction, cDNA synthesis, and qPCR were performed as described previously.

7.9 Statistics

SIET flux zonations were analyzed with a Two-Way repeated measures ANOVA followed by a Holm-Sidak test. SLC41a1 expression along the GI tract was compared using a One-Way ANOVA followed by a Tukey test. Transport kinetics were compared using repeated measures One-Way ANOVA followed by a Bonferroni test, followed by a linear regression. Finally, the non-everted and everted GI tract sacs and gill SIET measurements were analyzed using a repeated measures One-Way ANOVA followed by a Holm-Sidak test.

All statistical tests were carried out in SigmaPlot 11, with the specific post-hoc test used being recommended by the software for each experiment.

Results

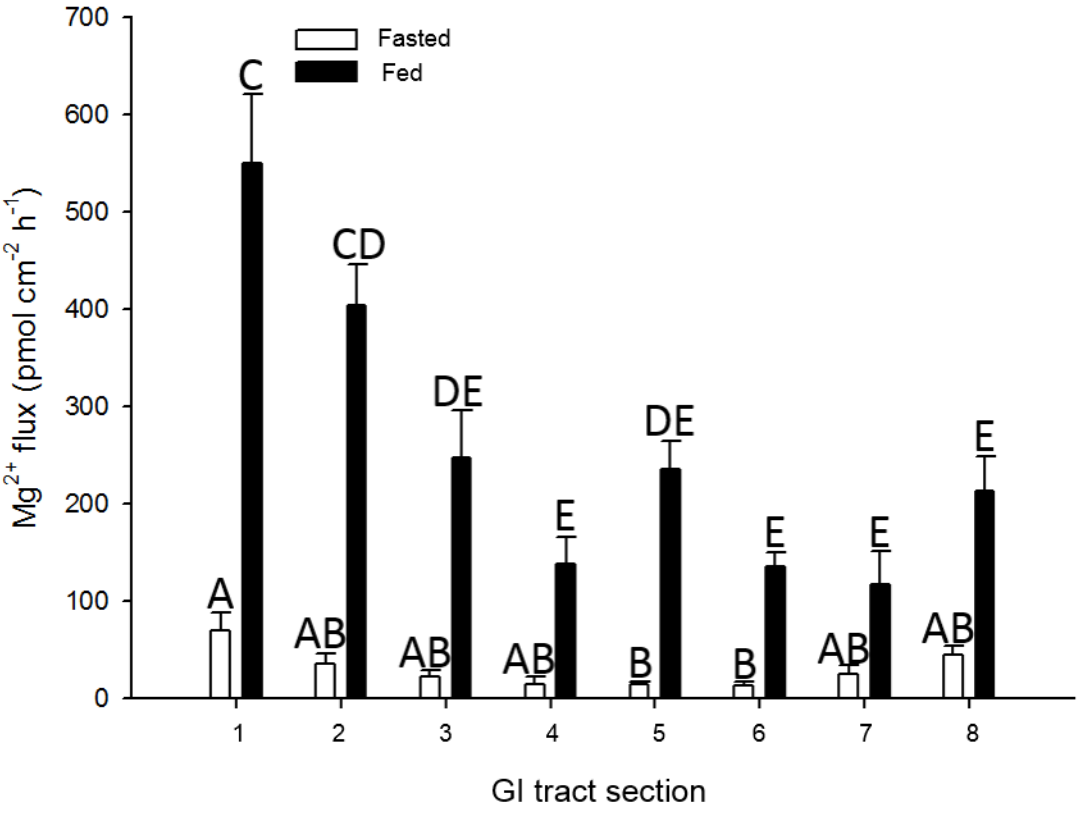

Figure 16: Mg^{2+} flux zonation along the GI tract. Magnesium flux was measured along the goldfish GI tract for both fed and fasted animals using SIET. The GI tract was divided into 8 equal length segments. A two-way repeated measures ANOVA followed by a Holm-Sidak test for pairwise comparisons was used to compare the different regions. Positive numbers indicate serosal secretion. Data shown is the average flux ± s.e.m. (n=5-7). Different letters indicate significant difference ($p<0.05$).

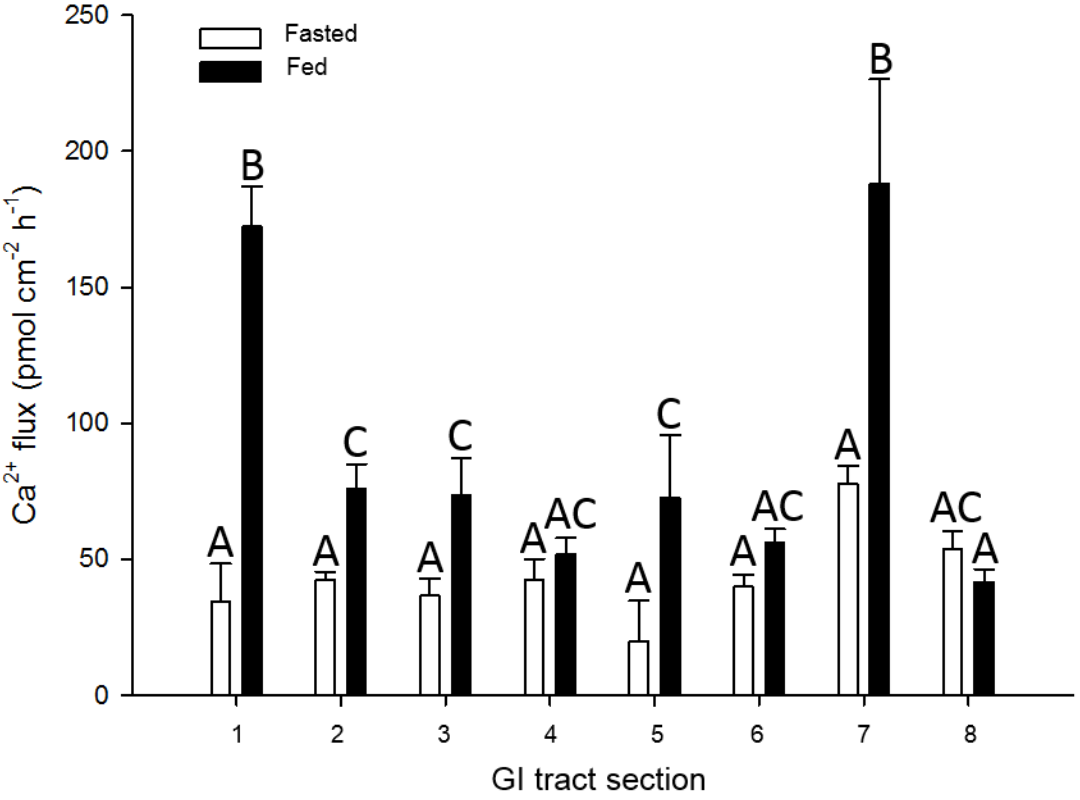

Figure 17: Ca^{2+} flux zonation along the GI tract. Calcium flux was measured along the goldfish GI tract for both fed and fasted animals using SIET. The GI tract was divided into 8 equal length segments. Positive numbers indicate serosal secretion. A two-way repeated measures ANOVA followed by a Holm-Sidak test for pairwise comparisons was used to compare the different regions. Data shown is the average flux ± s.e.m. (n=4). Different letters indicate significant difference ($p<0.05$).

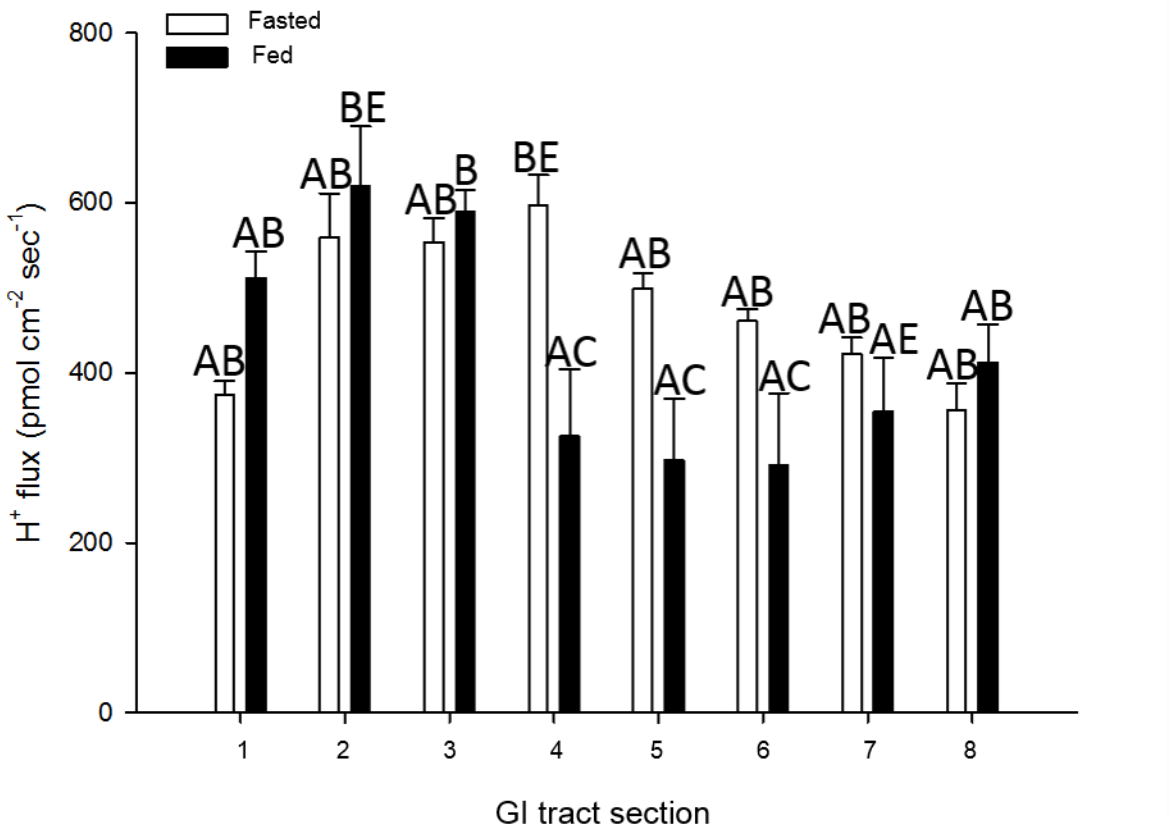

Figure 18: H^+ flux zonation along the GI tract. Proton flux was measured along the goldfish GI tract for both fed and fasted animals using SIET. The GI tract was divided into 8 equal length segments. Positive numbers indicate serosal secretion. A two-way repeated measures ANOVA followed by a Holm-Sidak test for pairwise comparisons was used to compare the different regions. Data shown is the average flux ± s.e.m. (n=4). Different letters indicate significant difference ($p<0.05$).

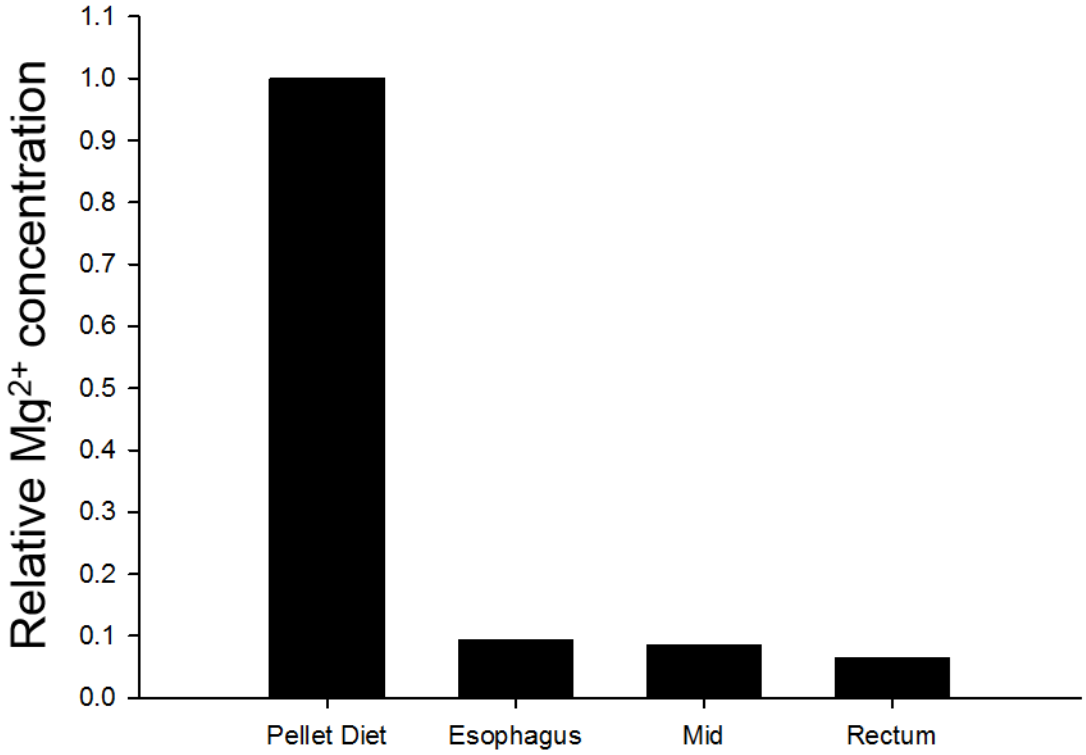

Figure 19: Relative Mg^{2+} chyme concentration. Mg^{2+} concentration in chyme samples from different segments along the intestine relative to the pellet diet the fish were fed. Samples were pooled from 5 fish and over dried. Samples were then suspended in ddH_2O (ml per g of dry weight) and quantified for Mg^{2+} content using ISMEs.

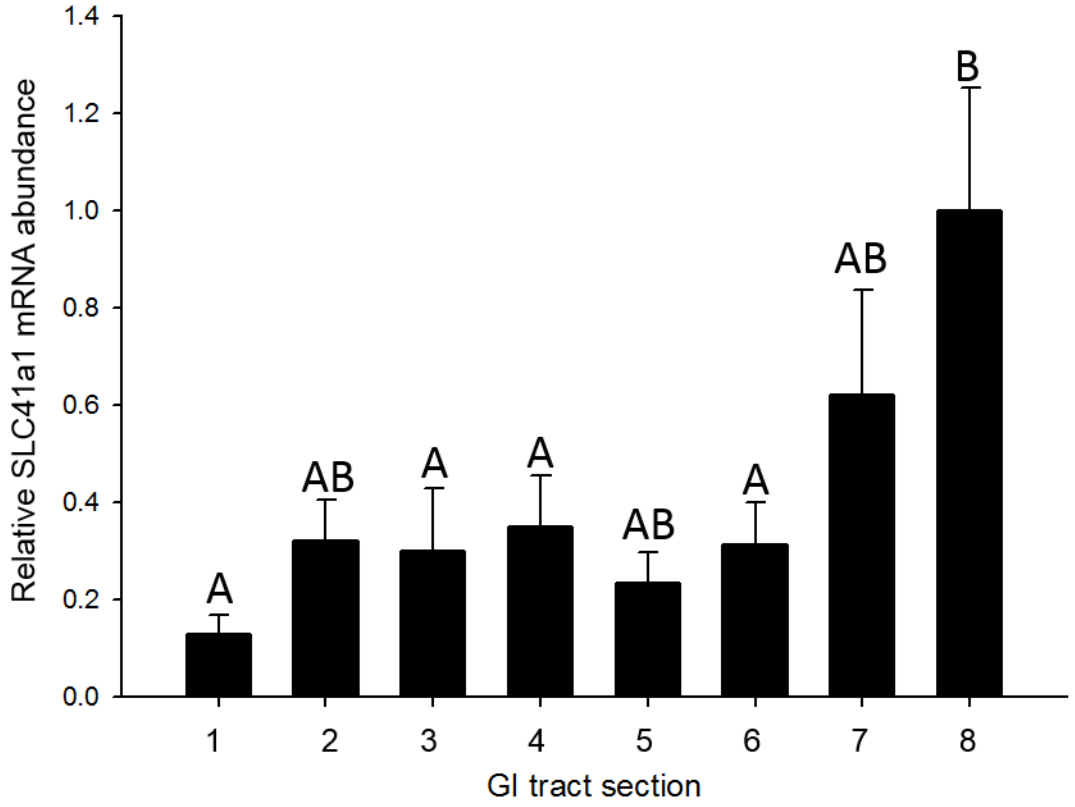

Figure 20: SLC41a1 expressional zonation along the GI tract. Relative mRNA SLC41a1 transcripts along 8 equal length segments in the GI tract of daily fed goldfish. A one-way ANOVA followed by a Tukey test was used to compare the different treatments (n=6-7). Data shown is the average relative (to the 8th segment) expression ± s.e.m. (n=4). Different letters show significance ($p<0.05$).

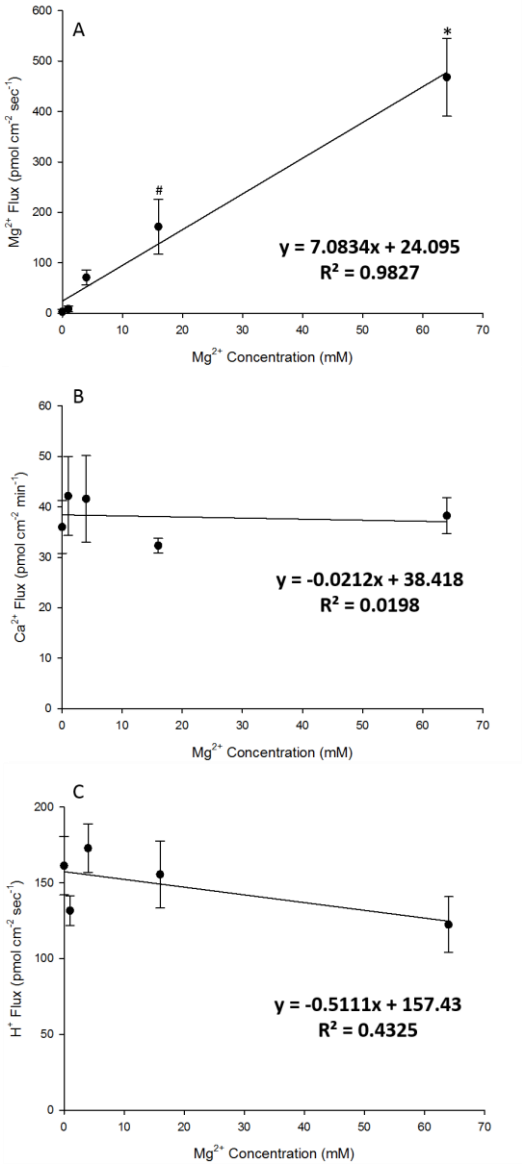

Figure 21: Mg^{2+} transport kinetics. Effect of application of Cortland's saline containing 0-64mM $MgSO_4$ to **the mucosal** side of fasted *C. auratus* 1st GI segments on the Mg^{2+} (A), Ca^{2+} (B) and H^+ (C) flux measured with SIET. All the different concentration Cortland's used as fill and the bathing Cortland's saline were all kept equimolar with the addition of meglumine (pH=7.4). All readings were taken at the serosal side. Positive flux numbers indicate ion movement from the mucosal to serosal surface of the 1st GI segments. Data shown is the average of the observed flux ± s.e.m. of n=4 (each from a distinct individual fish). A repeated measures one-way ANOVA was carried out for each individual ion, with only Mg^{2+} resulting in $p<0.05$ (* indicates statistical significance from 0-16mM concentrations; # indicates significant difference from 0-1mM concentrations; as determined by a post-hoc Bonferroni pairwise comparison resulting in $p<0.0125$).

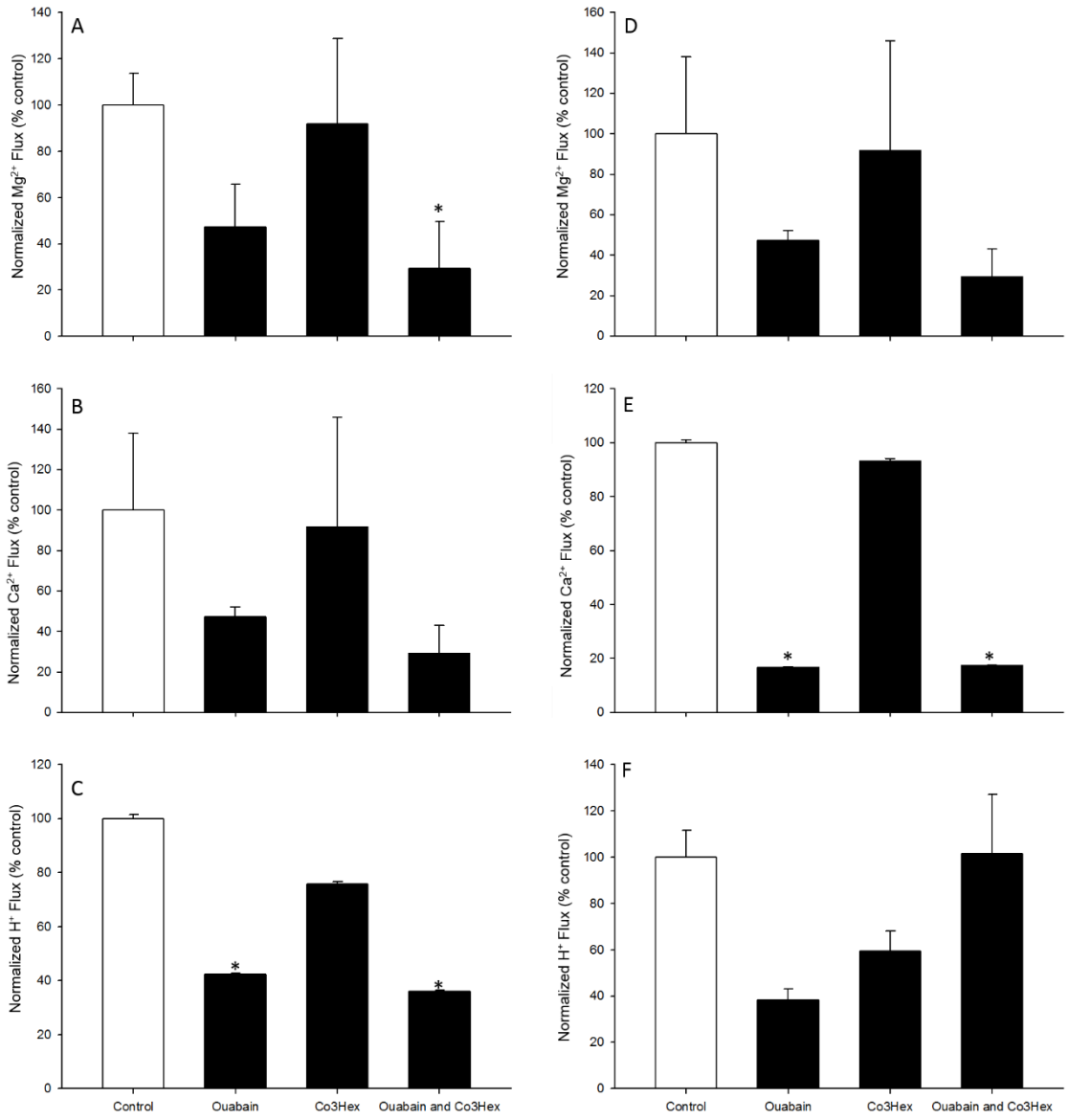

Figure 22: Serosal Mg^{2+}, Ca^{2+} and H^{+} flux in response to serosally applied drugs at the 1st and 8th GI segments. Effect of application of Cortland's saline containing 0.1mM ouabain, 0.1mM Co3Hex or both drugs at the same time to **the serosal side** of 1st (A, B, C) and 8th (D, E, F) GI tract segments from fasted *C. auratus* filled with regular Cortland's (control) on the Mg^{2+} (A, E), Ca^{2+} (B, E) and H^{+} (C, F) flux measured with SIET. Values are relative to the control treatment (regular Cortland's). The salines used on both sides of the tissues were buffered with 10mM HEPES (pH=7.4). All readings were taken at the serosal side. Positive flux numbers indicate ion movement from the mucosal to serosal surface of the 1st GI segments. Data shown is the average of the observed flux ± s.e.m. of n=4 (each from a distinct individual fish). A repeated measures one-way ANOVA was carried out for each ion; in case of $p<0.05$, a post-hoc Holm-Sidak test was used to compare individual treatments to the control (* indicates significant difference from control).

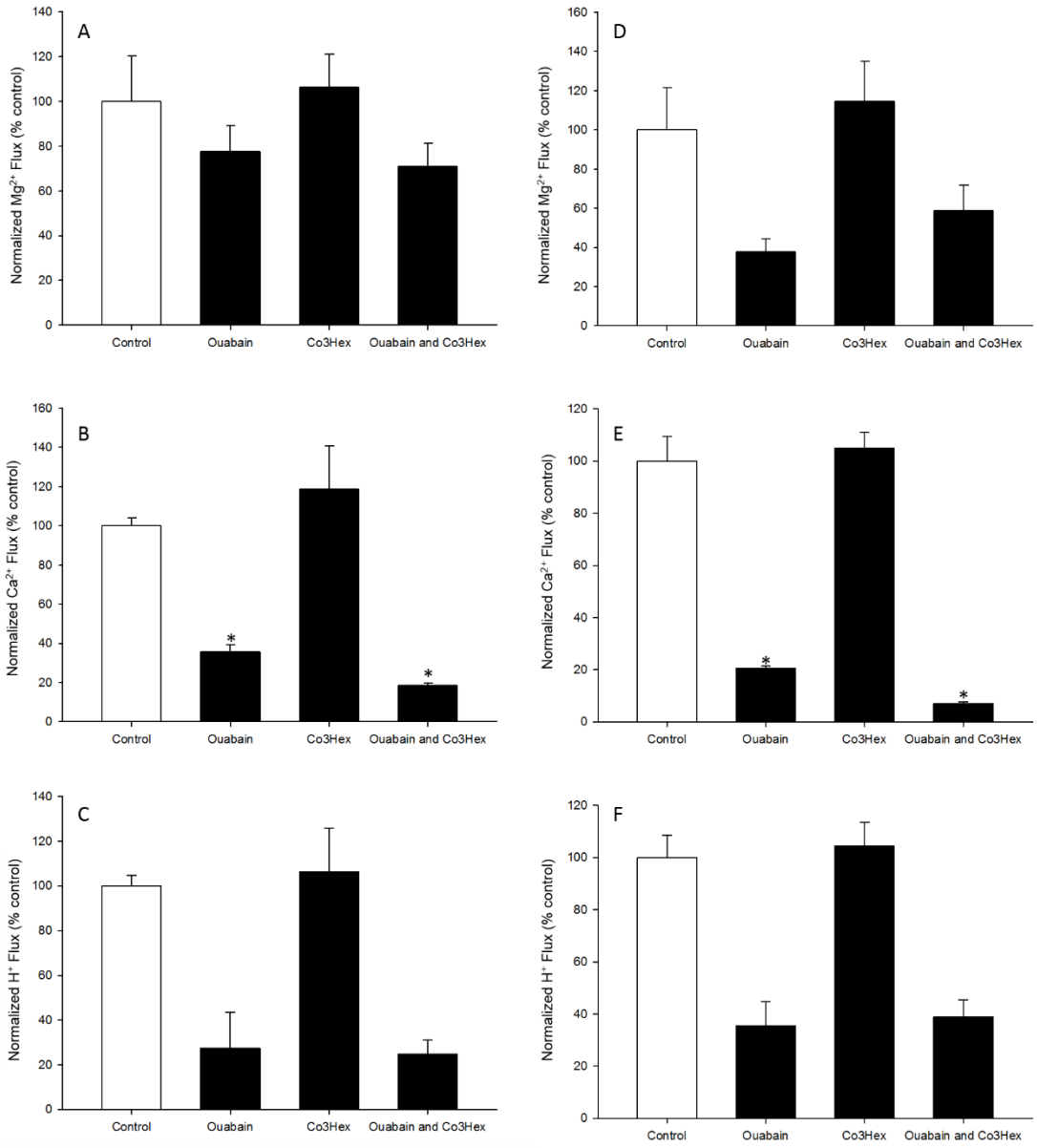

Figure 23: Serosal Mg^{2+}, Ca^{2+} and H^{+} flux in response to mucosally applied drugs at the 1st and 8th GI segments. Effect of application of Cortland's saline containing 0.1mM ouabain, 0.1mM Co3Hex or both drugs at the same time to **the mucosal side** of 1st (A, B, C) and 8th (D, E, F) GI segments from fasted *C. auratus* placed in regular Cortland's (control) on the Mg^{2+} (A, E), Ca^{2+} (B,E) and H^{+} (C,F) flux measured with SIET. Values are relative to the control treatment (regular Cortland's). The salines used on both sides of the tissues were buffered with 10mM HEPES (pH=7.4). All readings were taken at the serosal side. Positive flux numbers indicate ion movement from the mucosal to serosal surface of the 8th GI segments. Data shown is the average of the observed flux ± s.e.m. of n=4 (each from a distinct individual fish). A repeated measures one-way ANOVA was carried out for each ion; in case of $p<0.05$, a post-hoc Holm-Sidak test was used to compare individual treatments to the control (* indicates significant difference from control).

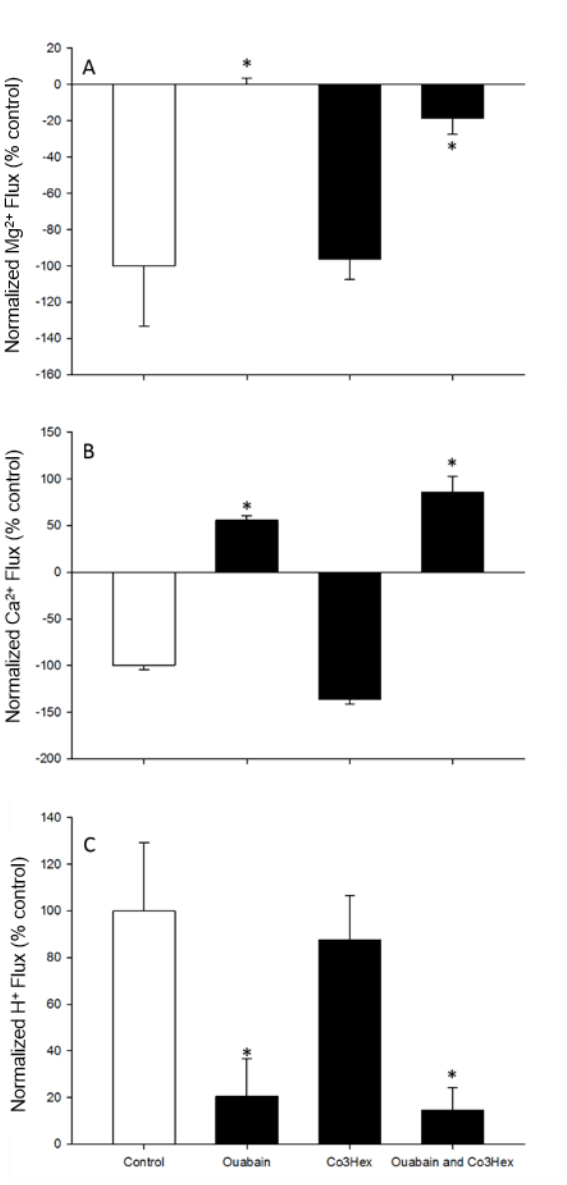

Figure 24: Mucosal Mg^{2+}, Ca^{2+} and H^{+} flux in response to serosally applied drugs at everted 1st GI segments. Effect of application of Cortland's saline containing 0.1mM ouabain, 0.1mM Co3Hex or both drugs at the same time to **the serosal side** of everted 1st GI segments from fasted *C. auratus* placed in regular Cortland's (control) on the Mg^{2+} (A), Ca^{2+} (B) and H^{+} (C) flux measured with SIET. Values are relative to the control treatment (regular Cortland's). The salines used on both sides of the tissues were buffered with 10mM HEPES (pH=7.4). All readings were taken at the mucosal side. Positive flux numbers indicate ion movement from the mucosal to serosal surface of the 1st GI segments, and vice versa. Data shown is the average of the observed flux ± s.e.m. of n=4 (each from a distinct individual fish). A repeated measures one-way ANOVA was carried out for each ion; in case of $p<0.05$, a post-hoc Holm-Sidak test was used to compare individual treatments to the control (* indicates significant difference from control).

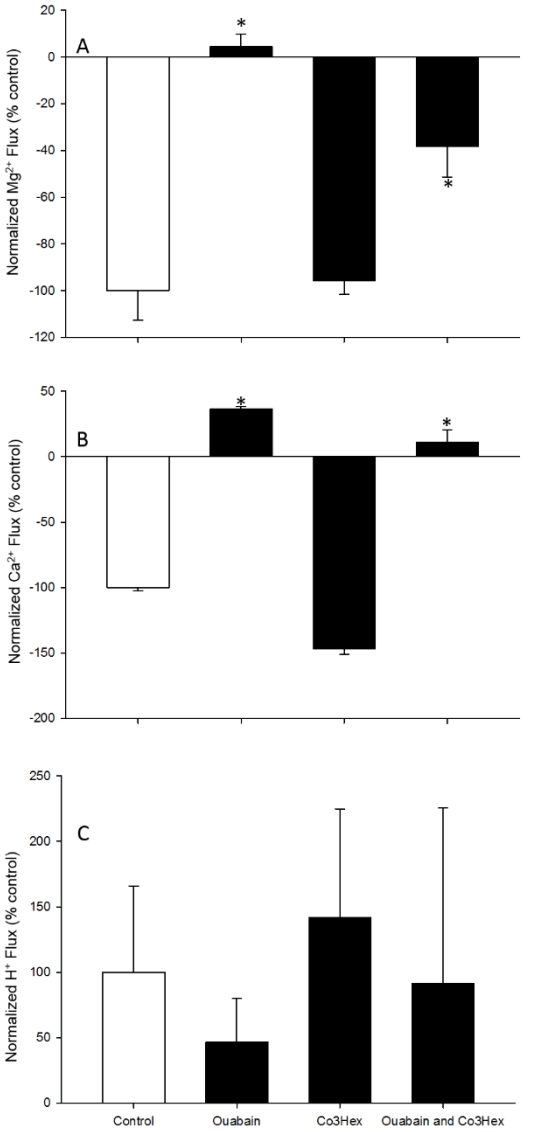

Figure 25: Mucosal Mg^{2+}, Ca^{+} and H^{+} flux in response to mucosally applied drugs at everted 1st GI segments. Effect of application of Cortland's saline containing 0.1mM ouabain, 0.1mM Co3Hex or both drugs at the same time to the bathing solution at **the mucosal side** of everted 1st GI segments from fasted *C. auratus* filled with regular Cortland's (control) on the Mg^{2+} (A), Ca^{2+} (B) and H^{+} (C) flux measured with SIET. Values are relative to the control treatment (regular Cortland's). The salines used on both sides of the tissues were buffered with 10mM HEPES (pH=7.4). All readings were taken at the mucosal side. Positive flux numbers indicate ion movement from the mucosal to serosal surface of the 1st GI segments, and vice versa. Data shown is the average of the observed flux ± s.e.m. of n=4 (each from a distinct individual fish). A repeated measures one-way ANOVA was carried out for each ion; in case of $p<0.05$, a post-hoc Holm-Sidak test was used to compare individual treatments to the control (* indicates significant difference from control).

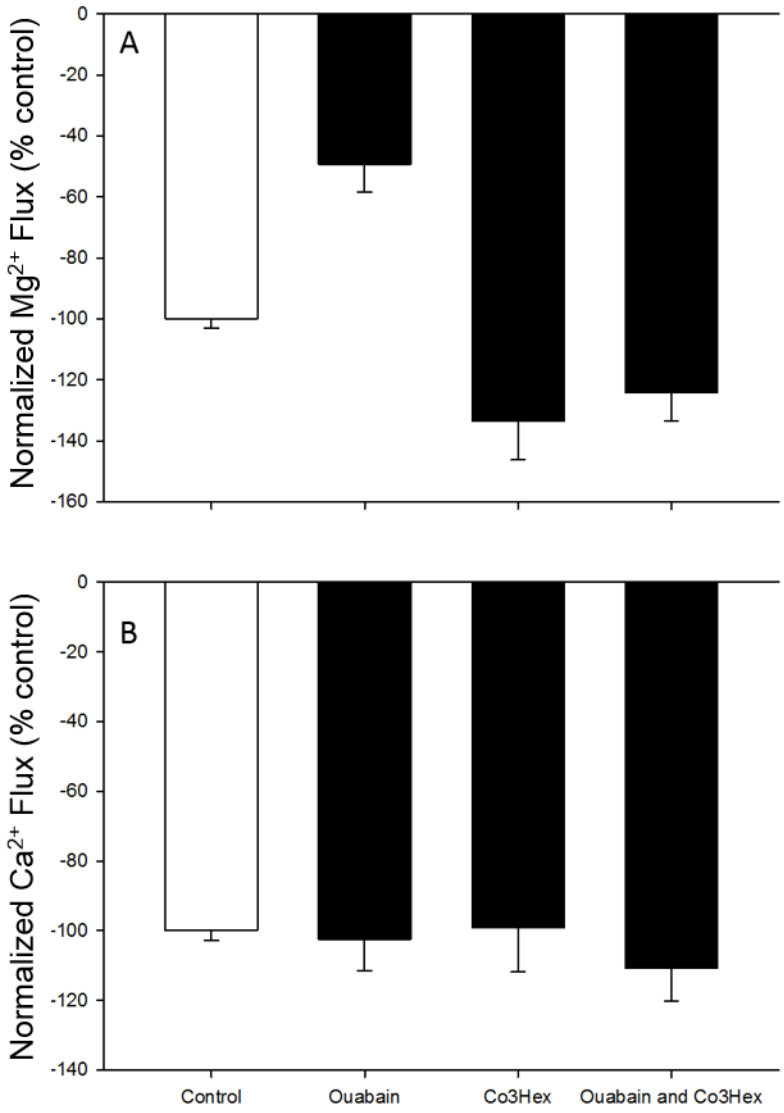

Figure 26: Branchial Mg^{2+}, Ca^{2+} and H^+ flux in response to drugs. Effect of application of 0.1mM ouabain, 0.1mM Co3Hex or both drugs at the same time to the bathing solution (dechlorinated FW) of *C. auratus* gill arches on the Mg^{2+} (A) and Ca^{2+} (B) measured with SIET relative to the control treatment (fresh water). All readings were taken at individual gill filament tips. Negative flux numbers indicate ion movement from the FW into the gill filaments. Data shown is the average of the observed flux ± s.e.m. of n=4 (each from a distinct individual fish). A repeated measures one-way ANOVA was carried out for each ion; in case of $p<0.05$, a post-hoc Holm-Sidak test was used to compare individual treatments to the control (* indicates significant difference from control).

8.1 Gastrointestinal zonation

Magnesium flux zonation was higher in all of the segments measured for fed fish, relative to those in fasted fish (Figure 16). Flux was highest at the 1st GI segment of fed fish (550±70 pmol $cm^{-2}hr^{-1}$) different from all other fed segments excluding the 2nd (404±41 pmol $cm^{-2}hr^{-1}$) (Figure 16). Within fed fish, the 2nd segment was different from the 4th (138±27 pmol $cm^{-2}hr^{-1}$), 6th (135±14 pmol $cm^{-2}hr^{-1}$) and 8th segment (212±36 pmol $cm^{-2}hr^{-1}$) (Figure 16). The fed 3rd (246±48 pmol $cm^{-2}hr^{-1}$) and 5th (234±29 pmol $cm^{-2}hr^{-1}$) segments were not different from any other fed segments, except for the 1st (Figure 16). The only difference within the fasted fish was between their 1st (69±17 pmol $cm^{-2}hr^{-1}$), 5th (14±7 pmol $cm^{-2}hr^{-1}$) and 6th (13±3 pmol $cm^{-2}hr^{-1}$) segments (Figure 16).

Calcium flux zonation followed a different pattern, wherein the 1st (172±14 pmol $cm^{-2}hr^{-1}$) and 7th (187±38 pmol $cm^{-2}hr^{-1}$) segments in fed fish showed the highest values, with the remainder of fed segments being lower and not different from one another (ranging from 51±6 pmol $cm^{-2}hr^{-1}$ at the 5th to 75±8.9 pmol $cm^{-2}hr^{-1}$ at the 2nd segment) (Figure 17). Finally, the 8th segment in fed fish had the lowest flux at 41±4.8 pmol $cm^{-2}hr^{-1}$. In fasted fish, the individual segments were not significantly different from one another, ranging from 77±6.6 pmol $cm^{-2}hr^{-1}$ at the 7th segment to 19.9±14 pmol cm^{-2} hr^{-1} at the 5th segment (Figure 17). Between the two treatments, fed 1st and 7th segments were different from all fasted segments, while the 2nd and 3rd and 5th segments were different from all fasted segments except for the 8th. Finally, the 4th, 6th and 8th segments were not different from any of the fasted segments (Figure 17).

The pattern of proton flux zonation was different from either of the divalent ions (Figure 18). The fed 2nd (619±70 pmol $cm^{-2}s^{-1}$) and 3rd (588±65 pmol $cm^{-2}s^{-1}$) segments and fasted 4th segment (597±35 pmol $cm^{-2}s^{-1}$) were all different from the fasted 4th (325±78 pmol $cm^{-2}s^{-1}$), 5th

(296±72 pmol $cm^{-2}s^{-1}$) and 7th (290±85 pmol $cm^{-2}s^{-1}$) (Figure 18). Furthermore, the fed 3rd segment was different from the fed 7th (354±63 pmol $cm^{-2}s^{-1}$) segment.

Chyme was also assessed for its Mg^{2+} concentration. Relative to food pellets, the measured concentration was highest at the anterior GI tract (9.29%), followed by the mid GI tract (8.5%) and lowest at the distal GI tract (6.4%) relative to the pellet diet (Figure 19).

Finally, the relative expression of SLC41a1 was highest at the 8th segment and lowest at the 1st segment (Figure 20). The 1st, 3rd, 4th and 6th segments were all significantly different from the 8th segment, ranging from 12.9% at the 1st, up to 34.8% at 4th (relative to the 8th) and there is a general increase in expression at the latter GI segments (Figure 20).

8.2 Mg^{2+}, Ca^{2+} and H^{+} transport kinetics with increasing luminal magnesium concentration

Mg^{2+}, Ca^{2+} and H^{+} were measured on the serosal side of tied 1st GI tract segment sacs filled with Cortland's saline with $MgSO_4$ concentration of 0, 1, 4, 16 and 64mM (Figures 21A, B and C, respectively). To ensure the saline on the mucosal and serosal sides of the tissue were equimolar, all solutions were equalized by adding appropriate concentrations of meglumine. The order of concentrations used to fill the preps was randomized for all three ions. Running a one-way repeated measures ANOVA showed that only magnesium flux responded to changes in the mucosal concentrations of Mg^{2+} ($p<0.05$). Magnesium flux at 64mM Mg^{2+} (468 pmol cm^{-2} sec^{-1} ± 77.15) was significantly elevated from all other concentrations (Bonferroni comparison; $p<0.0125$) (Figure 21A). Magnesium flux was also significantly different at 16mM (171 pmol cm^{-2} sec^{-1} ± 54.35) from the 0 and 1.9 mM concentrations (3.11 pmol cm^{-2} sec^{-1} ± 4.8 and 8.48 pmol cm^{-2} sec^{-1} ± 5.55, respectively), but not from the 4mM prep (71.08 pmol cm^{-2} sec^{-1} ± 14.64) (Figure 21A). The magnesium kinetics strongly fit a linear regression model, with the regression line having a y-intercept of 24.095 and a slope of 7.08. The R^2 value for the regression was 0.9827, meaning the

increasing Mg^{2+} concentration accounted for 98.27% of the observed variability in flux (Figure 21A).

Ca^{2+} and H^{+} fluxes showed no difference at different magnesium concentrations ($p>0.05$) (Figures 21B and C). Neither fit the linear regression model well, with a slope of -0.02 and -0.05, and a y-intercept of 38.4 and 157.4 for Ca^{2+} and H^{+} respectively (Figures 21B and C). The respective R^2 values were 0.019 and 0.43, implying the observed variability in flux could not be well explained with the increase in Mg^{2+} concentration (Figures 21B and C).

8.3 Ion fluxes at non-everted 1st and 8th GI segments

All fluxes for the divalent ions in all of the non-everted tissue preparations were positive, indicative of ion transport from the mucsoal surface to the serosal surface, or GI absorption (Figures 22 and 23). Proton fluxes were also positive, indicative of proton enrichment at the serosal surface (Figure 24). For magnesium fluxes, a significant reduction (to 29%) was observed when ouabain and Co3Hex was applied to the serosal side of the 1st GI segments only (Figure 22A). All other treatments had no significant effect on magnesium transport (Figures 22A and D and Figures 23A and D). In contrast, calcium fluxes were significantly reduced at the 8th segment when ouabain or ouabain + Co3Hex chloride was applied to either the serosal or mucosal side (Figures 22E and 23E). Co3Hex had no effect on calcium transport in either tissue, when applied to either side (Figures 22B and E and Figures 23B and E) suggesting the decrease when both drugs were applied is due to ouabain alone. Ouabain also decreased calcium fluxes at the 1st GI segments, but only when applied to the mucosal side of the preparation (Figure 23B). Proton fluxes at the 8th segment were unaffected by drug application to either the serosal (Figure 22F) or mucosal side of the preparation (Figure 23F). The drugs also did not affect proton fluxes at the 1st GI segments when applied to the mucosal side of the preparation (Figure 23C), however there was a significant

reduction in proton fluxes when ouabain and ouabain + Co3Hex were applied to the serosal side (Figure 22C). Again, a lack of impact of Co3Hex alone in this preparation suggests this decrease in due to ouabain alone.

8.4 Ion fluxes at everted 1st GI segment

The negative fluxes of divalent ions observed at the mucosal surface for everted tissues in the control treatment (regular saline) is indicative of ion absorption from the mucosal to the serosal side of the GI tract (Figures 24 and 25). In everted 1st GI segment preparations, ouabain reversed magnesium flux (to 0.5%) when applied to the mucosal side (in the bathing solution) and the serosal side (in the saline filling of the everted tissue; to 4.5%) (Figures 24A and 25A). The simultaneous addition of ouabain and Co3Hex reduced the flux significantly to 18% when applied to the mucosal bath and 38% when applied to the inside of the everted tissues (Figures 24A and 25A). Similarly, calcium fluxes were reversed in preparations containing ouabain, going up to 18 and 36% when applied to the saline and inside of the everted tissues, respectively (Figures 24B and 25B). Furthermore, calcium fluxes were also reversed when both drugs were present, going up to 22% when applied on the mucosal and 11% when applied on the serosal side (Figures 24B and 25B). Proton fluxes decreased with ouabain (to 42%) and both drugs (to 29%) when applied to the serosal side of the everted tissues, but not the mucosal surface (Figures 24C and 25C). Once again, Co3Hex failed to induce significant changes in any of the fluxes in everted 1st GI segments, regardless of the surface it was applied to (Figures 24C and 25C).

8.5 Ion transport in the gill

Both the magnesium and calcium fluxes measured at the gill were negative for the control treatment (gills in FW), indicative of transport from the FW bath into the tissue for both ions (Figures 26A and B). Proton flux was positive, indicative of secretion (not pictured). However,

neither ouabain or Co3Hex, nor both drugs added simultaneously to the FW bath in which the gills were kept caused a significant reduction in the flux of either Ca^{2+} or Mg^{2+} (Figures 26A and B).

Discussion

9.1 Overview

One of the major hurdles in our understanding of magnesium transport is the lack of appropriate magnesium radioisotopes, as the available ones either have very short half-lives (11.9 seconds and 9.8 minutes for Mg^{23} and Mg^{27}, respectively) or are cost-prohibitive (Mg^{28}) (Beyenbach 2000). Traditional approaches to studying magnesium have included everted GI tract sacs (e.g. Hardwick et al. 1990; Karbach et al. 1991), suggesting GI absorption is largely passive and paracellular, as well as plasma membrane preparations (e.g. Bijvelds et al. 1996; Bijvelds et al. 1997a; van der Velden et al. 1990) pointing to a secondary active, Na^+-dependent and ouabain-sensitive transcellular absorptive mechanism. Both of these approaches require isotopes that are barriers to research, as well GI tract sac approaches require large animals to obtain appropriate tissues for experimentation limiting the usefulness of the approach from a comparative aspect. Ultimately, alternative methodologies can be beneficial to the field of teleost magnesium transport, opening up comparisons between species that would otherwise not be possible with traditional approaches.

9.2 Zonation

The observed Mg^{2+} flux zonation of fed fish (Figure 16) was consistent with the observed Mg^{2+} chyme concentration (Figure 19), in that both decreased along the GI tract's length, although chyme concentrations only marginally so. A similar trend was observed in rats, where the proximal intestine displayed higher rates of magnesium transport compared to the distal intestine at high magnesium concentrations in the lumen (Lameris et al. 2015). Interestingly this zonation in transport was not detected lower luminal magnesium concentrations (Lameris et al. 2015) suggesting two transport pathways operating a different luminal magnesium concentrations. Fasted fish exhibited lower flux rates compared to their fed counterparts, likely due to the large

loss of passive transport associated with lower luminal Mg^{2+} concentrations when lacking digesta, and also displayed a lack of zonation at this lower concentration. This corresponds nicely to the mammalian data (Lameris et al. 2015).

Conversely, SLC41a1 transcript level was highest at the 8th segment, similar to observations in rats (Figure 20) (Kolisek et al. 2008). A possible explanation for this trend is that as passive transport presumably decreases with the decreased chemical gradient in latter segments of the GI tract, there is a greater reliance on active transport, and therefore active transporters such as SLC41a1 are expressed more highly, similar to rat GI tracts shown to express both SLC41a1 and TRPM6 more highly at latter segments (Goytain and Quamme 2005; Lameris et al. 2015). Alternatively, if SLC41a1 secretes magnesium across the apical membrane (as discussed in Chapter 2), it could reduce the measured magnesium flux, possibly explaining the lowest transport at the 8th segment. This is further discussed in the kinetics section

Calcium transport doesn't appear to follow the same pattern, with the 1st and 7th segments being hotspots for Ca^{2+} flux in fed fish, unlike feasted fish where transport was similar throughout (Figure 17). This is consistent with previous findings that calcium transport in the anterior GI tract is primarily regulated by luminal concentrations in the lake sturgeon, while latter segments are regulated by bodily requirement (Genz et al. 2013). While a mixture of secretion and absorption has been observed along the GI tract of FW *O. mykiss* for both divalent ions, the seemingly strictly absorptive function spread across the *C. auratus* GI tract could be explained by their lack of a stomach (Bucking and Wood 2007). The stomach has been implicated as the primary site of absorption for both calcium and magnesium (Bucking and Wood 2007) , and as such it's absorptive function could be fulfilled by different GI segments in stomach-lacking fish.

As expected, outward proton flux was observed along the entire length of the serosal side of the GI tract without a large deal of variance between segments and between fed and fasted fish (Figure 18). Lacking a stomach, an anterior region of large proton excretion was not expected, nor was it expected to increase proton secretion during digestion as observed in the stomach possessing rainbow trout (Bucking and Wood 2009). Furthermore, the FW-acclimated killifish, also lacking a stomach, displayed only marginal acidification of GI chyme during digestion as compared to fasting for 1-2 weeks, decreasing from pH 7.5 to pH 6.8 (Wood et al. 2010). While an increase in pH has been observed in chyme as it travels from the stomach to the GI tract of *O. mykiss*, this was likely due to alkaline bile and pancreatic secretions (Bucking and Wood 2009) and possibly not due to direct proton/base equivilant excretions to the lumen. The current experiment suggests that the tissue itself is not altering proton excretion and supports the hypothesis that pH changes in the GI tract are driven by digestive secretions.

An unfortunate limitation of the present study is the lack of selectivity of the magnesium ionophore used. We are unable to exclude the possibility that some of the zonational variation in magnesium flux observed is due to similar patterns of flux for calcium, such as the high 1st segment values. As such, while there may still be validity to the general trends observed for magnesium transport, it is unlikely the values measured are exact. There are alternative ionophores available for magnesium measurements, however, while the seemingly best choice, magnesium ionophore IV, is ~$10^{2.3}$ times more selective for Mg^{2+} vs Ca^{2+}, it is still around 10 times more selective for H^{+} (values from the Sigma-Aldrich website). The ionophore exhibits a near-Nernstian slope (~32.1) between 1 and 10mM Ca^{2+}-containing equimolar Cortland's saline (Figure 31). Calcium and proton zonation, alternatively, may be of more use, given the better selectivity of their respective ionophores.

9.3 Kinetics

Consistent with our hypothesis, Ca^{2+} and H^{+} flux remained unchanged with increasing luminal Mg^{2+} concentration (Figures 21B and C). Given the relatively low R^2 values, the variability in either flux can not be explained solely by the increase in luminal Mg2+ concentration (Figures 21B and C). Thus, it stands to reason that the inherently present flux for both ions would interfere roughly equally at all Mg^{2+} concentrations. As such, SIET could be used to accurately measure magnesium kinetics in the GI tract.

This is the first evidence of magnesium transport kinetics in the GI tract of a fish and the observed transport kinetics of magnesium at the 1st segment seemed to fit passive transport most closely, fitting really well into a linear regression model with a high R^2 value of 0.98 (Figure 21A). Contrasted with mammalian literature, which displayed a classic Michalis-Menten relationship indicative of transcellular, active transport (Hardwick et al. 1990; Karbach et al. 1991) this is a very different trend.

A possible explanation for this is found in the relative expression of SLC41a1 along the GI tract, as it is poorest at the 1st segment (Figure 20). Taking the relative expression of the transporter to be indicative of the segment's reliance on active transport, it is possible that Mg^{2+} kinetics would follow curvilinear relationship more closely at the 8th segment. Alternatively, if flux was less responsive to luminal concentration increase at the 8th segment, SLC41a1's proposed secretory function would be supported, as the increased cellular influx would need to be addressed either by basolateral extrusion or apical secretion. As such, further kinetics study of the *C. auratus* 8th segment is warranted, and may be more conclusive than the zonational approach, given the lack of responsiveness of H^{+} and Ca^{2+} fluxes to increased luminal concentration.

TRPM6 zonation has been studied in the rat GI tract, revealing higher expression in the rectum than ileum similar to SLC41a1 (Schlingmann et al. 2002; Figure 20). Given the presumed similarities in ion absorptive strategy between mammals and fish, we would expect transport to follow a similar trend in *C. auratus*, supportive of higher rates of active transport in the later segments of the GI tract.

9.4 Pharmacological effects on Mg^{2+} and Ca^{2+} transport at the 1st and 8th GI segments and gill

In agreement with our hypothesis, Mg^{2+}, Ca^{2+} and H^{+} fluxes were shown to be ouabain-sensitive, as preparations containing either just ouabain or both it and Co3Hex generally resulted in a reduction of transport for all three ions (Figures 22, 23, 24 and 25). This response was observed regardless of which side flux was measured or the drugs were applied, suggesting ouabain can cross the GI epithelium of *C. auratus*. Given that drugs were applied in randomized fashion in this experiment, all three fluxes appear to be recoverable when tissues are present in ouabain-free Cortland's for ~10 minutes. The ouabain-induced reduction in fluxes is likely due to inhibition of NKA at the basolateral membrane of cells, whose activity is required to maintain the high Na^{+} gradient driving Mg^{2+} and Ca^{2+} extrusion. Previously, ouabain has been shown to reduce both Mg^{2+} and Ca^{2+} fluxes in the GI tract of tilapia (Flik et al. 1993; van der Velden et al. 1990). Both divalent ions' transport is seemingly dependent on NKA activity, as inward fluxes were reduced in sodium-free saline (Flik et al. 1990; Flik et al. 1993; van der Velden et al. 1990). This is consistent with the current view that magnesium and calcium are both transported across the basolateral membrane via a sodium exchanger (NME and NCX1, respectively) (Bijvelds et al. 1998; Hwang et al. 2011). However, the reduction in magnesium fluxes should be viewed with caution, as the ionophore may have been detecting the reduced fluxes of calcium and/or protons

(Figures 22, 23, 24 and 25). Considering my evidence for paracellular transport at the 1st segment, this is likely the case.

Surprisingly, Co3Hex not only failed to exhibit synergistic effects with ouabain, but also failed to exhibit any response on its own in terms of magnesium fluxes. In contrast, the drug has been observed to reduce inward magnesium fluxes by over 50% in HEK-293 cells (Kolisek et al. 2008). A possible explanation for this difference with literature could stem from the different concentrations used, as HEK-293 cells were kept in a higher Mg^{2+} saline, 10mM or ~5 times higher than the mucosal concentration in the present experiment, and exposed to a ~10 fold higher concentration of Co3Hex (1mM) (Kolisek et al. 2008). Given Co3Hex is a competitive inhibitor for (presumably) the TRPM6/7 channel complexes in enterocytes, it's concentration relative to Mg^{2+} is about 2 times higher in the HEK-293 experiments relative to the present study (Kolisek et al. 2008). An additional explanation for the lack of effect is again the observed paracellular transport at the 1st segment. If my hypothesis that transcellular transport would be relied on more at the 8th segment, I would expect to observe an effect there instead.

Finally, absorption-indicative negative flux was observed at the gill for both divalent ions (negative numbers), along with H^+ secretion (positive numbers). The difference in pharmacological response compared to the GI segments could possibly be explained with the incubation time available to the tissue. Given that gills were kept in DTW rather than a saline, there was a visible colour change and rapid degradation. As such, for consistency's sake, readings were only taken prior to those changes, which likely limited the time required for the tissue's ion transport to be disrupted by the ouabain. Magnesium and calcium absorption have been a long-standing assumption of FW fish ionregulation, as body content has been reported to exceed dietary availability (Shearer and Åsgård 1992). Furthermore, gills are an important organ for acid-base

balance in FW fish, secreting protons (Evans et al. 2005). Thus, my results fit the expected ion transport profile at the gill for the three ions.

9.5 Proposed SLC41a1 role in magnesium secretion

If the suggested secretory function of SLC41a1 is correct, it would likely be reflected in differences in transport kinetics along the GI tract. If absorption is largely passive, and SLC41a1 is continuously secreting Mg^{2+} back into the lumen at a relatively low rate, we would expect to observe flux similar to example B in Figure 27, as was the case at the 1st segment (Figure 21A). In other words, we would observe a linear relationship between increasing luminal concentration and transport. Furthermore, if SLC41a1 secretes magnesium we would expect higher rates of secretion with increased SLC41a1 expression (Figure 27C). Thus, we should be able to observe a relatively-lower, linear relationship between transport and concentration at the 1st segment at increased SLC41a1 expression levels.

Conversely, if SLC41a1 carries out basolateral NME function, and is part of an active absorptive mechanism, we would expect a curvilinear relationship, suggestive of a mixture of both active and passive transport more similar to Figure 27A. I would predict this will be observed in the 8th segment, corresponding to my hypothesis that paracellular transport decreases and transcellular transport increases along the GI tract and in accordance with the observed mammalian (and presumed teleost) TRPM6/7 expression (Schlingmann et al. 2002). Alternatively, GI segments relying more on active transport would have increased magnesium entry. If the channels cannot be inactivated at a rapid enough rate when faced with a sudden influx of magnesium (such as a meal), it is possibly SLC41a1 provides further protection from deleterious accumulation of cellular Mg^{2+}.

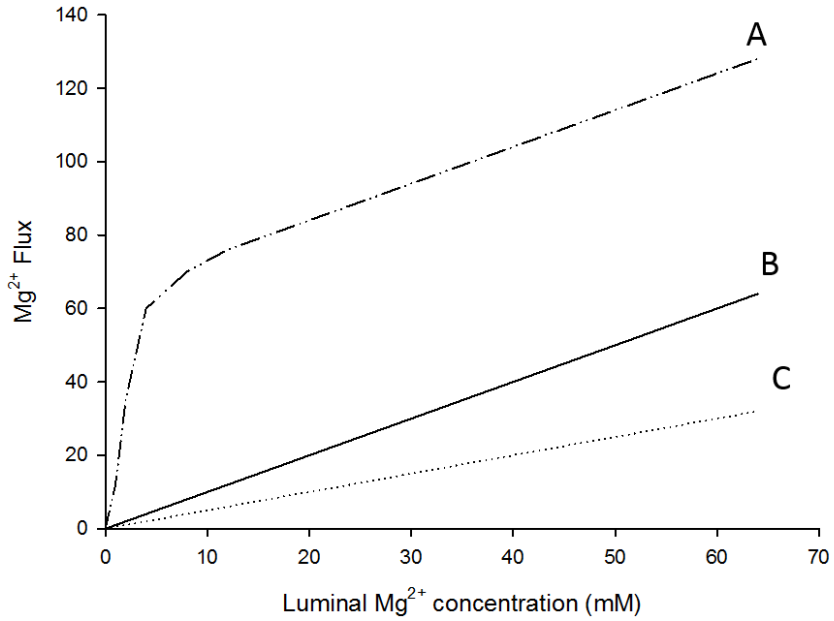

Figure 27: Different possible Mg^{2+} transport kinetics. Three hypothetical Mg^{2+} flux kinetics indicative of a mixture of active and passive transport (A), passive transport (B) and passive transport with secretion (C).

Chapter 4: Overall significance, conclusions and future directions

The present study is novel, in that it is the first to look at SLC41a1 mRNA transcript regulation in the ion regulatory organs in response to temperature change, dietary frequency, IPW exposure and diet manipulation in an adult stenohaline FW teleost. The transcriptional regulation is suggestive of a excretory role, minimizing expression during magnesium restrictions and increasing expressing during magnesium enhancements.

It is also the first to examine magnesium transport using the SIET approach, which revealed dominant paracellular kinetics at the 1st GI segment as well as possible zonation along the GI tract. However there continues to be a relatively minimal understanding of how cellular magnesium transport is regulated in response to osmoregulatory factors such as diet, temperature and water salinity. A multitude of future directions can be explored as follows.

Firstly, the channel complex (TRPM6/TRPM7) proposed as the entry point of the transcellular pathway appears to be regulated paradoxically. TRPM6 was upregulated at the gill, but not kidney or GI tract, of *D. rerio* at lower ambient Mg^{2+} (Arjona et al. 2013). This is consistent with the channel's proposed function, in that if availability in the water decreases, the absorptive mechanism at the gill must be upregulated to compensate. Conversely, TRPM7 was also upregulated at the GI tract of *Salmo salar* when transferred to SW from FW (Esbaugh et al. 2014). This upregulation is puzzling, as one would either expect a downregulation in expression when fish are transferred to SW, due to the sudden influx of ions, or a maintenance of expression level, as both TRPM6 and 7 are sensitive and can be inactivated by high cellular magnesium concentration (Demeuse et al. 2006).

Given the interaction between the two channel forms the heterodimer through which Mg^{2+} is believed to enter cells (regulated via TRPM6 phosphorylating TRPM7), future studies in teleosts

must address how the two transcripts are regulated simultaneously (Schlingmann et al. 2002; Schmitz et al. 2005). As well, zonation of TRPM6 and 7 along the GI tract should be investigated to observe how expression relates to the observed zonation of SLC41a1 (Figure 20).

Magnesium must then be transported across the basolateral membrane, likely via a NME exchanger, believed to be SLC41a1 (Bijvelds et al. 1998). Alternatively, SLC41a1 could be a part of an apical membrane-associated magnesium secretory mechanism in the vertebrate cell, as suggested by mRNA transcripts that were upregulated in the proximal tubules (excretory in nature) of mefugu transferred from FW to SW (Islam et al. 2013). Similarly, the present results show that SLC41a1 expression is regulated at the transcript level in a tissue-dependant manner consistent with the protein playing a role in secretory function. Expression appears to decrease when Mg^{2+} availability decreases (e.g. when feeding frequency decreases to every 48 hours as opposed to every 24 hours or fish are fed magnesium-poor shrimp) and increases when excess magnesium is presented (e.g. the kidney upregulates it when presented with a magnesium enriched diet). Future experiments should focus on the localization of SLC41a1 in the different ion regulatory tissues. A basolateral localization would make a strong case for the protein fulfilling the role of the hypothesized basolateral NME involved in absorption. Alternatively, an apical or vesicular localization would make a case for excretory function. Localization must therefore be studied using immunohistochemistry and developing a custom antibody for the *C. auratus* protein.

Furthermore, a marked limitation of both Islam et al. 2013's and the present methodology is using a genomic and not proteomic approach. Thus, both fail to account for proposed post-transcriptional regulation (Mandt et al. 2011). This could provide an alternate explanation to the mefugu findings, as the SLC41a1-containing vesicles observed may have been endosomes transporting SLC41a1 away from the apical surface. Since the immunohistochemical study of

SLC41a1 in Islam et al. 2013 was carried out in SW acclimated fish, it stands to reason the proximal tubule cells observed would not be Mg^{2+} deficient. As such, it is possible SLC41a1 would be continuously transported away from the surface and degraded, resulting in a minimal localization to the apical membrane. To study this, western blots can be utilized (again, using a custom antibody) along with plasma membrane protein isolation (using a commercially available kit) to quantify the relative expression of the protein at the membrane at a given time point. Together with immunohistochemistry, this would allow us to better understand the localization and regulation, and therefore function, of SLC41a1 in a FW fish.

Furthermore, we must better understand other proposed magnesium transporters and their respective function. For example, two more members of the SLC41 family have been uncovered, namely SLC41a2 and SLC41a3. SLC41a2 has been shown to facilitate transport for Mg^{2+} as well as a variety of divalent cations, however, its regulation and role are still not well understood (Goytain and Quamme 2005). Its subcellular localization has also not been fully understood, with evidence suggesting it is either found on the plasma membrane or on organelle membranes facilitating magnesium transport inside the cell (Fleig et al. 2013). Unlike SLC41a1, a2 is not universally expressed and mRNA transcripts were not detected in respiratory epithelia, pancreas, thyroid and uterine glands in humans (Fleig et al. 2013). Similarly, SLC41a3 is poorly understood. Its localization and expression have not been shown (Fleig et al. 2013). There has been recent evidence that it is somehow a factor in magnesium transport, as a deletion mutation for it has been correlated to unilateral hydronephrosis (kidney swelling) in mice (de Baaij et al. 2016). The deletion did not cause a reduction in GI absorption of $^{25}Mg^{2+}$, so its exact function remains unknown (de Baaij et al. 2016). Another family of potential magnesium transporters is the cyclin

M (Cnnm) family, two members (Cnnm2 and 3) have been shown to hold NME function (Islam et al. 2014).

Additionally, like the gill, there is evidence that FW teleost skin not only serves as a semi-permeable barrier between the fish tissues and environment, but also can play an active role in transport (reviewed by Glover et al. 2013). However, little work exists focusing on ion transport across this tissue. An early study revealed that skin preparations for *Oreochromis niloticus* exposed to FW on the mucosal side and saline on the serosal side exhibited inward fluxes for sodium, chloride and calcium against concentration gradients (Burgess et al. 1998). This study supports the notion that the skin is not only a barrier to diminish ion loss and water gain, but is also actively involved in homeostasis. The presence of SLC41a1 in the skin of *C. auratus* (Figure 9) and TRMP6/7 in the scales of *D. rerio* (Arjona et al. 2013) further suggests that magnesium transport occurs in this tissue, although the role in homeostasis is not clear.

Paracellular transport should also be examined, especially considering our evidence for diffusive kinetics at the 1st GI segment (Figure 21A). For example, human CACO-2 cell monolayers treated with omeprazole, a drug associated with hypomagnesemia upon long term use, displayed reduced expression for claudins 7 and 12 and lower rates of passive magnesium transport (Thongon and Krishnamra 2012). Orthologues to both claudins have been found to be expressed in the GI tract of *C. auratus* and *D. rerio*, however, their relationship with magnesium homeostasis in fish remains largely understudied (reviewed in Kolosov et al. 2013).

Obtaining the sequence for all of these genes in *C. auratus* and repeating the discussed experiments, quantifying both mRNA transcripts and protein expression (using Western blots), we could better understand the individual roles of each of these potential magnesium transporters and TJ proteins on magnesium homeostasis. Furthermore, gene knock downs (possibly via CRISPR

deletion) could be used along with SIET to possibly study the impact of each protein on the transport rates and kinetics of magnesium at the gill and GI tract.

Finally, given the lack of a highly selective magnesium ionophore, the used set-up is of limited use for magnesium study, unless calcium and proton fluxes can be shown to be stable (as in the magnesium transport kinetics experiment or focusing on a single zone of transport). While experiments conducted in a ion-rich media such as Cortland's saline are bound to exhibit interference, flux is likely less impacted in a ion-poor media such DTW, making it a strong potential tool for studying branchial transport. An alternative approach to address this could be the limitation or exclusion of interfering ions (such as calcium) from the bathing saline. However, this would possibly impact the physiology of the tissue. As well, while branchial transport for the divalent ions has been studied before, direct measurements of the transport flux are challenging to obtain and are often measured indirectly. The present study directly measured magnesium and calcium absorption at the gill offering a potential novel technique to study into transport across the tissue on a microscale, identifying transport rich areas. Taken together, SIET can be very useful in future studies of GI and branchial transport studies for ions but more work is required to establish the technique.

References

Arjona FJ, **Chen YX**, **Flik G**, **Bindels RJ**, **Hoenderop JG**. Tissue-specific expression and in vivo regulation of zebrafish orthologues of mammalian genes related to symptomatic hypomagnesemia. *Pflugers Arch Eur J Physiol* 465: 1409–1421, 2013.

Bagherie-Lachidan M, **Wright SI**, **Kelly SP**. Claudin-3 tight junction proteins in *Tetraodon nigroviridis*: cloning, tissue-specific expression, and a role in hydromineral balance. *Am J Physiol Regul Integr Comp Physiol* 294: R1638-47, 2008.

Bagherie-Lachidan M, **Wright SI**, **Kelly SP**. Claudin-8 and -27 tight junction proteins in puffer fish *Tetraodon nigroviridis* acclimated to freshwater and seawater. *J Comp Physiol B* 179: 419–431, 2009.

Barish ME. A transient calcium-dependent chloride current in the immature Xenopus oocyte. *J Physiol* 342: 309–25, 1983.

Beamish FWH. Respiration of fishes with special emphasis on standard oxygen consumption II. Influence of weight and temperature on respiration of several species. *Can J Zool* 42: 177–188, 1964.

Behar J. Magnesium absorption by the rat ileum and colon. *Am J Physiol* 227: 334–340, 1974.

Beyenbach KW. Renal handling of magnesium in fish: from whole animal to brush border membrane vesicles. *Front Biosci* 5: D712-9, 2000.

Bijvelds MJC, Kolar Z, Bonga S, Flik G. Mg^{2+} transport in plasma membrane vesicles of renal epithelium of the Mozambique tilapia (*Oreochromis mossambicus*). *J Exp Biol* 200: 1931–9, 1997a.

Bijvelds MJC, **Velden JA**, **Kolar ZI**, **Flik G**. Magnesium transport in freshwater teleosts. *J Exp Biol* 201: 1981, 1998.

Bijvelds MJC, **Flik G**, **Kolar ZI**, **Wendelaar Bonga SE**. Uptake, distribution and excretion of magnesium in Oreochromis mossambicus: dependence on magnesium in diet and water. *Fish Physiol Biochem* 15: 287–298, 1996.

Bijvelds MJC, **Flik G**, **Wendelaar Bonga SE**. Mineral balance in *Oreochromis mossambicus*: dependence on magnesium in diet and water. *Fish Physiol Biochem* 16: 323–331, 1997b.

Bijvelds MJC, **Kolar ZI**, **Flik G**. Electrodiffusive magnesium transport across the intestinal brush border membrane of tilapia (*Oreochromis mossambicus*). *Eur J Biochem* 268: 2867–2872, 2001.

Boisen AMZ, **Amstrup J**, **Novak I**, **Grosell M**. Sodium and chloride transport in soft water and hard water acclimated zebrafish (*Danio rerio*). *Biochim Biophys Acta - Biomembr* 1618:

207–208, 2003.

Bradford MM. A rapid and sensitive method for the quantitation of microgram quantities of protein utilizing the principle of protein-dye binding. *Anal Biochem* 72: 248–254, 1976.

Braun EJ, **Dantzler WH**, **Braun EJ**, **Dantzler WH**. Vertebrate renal system. In: *Comprehensive Physiology*. John Wiley & Sons, Inc.

Bucking C, **Landman MJ**, **Wood CM**. The role of the kidney in compensating the alkaline tide, electrolyte load, and fluid balance disturbance associated with feeding in the freshwater rainbow trout, Oncorhynchus mykiss. *Comp Biochem Physiol Part A* 156: 74–83, 2010.

Bucking C, **Wood CM**. Gastrointestinal processing of Na^+, Cl^- , and K^+ during digestion: implications for homeostatic balance in freshwater rainbow trout. *Am J Physiol Regul Integr Comp Physiol* 291: 1764–1772, 2006a.

Bucking C, **Wood CM**. Water dynamics in the digestive tract of the freshwater rainbow trout during the processing of a single meal. *J Exp Biol* 209: 1883–1893, 2006b.

Bucking C, **Wood CM**. Gastrointestinal transport of Ca^{2+} and Mg^{2+} during the digestion of a single meal in the freshwater rainbow trout. *J Comp Physiol B* 177: 349–360, 2007.

Bucking C, **Wood CM**. The effect of postprandial changes in pH along the gastrointestinal tract on the distribution of ions between the solid and fluid phases of chyme in rainbow trout. *Aquac Nutr* 15: 282–296, 2009.

Burgess DW, **Marshall WS**, **Wood CM**. Ionic transport by the opercular epithelia of freshwater acclimated tilapia (*Oreochromis niloticus*) and killifish (*Fundulus heteroclitus*). *Comp Biochem Physiol Part A Mol Integr Physiol* 121: 155–164, 1998.

Chandra S, Morrison GH, Beyenbach KW. Identification of Mg-transporting renal tubules and cells by ion microscopy imaging of stable isotopes. Am J Physiol Renal Physiol 273:F939-948, 1997.

Chasiotis H, **Effendi JC**, **Kelly SP**. Occludin expression in goldfish held in ion-poor water. *J Comp Physiol B* 179: 145–154, 2009.

Chasiotis H, **Kelly SP**. Occludin immunolocalization and protein expression in goldfish. *J Exp Biol* 211: 1524–34, 2008.

Chasiotis H, **Kolosov D**, **Bui P**, **Kelly SP**. Tight junctions, tight junction proteins and paracellular permeability across the gill epithelium of fishes: A review. *Respir Physiol Neurobiol* 184: 269–281, 2012.

Choe KP, **Morrison-Shetlar AI**, **Wall BP**, **Claiborne JB**. Immunological detection of Na^+/H^+ exchangers in the gills of a hagfish, *Myxine glutinosa*, an elasmobranch, *Raja erinacea*, and

a teleost, *Fundulus heteroclitus*. *Comp Biochem Physiol Part A Mol Integr Physiol* 131: 375–385, 2002.

Chubanov V, **Gudermann T**, **Schlingmann KP**. Essential role for TRPM6 in epithelial magnesium transport and body magnesium homeostasis. *Pflugers Arch Eur J Physiol* 451: 228–234, 2005.

Chubanov V, **Waldegger S**, **Schnitzler MM**, **Vitzthum H**, **Sassen MC**, **Seyberth HW**, **Konrad M**, **Gudermann T**. Disruption of TRPM6/TRPM7 complex formation by a mutation in the TRPM6 gene causes hypomagnesemia with secondary hypocalcemia. *Proc Natl Acad Sci* 101: 2894–2899, 2004.

Claiborne JB, **Blackston CR**, **Choe KP**, **Dawson DC**, **Harris SP**, **MacKenzie LA**, **Morrison-Shetlar AI**. A mechanism for branchial acid excretion in marine fish: identification of multiple Na^+/H^+ antiporter (NHE) isoforms in gills of two seawater teleosts *J Exp Biol* 202: 315–234, 1999.

Cliff WH, **Beyenbach KW**. Secretory renal proximal tubules in seawater- and freshwater-adapted killifish. *Am J Physiol - Ren Physiol* 262, 1992.

Dabrowska H, **Meyer-Burgdorff KH**, **Gunther KD**. Magnesium status in freshwater fish, common carp (*Cyprinus carpio*) and the dietary protein-magnesium interaction. *Fish Physiol Biochem* 9: 165–172, 1991.

Dai LJ, **Quamme GA**. Intracellular Mg^{2+} and magnesium depletion in isolated renal thick ascending limb cells. *J Clin Invest* 88: 1255–64, 1991.

Dai LJ, **Raymond L**, **Friedman PA**, **Quamme GA**. Mechanisms of amiloride stimulation of Mg^{2+} uptake in immortalized mouse distal convoluted tubule cells. *Am J Physiol* 272: 249-256, 1997.

Dantzler WH. Regulation of renal proximal and distal tubule transport: sodium, chloride and organic anions. *Comp Biochem Physiol A Mol Integr Physiol* 136: 453–78, 2003.

Dascal N. Voltage clamp recordings from Xenopus oocytes. *Curr Protoc Neurosci* Chapter 6: Unit 6.12, 2001.

Davis EM, **Musch mark W**, **Goldstein L**. Transfection of an inducible trout anion exchanger (AE1) into HEK-EcR cells. *J Exp Zool* 293: 46–57, 2002.

de Baaij JHF, **Arjona FJ**, **van den Brand M**, **Lavrijsen M**, **Lameris ALL**, **Bindels RJM**, **Hoenderop JGJ**. Identification of SLC41A3 as a novel player in magnesium homeostasis. *Sci Rep* 6: 28565, 2016.

Del Duca O, **Nasirian A**, **Galperin V**, **Donini A**. Pharmacological characterisation of apical Na^+ and Cl^- transport mechanisms of the anal papillae in the larval mosquito *Aedes aegypti*. *J*

Exp Biol 214: 3992–3999, 2011.

Demeuse P, **Penner R**, **Fleig A**. TRPM7 channel is regulated by magnesium nucleotides via its kinase domain. *J Gen Physiol* 127: 421–434, 2006.

de Rouffignac C, **Corman B**, **Roinel N**. Stimulation by antidiuretic hormone of electrolyte tubular reabsorption in rat kidney. *Am J Physiol* 244: 156–164, 1983.

de Rouffignac C, **Quamme G**. Renal magnesium handling and its hormonal control. *Physiol Rev* 74: 305–22, 1994.

Donini A, **O'Donnell MJO**. Analysis of Na^+ , Cl^- , K^+ , H^+ and $NH4^+$ concentration gradients adjacent to the surface of anal papillae of the mosquito *Aedes aegypti* : application of self-referencing ion-selective microelectrodes. *J Exp Biol* 208: 603–610, 2005.

Edmonds J, **Caputi N**, **Morita M**, **Edmonds J**, **Caputi N**, **Morita M**. Stock discrimination by trace-element analysis of otoliths of orange roughy (*Hoplostethus atlanticus*), a deep-water marine teleost. *Mar Freshw Res* 42: 383, 1991.

Edwards SL, **Tse CM**, **Toop T**. Immunolocalisation of NHE3-like immunoreactivity in the gills of the rainbow trout (*Oncorhynchus mykiss*) and the blue-throated wrasse (*Pseudolabrus tetrious*). *J Anat* 195: 465–469, 1999.

Elizondo MR, **Arduini BL**, **Paulsen J**, **MacDonald EL**, **Sabel JL**, **Henion PD**, **Cornell RA**, **Parichy DM**. Defective skeletogenesis with kidney stone formation in dwarf zebrafish mutant for TRPM7. *Curr Biol* 15: 667-671, 2005.

Esbaugh AJ, **Kristensen T**, **Takle H**, **Grosell M**. The effects of sustained aerobic swimming on osmoregulatory pathways in Atlantic salmon *Salmo salar* smolts. *J Fish Biol* 85: 1355–1368, 2014.

FAO. The State of World Fisheries and Aquaculture 2016. Contributing to food security and nutrition for all. Rome. 200 pp.

Fleig A, **Schweigel-Röntgen M**, **Kolisek M**. Solute carrier family SLC41: What do we really know about it? *Wiley Interdiscip Rev Membr Transp Signal* 2: 227–239, 2013.

Flik G, **Schoenmakers TJ**, **Groot JA**, **van Os CH**, **Wendelaar Bonga SE**. Calcium absorption by fish intestine: the involvement of ATP- and sodium-dependent calcium extrusion mechanisms. *J Membr Biol* 113: 13–22, 1990.

Flik G, **Van Der Velden JA**, **Dechering KJ**, **Verbost PM**, **Schoenmakers TJM**, **Kolar ZI**, **Bonga SEW**. Ca^{2+} and Mg^{2+} transport in gills and gut of tilapia,*Oreochromis mossambicus*: A review. *J Exp Zool* 265: 356–365, 1993.

Freire CA, **Kinne RK**, **Kinne-Saffran E**, **Beyenbach KW**. Electrodiffusive transport of Mg across renal membrane vesicles of the rainbow trout *Oncorhynchus mykiss*. *Am J Physiol* 270: F739-48, 1996.

Fuentes J, **Eddy FB**. Drinking in marine, euryhaline and freshwater teleost fish. In: *Ionic Regulation in Animals: A Tribute to Professor W.T.W.Potts*. Springer Berlin Heidelberg, p. 135–149.

Galvez F, **Reid SD**, **Hawkings G**, **Goss GG**. Isolation and characterization of mitochondria-rich cell types from the gill of freshwater rainbow trout. *Am J Physiol Regul Integr Comp Physiol* 282: R658-68, 2002.

Gatlin DM, **Robinson EH**, **Poe WE**, **Wilson RP**. Magnesium requirement of fingerling channel catfish and signs of magnesium deficiency. *J Nutr* 112: 1182–7, 1982.

Glover CN, **Bucking C**, **Wood CM**. The skin of fish as a transport epithelium: a review. *J Comp Physiol B Biochem Syst Environ Physiol* 183: 877–891, 2013.

Goss GG, **Adamia S**, **Galvez F**. Peanut lectin binds to a subpopulation of mitochondria-rich cells in the rainbow trout gill epithelium. *Am J Physiol Regul Integr Comp Physiol* 281: R1718-25, 2001.

Goytain A, **Quamme GA**. Functional characterization of human SLC41A1, a Mg^{2+} transporter with similarity to prokaryotic MgtE Mg^{2+} transporters. *Physiol Genomics* 21: 337–342, 2005.

Grant FB, **Pang PK.**, **Griffith RW**. The twenty-four-hour seminal hydration response in goldfish (*Carassius auratus*) sodium, potassium, calcium, magnesium, chloride and osmolality of serum and seminal fluid. *Comp Biochem Physiol* 30: 273–280, 1969.

Grosell M, **Hogstrand C**, **Wood C.**, **Hansen HJ.** A nose-to-nose comparison of the physiological effects of exposure to ionic silver versus silver chloride in the European eel (*Anguilla anguilla*) and the rainbow trout (*Oncorhynchus mykiss*). *Aquat Toxicol* 48: 327–342, 2000.

Grosell M, **Nielsen C**, **Bianchini A**. Sodium turnover rate determines sensitivity to acute copper and silver exposure in freshwater animals. *Comp Biochem Physiol C Toxicol Pharmacol* 133: 287–303, 2002.

Han D, **Liu H**, **Liu M**, **Xiao X**, **Zhu X**, **Yang Y**, **Xie S**. Effect of dietary magnesium supplementation on the growth performance of juvenile gibel carp, *Carassius auratus gibelio*. *Aquac Nutr* 18: 512–520, 2012.

Handeland SO, **Imsland AK**, **Stefansson SO**. The effect of temperature and fish size on growth, feed intake, food conversion efficiency and stomach evacuation rate of Atlantic salmon post-smolts. *Aquaculture* 283: 36–42, 2008.

Hardwick LL, **Jones MR**, **Buddington RK**, **Clemens RA**, **Lee DB**. Comparison of calcium and magnesium absorption: in vivo and in vitro studies. *Am J Physiol - Gastrointest Liver Physiol* 259, 1990.

Hartzell HC, **White RE**. Effects of magnesium on inactivation of the voltage-gated calcium current in cardiac myocytes. *J Gen Physiol* 94: 745–67, 1989.

Hentschel H, Zierold K. Morphology and element distribution of magnesium-secreting epithelium: the proximal tubule segment PII of dogfish, *Scyliorhinus caniculus*. *Eur J Cell Biol* 63:32–42, 1994.

Hickman C, **Trump B**. The kidney. In: Fish Physiology. Vol 1. New York: Academic Press, 1969, p. 91–239.

Hobe H, **Wood CM**, **McMahon BR**. Mechanisms of acid-base and ionoregulation in white suckers (*Catostomus commersoni*) in natural soft water. *J Comp Physiol B* 154: 35–46, 1984.

Horie M, **Irisawa H**, **Noma A**. Voltage-dependent magnesium block of adenosine-triphosphate-sensitive potassium channel in guinea-pig ventricular cells. *J Physiol* 387: 251–72, 1987.

Hoskins LJ, **Xu M**, **Volkoff H**. Interactions between gonadotropin-releasing hormone (GnRH) and orexin in the regulation of feeding and reproduction in goldfish (*Carassius auratus*). *Horm Behav* 54: 379–85, 2008.

Islam Z, **Hayashi N**, **Inoue H**, **Umezawa T**, **Kimura Y**, **Doi H**, **Romero MF**, **Hirose S**, **Kato A**. Identification and lateral membrane localization of cyclin M3, likely to be involved in renal Mg^{2+} handling in seawater fish. *Am J Physiol - Regul Integr Comp Physiol* 307: R525-537, 2014.

Islam Z, **Hayashi N**, **Yamamoto Y**, **Doi H**, **Romero MF**, **Hirose S**, **Kato A**. Identification and proximal tubular localization of the Mg^{2+} transporter, SLC41a1, in a seawater fish. *Am J Physiol Regul Integr Comp Physiol* 305: R385-96, 2013.

Karbach U, **Feldmeier H**. New clinical and experimental aspects of intestinal magnesium transport. *Magnes Res* 4: 9–22, 1991.

Karbach U, **Schmitt A**, **Saner FH**. Different mechanism of magnesium and calcium transport across rat duodenum. *Dig Dis Sci* 36: 1611–1618, 1991.

Knox D, **Cowey A N CB**. Studies on the nutrition of salmonid fish. The magnesium requirement of rainbow trout (*Safmo gairdneri*). *Br J Nutr* 45, 1981.

Kolisek M, **Launay P**, **Beck A**, **Sponder G**, **Serafini N**, **Brenkus M**, **Froschauer EM**, **Martens H**, **Fleig A**, **Schweigel M**. SLC41A1 is a novel mammalian Mg^{2+} carrier. *J Biol Chem* 283:

16235–16247, 2008.

Kolisek M, **Nestler A**, **Vormann J**, **Schweigel-Rontgen M**. Human gene SLC41A1 encodes for the Na^+/Mg^{2+} exchanger. *AJP Cell Physiol* 302: C318–C326, 2012.

Kolosov D, **Bui P**, **Chasiotis H**, **Kelly SP**. Claudins in teleost fishes. *Tissue Barriers* 1: e25391, 2013.

Kolosov D, **Chasiotis H**, **Kelly SP**, Tight junction protein gene expression patterns and changes in transcript abundance during development of model fish gill epithelia. *J Exp Biol* 217: 1667–81, 2014.

Kozak JA, **Cahalan MD**. MIC channels are inhibited by internal divalent cations but not ATP. *Biophys J* 84: 922–7, 2003.

Kucharski LM, **Lubbe WJ**, **Maguire ME**. Cation hexaammines are selective and potent inhibitors of the CorA magnesium transport system. *J Biol Chem* 275: 16767–73, 2000.

Lameris AL, **Nevalainen PI**, **Reijnen D**, **Simons E**, **Eygensteyn J**, **Monnens L**, **Bindels RJM**, **Hoenderop JGJ**. Segmental transport of Ca^{2+} and Mg^{2+} along the gastrointestinal tract. *Am J Physiol Gastrointest Liver Physiol* 308: G206-16, 2015.

Laurent P, **Perry SF**. Effects of cortisol on gill chloride cell morphology and ionic uptake in the freshwater trout, Salmo gairdned. *Cell Tissue Res* 259: 429–442, 1990.

Le Grimellec C, **Roinel N**, **Morel F**, **Philippe P**, **Malorey P**. Simultaneous Mg, Ca, P, K, Na and Cl analysis in rat tubular fluid. *Pflügers Arch* 340: 181–196, 1973.

Li M, **Jiang J**, **Yue L**. Functional Characterization of Homo- and Heteromeric Channel Kinases TRPM6 and TRPM7. *J Gen Physiol* 127: 525–537, 2006.

Lin H, **Pfeiffer D**, **Vogl A**, **Pan J**, **Randall D**. Immunolocalization of H+-ATPase in the gill epithelia of rainbow trout. *J Exp Biol* 195: 169–83, 1994.

Lin LY, **Horng JL**, **Kunkel JG**, **Hwang PP**. Proton pump-rich cell secretes acid in skin of zebrafish larvae. *Am J Physiol Cell Physiol* 290: C371-8, 2006.

Lo CJ, **Leake MC**, **Berry RM**. Fluorescence measurement of intracellular sodium concentration in single *Escherichia coli* cells. *Biophys J* 90: 357–65, 2006.

Low SE, **Amburgey K**, **Horstick E**, **Linsley J**, **Sprague SM**, **Cui WW**, **Zhou W**, **Hirata H**, **Saint-Amant L**, **Hume RI**, **Kuwada JY**. TRPM7 Is Required within Zebrafish Sensory Neurons for the Activation of Touch-Evoked Escape Behaviors. *J Neurosci* 31: 11633–11644, 2011.

Mandt T, **Song Y**, **Scharenberg AM**, **Sahni J**. SLC416A1 Mg^{2+} transport is regulated via Mg^{2+}

-dependent endosomal recycling through its N-terminal cytoplasmic domain. *Biochem J* 439: 129–139, 2011.

Marlatt VL, **Martyniuk CJ**, **Zhang D**, **Xiong H**, **Watt J**, **Xia X**, **Moon T**, **Trudeau VL**. Auto-regulation of estrogen receptor subtypes and gene expression profiling of 17beta-estradiol action in the neuroendocrine axis of male goldfish. *Mol Cell Endocrinol* 283: 38–48, 2008.

Marshall WS, **Grosell M**. *Ion Osmoregulation , and Acid – Base Balance*. 2005.

Marshall WS. Na^+, Cl^-, Ca^{2+} and Zn^{2+} transport by fish gills: Retrospective review and prospective synthesis. *J Exp Zool* 293: 264–283, 2002.

McCord JM, **Fridovich I**. Superoxide Dismutase: an enzymatic function for Erythrocuprein (Hemocuprein). *J Biol Chem* 244: 6049–6055, 1969.

McNeill MS, **Paulsen J**, **Bonde G**, **Burnight E**, **Hsu M-Y**, **Cornell RA**. Cell Death of Melanophores in Zebrafish TRPM7 Mutant Embryos Depends on Melanin Synthesis. *J Invest Dermatol* 127: 2020–2030, 2007.

Miledi R, **Parker I**. Chloride current induced by injection of calcium into Xenopus oocytes. *J Physiol* 357: 173–83, 1984.

Monteilh-Zoller MK, **Hermosura MC**, **Nadler MJS**, **Scharenberg AM**, **Penner R**, **Fleig A**. TRPM7 Provides an Ion Channel Mechanism for Cellular Entry of Trace Metal Ions. *J Gen Physiol* 121: 49–60, 2003.

Monteiro J, **Aires R**, **Becker JD**, **Jacinto A**, **Certal AC, Rodriguez-Leon, J**. V-ATPase Proton Pumping Activity Is Required for Adult Zebrafish Appendage Regeneration V-ATPase Proton Pumping Activity Is Required for Adult Zebrafish Appendage Regeneration. *PLoS One* 9:1-11, 2014.

Morel F, **Roinel N**, **Le Grimellec C**. Electron Probe Analysis of Tubular Fluid Composition. *Nephron* 6: 350–364, 1969.

Nadler MJ, **Hermosura MC**, **Inabe K**, **Perraud AL**, **Zhu Q**, **Stokes AJ**, **Kurosaki T**, **Kinet JP**, **Penner R**, **Scharenberg AM**, **Fleig A**. LTRPC7 is a Mg.ATP-regulated divalent cation channel required for cell viability. *Nature* 411: 590–5, 2001.

Nguyen H, **Donini A**. Larvae of the midge *Chironomus riparius* possess two distinct mechanisms for ionoregulation in response to ion-poor conditions. *Am J Physiol Regul Integr Comp Physiol* 299: R762–R773, 2010.

Nishimura H, **Imai M**, **Ogawa M**. Sodium chloride and water transport in the renal distal tubule of the rainbow trout. *Am J Physiol* 244: F247-54, 1983.

Ogino C, **Chiou JY**. Mineral requirements in fish. II. Magnesium requirement of carp. *Bull Jap*

Soc scient Fish 42: 71–75, 1976.

Ogino C, **Takashima F**, **Chiou J.** Requirement of rainbow trout for dietary magnesium. *Bull Jap Soc scient Fish* 44: 1105–1108, 1978.

Oikari AJ, **Rankin JC**. Renal excretion of magnesium in a freshwater teleost, *Salmo gairdneri*. *J exp Biol* 117: 319–333, 1985.

Paravicini TM, **Chubanov V**, **Gudermann T**. TRPM7: A unique channel involved in magnesium homeostasis. *Int J Biochem Cell Biol* 44: 1381–1384, 2012.

Perry SF, **Rivero-Lopez L**, **McNeill B**, **Wilson J**. Fooling a freshwater fish: how dietary salt transforms the rainbow trout gill into a seawater gill phenotype. *J Exp Biol* 209, 2006.

Pusch M, **Conti F**, **Stühmer W**. Intracellular magnesium blocks sodium outward currents in a voltage- and dose-dependent manner. *Biophys J* 55: 1267–71, 1989.

Quamme GA. Molecular identification of ancient and modern mammalian magnesium transporters. *Am J Physiol Cell Physiol* 298: 407–429, 2010.

Quamme GA. Recent developments in intestinal magnesium absorption. *Curr Opin Gastroenterol* 24: 230–235, 2008.

Quamme GA, **Carney SL**, **Wong NLM**, **Dirks JH**. Effect of parathyroid hormone on renal calcium and magnesium reabsorption in magnesium deficient rats. *Pflügers Arch* 386: 59–65, 1980.

Quamme GA, **De Rouffignac C**. Epithelial magnesium transport and regulation by the kidney. *Front Biosci* 5: 694–711, 2000.

Renfro JL, **Shustock E**. Peritubular uptake and brush border transport of ^{28}Mg by flounder renal tubules. *Am J Physiol* 249: F497-506, 1985.

Rheault MR, **O'Donnell MJO**. Organic cation transport by Malpighian tubules of Drosophila melanogaster : application of two novel electrophysiological methods. *J Exp Biol* 207: 2173–2184, 2004.

Rubin H. Magnesium deprivation reproduces the coordinate effects of serum removal or cortisol addition on transport and metabolism in chick embryo fibroblasts. *J Cell Physiol* 89: 613–25, 1976.

Runnels LW, **Yue L**, **Clapham DE**. TRP-PLIK, a bifunctional protein with kinase and ion channel activities. *Science* 291: 1043–7, 2001.

Ryazanova LV, **Pavur KS**, **Petrov AN**, **Dorovkov MV**, **Ryazanov AG**. Novel Type of Signaling Molecules: Protein Kinases Covalently Linked with Ion Channels. *Mol Biol* 35: 271–283,

2001.

Sardet C, **Pisam M**, **Maetz J**. The surface epithelium of teleostean fish gills. Cellular and junctional adaptations of the chloride cell in relation to salt adaptation. *J Cell Biol* 80: 96–117, 1979.

Schlingmann KP, **Waldegger S**, **Konrad M**, **Chubanov V**, **Gudermann T**. TRPM6 and TRPM7—Gatekeepers of human magnesium metabolism. *Biochem Biophys Acta* 1772: 813–821, 2007.

Schlingmann KP, **Weber S**, **Peters M**, **Niemann Nejsum L**, **Vitzthum H**, **Klingel K**, **Kratz M**, **Haddad E**, **Ristoff E**, **Dinour D**, **Syrrou M**, **Nielsen S**, **Sassen M**, **Waldegger S**, **Seyberth HW**, **Konrad M**. Hypomagnesemia with secondary hypocalcemia is caused by mutations in TRPM6, a new member of the TRPM gene family. *Nat Genet* 31: 166–170, 2002.

Schmitz C, **Dorovkov MV**, **Zhao X**, **Davenport BJ**, **Ryazanov AG**, **Perraud AL**. The channel kinases TRPM6 and TRPM7 are functionally nonredundant. *J Biol Chem* 280: 37763–37771, 2005.

Schmitz C, **Perraud AL**, **Johnson CO**, **Inabe K**, **Smith MK**, **Penner R**, **Kurosaki T**, **Fleig A**, **Scharenberg AM**. Regulation of vertebrate cellular Mg^{2+} homeostasis by TRPM7. *Cell* 114: 191–200, 2003.

Schwarzbaum P, **Niederstätter H**, **Wieser W**. Effects of temperature on the $(Na^{+}+ K^{+})$-ATPase and oxygen consumption in hepatocytes of two species of freshwater fish, roach (*Rutilus rutilus*) and brook trout (*Salvelinus fontinalis*). *Physiol Zool* 65: 699-711, 1992.

Schweigel M, **Martens H**. Magnesium transport in the gastrointestinal tract. *Front Biosci* 5: D666–D677, 2000.

Shearer KD. Whole body magnesium concentration as an indicator of magnesium status in rainbow trout (*Salmo gairdneri*). *Aquaculture* 77: 201–210, 1989.

Shearer KD, **Åsgård T**. The effect of water-borne magnesium on the dietary magnesium requirement of the rainbow trout (*Oncorhynchus mykiss*). *Fish Physiol Biochem* 9: 387–392, 1992.

Shih TH, **Horng JL**, **Hwang PP**, **Lin LY**. Ammonia excretion by the skin of zebrafish (*Danio rerio*) larvae. *Am J Physiol Cell Physiol* 295: C1625-32, 2008.

Shim KF, **Ng SH**. Cyclic AMP and ouabain-binding sites in the rectal gland of the dogfish (Scyliorhinus canicula). *J Exp Physiol Zool* 206: 297–302, 1978.

Shuttleworth TJ, Thompson JL. Magnesium requirement of the guppy (*Poecilia reticulata*). *Aquaculture* 73: 131–141, 1988.

Smith PJS, **Hammar K**, **Porterfield DM**, **Sanger RH**, **Trimarchi JR**. Self-Referencing , Non-Invasive , Ion Selective Electrode for Single Cell Detection of Trans-Plasma Membrane Calcium Flux. *Microsc Res Tech* 417: 398–417, 1999.

Sponder G, **Rutschmann K**, **Kolisek M**. "Inside-in" or "inside-out"? The membrane topology of SLC41A1. *Magnes Res* 26: 176–181, 2013.

Tamura K, **Stecher G**, **Peterson D**, **Filipski A**, **Kumar S**. MEGA6: Molecular Evolutionary Genetics Analysis Version 6.0. *Mol Biol Evol* 30: 2725–2729, 2013.

Thongon N, **Krishnamra N**. Apical acidity decreases inhibitory effect of omeprazole on Mg^{2+} absorption and claudin-7 and -12 expression in Caco-2 monolayers. *Exp Mol Med* 44: 684–693, 2012.

Tinoco AB, **Nisembaum LG**, **Isorna E**, **Delgado MJ**, **de Pedro N**. Leptins and leptin receptor expression in the goldfish (*Carassius auratus*). Regulation by food intake and fasting/overfeeding conditions. *Peptides* 34: 329–35, 2012.

Usher ML, **Talbot C**, **Eddy FB**. Drinking in Atlantic salmon smolts transferred to seawater and the relationship between drinking and feeding. *Aquaculture* 73: 237–246, 1988.

van der Velden JA, **Groot JA**, **Flik G**, **Polak P**, **Kolar ZI**. Magnesium transport in fish intestine. *J Exp Biol* 152: 587–592, 1990.

Voets T, **Nilius B**, **Hoefs S**, **Van Der Kemp AWCM**, **Droogmans G**, **Bindels RJM**, **Hoenderop JGJ**. TRPM6 forms the Mg^{2+} influx channel involved in intestinal and renal Mg^{2+} absorption. *Am Soc Biochem Mol Biol* 279: 19–25, 2004.

Wabakken T, **Rian E**, **Kveine M**, **Aasheim HC**. The human solute carrier SLC41A1 belongs to a novel eukaryotic subfamily with homology to prokaryotic MgtE Mg^{2+} transporters. *Biochem Biophys Res Commun* 306: 718–724, 2003.

Wendelaar Bonga SE, **Löwik CJ**, **van der Meij JC**. Effects of external Mg^{2+} and Ca^{2+} on branchial osmotic water permeability and prolactin secretion in the teleost *Sarotherodon mossambicus*. *Gen Comp Endoc* 52: 222-231, 1983.

Wilson JM, **Laurent P**. Fish gill morphology: inside out. *J Exp Zool* 293: 192–213, 2002.

Wilson JM, Laurent P, Tufts BL, Benos, DJ, Donowitz M, Vogl AW, Randall DJ. NaCl uptake by the branchial epithelium in freshwater teleost fish: an immunological approach to ion-transport protein localization. *J Exp Biol* 203: 2279-2296, 2000.

Wilson RW, **Grosell M**. Intestinal bicarbonate secretion in marine teleost fish—source of bicarbonate, pH sensitivity, and consequences for whole animal acid–base and calcium

homeostasis. *Biochim Biophys Acta - Biomembr* 1618: 163–174, 2003.

Wood CM, **Bucking C**, **Grosell M**. Acid–base responses to feeding and intestinal Cl– uptake in freshwater- and seawater-acclimated killifish, *Fundulus heteroclitus* , an agastric euryhaline teleost. *J Exp Biol* 213: 2681–2692, 2010.

Wood CM, **Kelly SP**, **Zhou B**, **Fletcher M**, **O'Donnell M**, **Eletti B**, **Pärt P**. Cultured gill epithelia as models for the freshwater fish gill. *Biochim Biophys Acta - Biomembr* 1566: 72–83, 2002.

Appendix

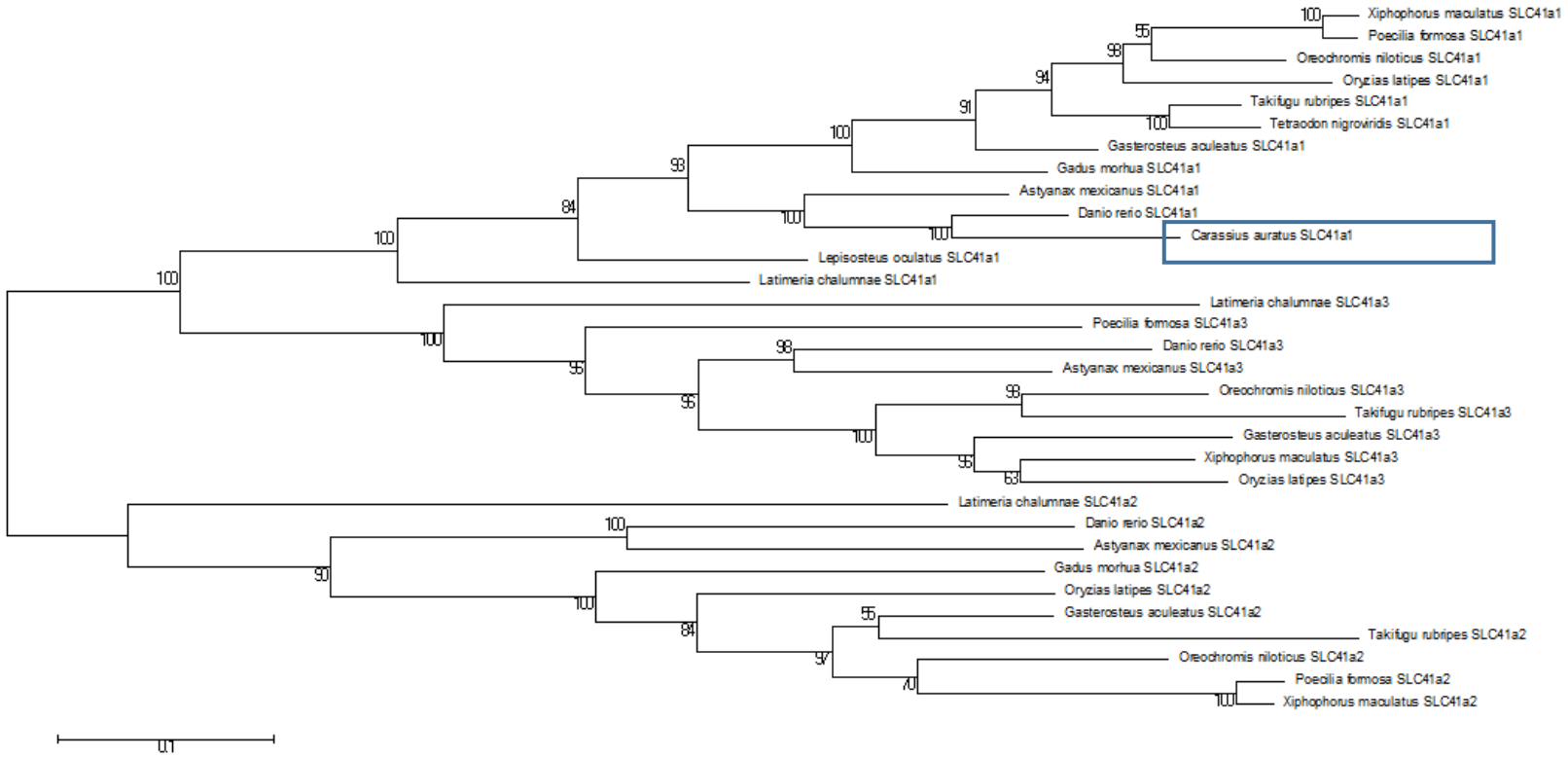

Figure 28: SLC41a1, a2 and a3 nucleotide phylogeny. Phylogenetic analysis of several teleost species for the SLC41a1, a2 and a3 genes, using cDNA sequences available on ensembl. The evolutionary history was inferred by using the Maximum Likelihood method based on the Tamura-Nei model (Tamura and Nei 1993). The tree with the highest log likelihood (-32117.0760) is shown. The percentage of trees in which the associated taxa clustered together is shown next to the branches. Initial tree(s) for the heuristic search were obtained automatically by applying Neighbor-Join and BioNJ algorithms to a matrix of pairwise distances estimated using the Maximum Composite Likelihood (MCL) approach, and then selecting the topology with superior log likelihood value. The tree is drawn to scale, with branch lengths measured in the number of substitutions per site. The analysis involved 32 nucleotide sequences. Codon positions included were 1st+2nd+3rd+Noncoding. There were a total of 2352 positions in the final dataset. Evolutionary analyses were conducted in MEGA6 (Tamura et al. 2013)

Figure 28 was constructed with the SLC41a1 sequences listed in Chapter 2, along with the following SLC41a2 and a3 sequences: *Danio rerio* (SLC41a2:ENSDARG00000075803; SLC41a3:ENSDARG00000061272), *Astyanax mexicanus* (SLC41a2:NSAMXG00000000997; SLC41a3:ENSAMXG00000012871), *Gadus morhua* (SLC41a2:ENSGMOG00000003515), *Oryzias latipes* (SLC41a2:ENSORLG00000016413; SLC41a3:ENSORLG00000001156), *Oreochromis niloticus* (SLC41a2:ENSONIG00000010462; SLC41a3:ENSONIG00000009165), *Poecilia formosa* (SLC41a2:ENSPFOG00000011668; SLC41a3:ENSPFOG00000002002), *Xiphophorus maculatus* (SLC41a2:ENSXMAG00000019285; SLC41a3:ENSXMAG00000001327), *Gasterosteus aculeatus* (SLC41a2:ENSGACG00000013493; SLC41a3:ENSGACG00000003711), *Takifugu rubripes* (SLC41a2:ENSTRUG00000001488; SLC41a3:ENSTRUG00000014991), *Latimeria chalumnae* (SLC41a2:ENSLACG00000012354; SLC41a3:ENSLACG00000014415).

```
Danio rerio                --- --- --- --- --- --- --- --- --- --- --- --- --- --- --- --- --- ---  [  48]
Xiphophorus maculatus      --- --- --- --- --- --- --- --- --- --- --- --- --- --- --- --- --- ---  [  48]
Tetraodon nigroviridis     --- --- --- --- --- --- --- --- --- --- --- --- --- --- --- --- --- ---  [  48]
Takifugu rubripes          --- --- --- --- --- --- --- --- --- --- --- --- --- --- --- --- --- ---  [  48]
Takifugu obscurus          --- --- --- --- --- --- --- --- --- --- --- --- --- --- --- --- --- ---  [  48]
Poecilia formosa           --- --- --- --- --- --- --- --- --- --- --- --- --- --- --- --- --- ---  [  48]
Oryzias latipes            --- --- --- --- --- --- --- --- --- --- --- --- --- --- --- --- --- ---  [  48]
Oreochromis niloticus      ATG ACT GTC CAC TCT GGT TGG AGA GAT ACT TTT CCA CAG TTG GTA ATT  [  48]
Lepisosteus oculatus       --- --- --- --- --- --- --- --- --- --- --- --- --- --- --- --- --- ---  [  48]
Latimeria chalumnae        --- --- --- --- --- --- --- --- --- --- --- --- --- --- --- --- --- ---  [  48]
Gasterosteus aculeatus     --- --- --- --- --- --- --- --- --- --- --- --- --- --- --- --- --- ---  [  48]
Gadus morhua               --- --- --- --- --- --- --- --- --- --- --- --- --- --- --- --- --- ---  [  48]
Carassius auratus          --- --- --- --- --- --- --- --- --- --- --- --- --- --- --- --- --- ---  [  48]
Astyanax mexicanus         --- --- --- --- --- --- --- --- --- --- --- --- --- --- --- --- --- ---  [  48]

Danio rerio                --- --- --- --- --- --- --- --- --- --- --- --- --- --- --- --- --- ---  [  96]
Xiphophorus maculatus      --- --- --- --- --- --- --- --- --- --- --- --- --- --- --- --- --- ---  [  96]
Tetraodon nigroviridis     --- --- --- --- --- --- --- --- --- --- --- --- --- --- --- --- --- ---  [  96]
Takifugu rubripes          --- --- --- --- --- --- --- --- --- --- --- --- --- --- --- --- --- ---  [  96]
Takifugu obscurus          --- --- --- --- --- --- --- --- --- --- --- --- --- --- --- --- --- ---  [  96]
Poecilia formosa           --- --- --- --- --- --- --- --- --- --- --- --- --- --- --- --- --- ---  [  96]
Oryzias latipes            --- --- --- --- --- --- --- --- --- --- --- --- --- --- --- --- --- ---  [  96]
Oreochromis niloticus      CAA TCC TCA TAC TGA GAC CTT TAA ATA TCT CAT TTG AAA ACC GTC CAG  [  96]
Lepisosteus oculatus       --- --- --- --- --- --- --- --- --- --- --- --- --- --- --- --- --- ---  [  96]
Latimeria chalumnae        --- --- --- --- --- --- --- --- --- --- --- --- --- --- --- --- --- ---  [  96]
Gasterosteus aculeatus     --- --- --- --- --- --- --- --- --- --- --- --- --- --- --- --- --- ---  [  96]
Gadus morhua               --- --- --- --- --- --- --- --- --- --- --- --- --- --- --- --- --- ---  [  96]
Carassius auratus          --- --- --- --- --- --- --- --- --- --- --- --- --- --- --- --- --- ---  [  96]
Astyanax mexicanus         --- --- --- --- --- --- --- --- --- --- --- --- --- --- --- --- --- ---  [  96]

Danio rerio                --- --- --- --- --- --- --- --- --- --- --- --- --- --- --- --- --- ---  [ 144]
Xiphophorus maculatus      --- --- --- --- --- --- --- --- --- --- --- --- --- --- --- --- --- ---  [ 144]
Tetraodon nigroviridis     --- --- --- --- --- --- --- --- --- --- --- --- --- --- --- --- --- ---  [ 144]
Takifugu rubripes          --- --- --- --- --- --- --- --- --- --- --- --- --- --- --- --- --- ---  [ 144]
Takifugu obscurus          --- --- --- --- --- --- --- --- --- --- --- --- --- --- --- --- --- ---  [ 144]
Poecilia formosa           --- --- --- --- --- --- --- --- --- --- --- --- --- --- --- --- --- ---  [ 144]
Oryzias latipes            --- --- --- --- --- --- --- --- --- --- --- --- --- --- --- --- --- ---  [ 144]
Oreochromis niloticus      CGG CCA CGT GGT GTA AAG TGA GAC GTT TGA AGC CCT GTG CAG CGA CCA  [ 144]
Lepisosteus oculatus       --- --- --- --- --- --- --- --- --- --- --- --- --- --- --- --- --- ---  [ 144]
Latimeria chalumnae        --- --- --- --- --- --- --- --- --- --- --- --- --- --- --- --- --- ---  [ 144]
Gasterosteus aculeatus     --- --- --- --- --- --- --- --- --- --- --- --- --- --- --- --- --- ---  [ 144]
Gadus morhua               --- --- --- --- --- --- --- --- --- --- --- --- --- --- --- --- --- ---  [ 144]
Carassius auratus          --- --- --- --- --- --- --- --- --- --- --- --- --- --- --- --- --- ---  [ 144]
Astyanax mexicanus         --- --- --- --- --- --- --- --- --- --- --- --- --- --- --- --- --- ---  [ 144]
```

```
Danio rerio                --- --- --- --- --- --- --- --- --- --- --- --- --- --- --- --- ---  [ 192]
Xiphophorus maculatus      --- --- --- --- --- --- --- --- --- --- --- --- --- --- --- --- ---  [ 192]
Tetraodon nigroviridis     --- --- --- --- --- --- --- --- --- --- --- --- --- --- --- --- ---  [ 192]
Takifugu rubripes          --- --- --- --- --- --- --- --- --- --- --- --- --- --- --- --- ---  [ 192]
Takifugu obscurus          --- --- --- --- --- --- --- --- --- --- --- --- --- --- --- --- ---  [ 192]
Poecilia formosa           --- --- --- --- --- --- --- --- --- --- --- --- --- --- --- --- ---  [ 192]
Oryzias latipes            --- --- --- --- --- --- --- --- --- --- --- --- --- --- --- --- ---  [ 192]
Oreochromis niloticus      GTC TCA CAT GGA CAG CAG ACT GAC AGC ATG ACC GGT GCC ACT GCG GGT  [ 192]
Lepisosteus oculatus       --- --- --- --- --- --- --- --- --- --- --- --- --- --- --- --- ---  [ 192]
Latimeria chalumnae        --- --- --- --- --- --- --- --- --- --- --- --- --- --- --- --- ---  [ 192]
Gasterosteus aculeatus     --- --- --- --- --- --- --- --- --- --- --- --- --- --- --- --- ---  [ 192]
Gadus morhua               --- --- --- --- --- --- --- --- --- --- --- --- --- --- --- --- ---  [ 192]
Carassius auratus          --- --- --- --- --- --- --- --- --- --- --- --- --- --- --- --- ---  [ 192]
Astyanax mexicanus         --- --- --- --- --- --- --- --- --- --- --- --- --- --- --- --- ---  [ 192]

Danio rerio                --- --- --- --- --- --- --- --- --- --- --- --- --- --- --- --- ---  [ 240]
Xiphophorus maculatus      --- --- --- --- --- --- --- --- --- --- --- --- --- --- --- --- ---  [ 240]
Tetraodon nigroviridis     --- --- --- --- --- --- --- --- --- --- --- --- --- --- --- --- ---  [ 240]
Takifugu rubripes          --- --- --- --- --- --- --- --- --- --- --- --- --- --- --- --- ---  [ 240]
Takifugu obscurus          --- --- --- --- --- --- --- --- --- --- --- --- --- --- --- --- ---  [ 240]
Poecilia formosa           --- --- --- --- --- --- --- --- --- --- --- --- --- --- --- --- ---  [ 240]
Oryzias latipes            --- --- --- --- --- --- --- --- --- --- --- --- --- --- --- --- ---  [ 240]
Oreochromis niloticus      CTC TGA TTT ACA TAT TTT TCC AGC TTG TAC TGA ACT GCT AAG GAC TGT  [ 240]
Lepisosteus oculatus       --- --- --- --- --- --- --- --- --- --- --- --- --- --- --- --- ---  [ 240]
Latimeria chalumnae        --- --- --- --- --- --- --- --- --- --- --- --- --- --- --- --- ---  [ 240]
Gasterosteus aculeatus     --- --- --- --- --- --- --- --- --- --- --- --- --- --- --- --- ---  [ 240]
Gadus morhua               --- --- --- --- --- --- --- --- --- --- --- --- --- --- --- --- ---  [ 240]
Carassius auratus          --- --- --- --- --- --- --- --- --- --- --- --- --- --- --- --- ---  [ 240]
Astyanax mexicanus         --- --- --- --- --- --- --- --- --- --- --- --- --- --- --- --- ---  [ 240]

Danio rerio                --- --- --- --- --- --- --- --- --- --- --- --- --- --- --- --- ---  [ 288]
Xiphophorus maculatus      --- --- --- --- --- --- --- --- --- --- --- --- --- --- --- --- ---  [ 288]
Tetraodon nigroviridis     --- --- --- --- --- --- --- --- --- --- --- --- --- --- --- --- ---  [ 288]
Takifugu rubripes          --- --- --- --- --- --- --- --- --- --- --- --- --- --- --- --- ---  [ 288]
Takifugu obscurus          --- --- --- --- --- --- --- --- --- --- --- --- --- --- --- --- ---  [ 288]
Poecilia formosa           --- --- --- --- --- --- --- --- --- --- --- --- --- --- --- --- ---  [ 288]
Oryzias latipes            --- --- --- --- --- --- --- --- --- --- --- --- --- --- --- --- ---  [ 288]
Oreochromis niloticus      TTG CAG CTG AAT GCA GGG GAA TTC TGT GGT GAG TCC CCT CCC TGT TGT  [ 288]
Lepisosteus oculatus       --- --- --- --- --- --- --- --- --- --- --- --- --- --- --- --- ---  [ 288]
Latimeria chalumnae        --- --- --- --- --- --- --- --- --- --- --- --- --- --- --- --- ---  [ 288]
Gasterosteus aculeatus     --- --- --- --- --- --- --- --- --- --- --- --- --- --- --- --- ---  [ 288]
Gadus morhua               --- --- --- --- --- --- --- --- --- --- --- --- --- --- --- --- ---  [ 288]
Carassius auratus          --- --- --- --- --- --- --- --- --- --- --- --- --- --- --- --- ---  [ 288]
Astyanax mexicanus         --- --- --- --- --- --- --- --- --- --- --- --- --- --- --- --- ---  [ 288]
```

```
Danio rerio                --- --- --- --- --- --- --- --- --- --- --- --- --- --- --- --- ---  [ 336]
Xiphophorus maculatus      --- --- --- --- --- --- --- --- --- --- --- --- --- --- --- --- ---  [ 336]
Tetraodon nigroviridis     --- --- --- --- --- --- --- --- --- --- --- --- --- --- --- --- ---  [ 336]
Takifugu rubripes          --- --- --- --- --- --- --- --- --- --- --- --- --- --- --- --- ---  [ 336]
Takifugu obscurus          --- --- --- --- --- --- --- --- --- --- --- --- --- --- --- --- ---  [ 336]
Poecilia formosa           --- --- --- --- --- --- --- --- --- --- --- --- --- --- --- --- ---  [ 336]
Oryzias latipes            --- --- --- --- --- --- --- --- --- --- --- --- --- --- --- --- ---  [ 336]
Oreochromis niloticus      TTT CTA TCC TTT TCT GTG TTG AAC CAG TAT GCC TTC TGT TTT TTG CCG  [ 336]
Lepisosteus oculatus       --- --- --- --- --- --- --- --- --- --- --- --- --- --- --- --- ---  [ 336]
Latimeria chalumnae        --- --- --- --- --- --- --- --- --- --- --- --- --- --- --- --- ---  [ 336]
Gasterosteus aculeatus     --- --- --- --- --- --- --- --- --- --- --- --- --- --- --- --- ---  [ 336]
Gadus morhua               --- --- --- --- --- --- --- --- --- --- --- --- --- --- --- --- ---  [ 336]
Carassius auratus          --- --- --- --- --- --- --- --- --- --- --- --- --- --- --- --- ---  [ 336]
Astyanax mexicanus         --- --- --- --- --- --- --- --- --- --- --- --- --- --- --- --- ---  [ 336]

Danio rerio                --- --- --- --- --- --- --- --- --- --- --- --- --- --- --- --- ---  [ 384]
Xiphophorus maculatus      --- --- --- --- --- --- --- --- --- --- --- --- --- --- --- --- ---  [ 384]
Tetraodon nigroviridis     --- --- --- --- --- --- --- --- --- --- --- --- --- --- --- --- ---  [ 384]
Takifugu rubripes          --- --- --- --- --- --- --- --- --- --- --- --- --- --- --- --- ---  [ 384]
Takifugu obscurus          --- --- --- --- --- --- --- --- --- --- --- --- --- --- --- --- ---  [ 384]
Poecilia formosa           --- --- --- --- --- --- --- --- --- --- --- --- --- --- --- --- ---  [ 384]
Oryzias latipes            --- --- --- --- --- --- --- --- --- --- --- --- --- --- --- --- ---  [ 384]
Oreochromis niloticus      GCC TAA CCT GAG CAC CTT GCA GTG AAT GGA GAA CAT ACT GGT TCT GCT  [ 384]
Lepisosteus oculatus       --- --- --- --- --- --- --- --- --- --- --- --- --- --- --- --- ---  [ 384]
Latimeria chalumnae        --- --- --- --- --- --- --- --- --- --- --- --- --- --- --- --- ---  [ 384]
Gasterosteus aculeatus     --- --- --- --- --- --- --- --- --- --- --- --- --- --- --- --- ---  [ 384]
Gadus morhua               --- --- --- --- --- --- --- --- --- --- --- --- --- --- --- --- ---  [ 384]
Carassius auratus          --- --- --- --- --- --- --- --- --- --- --- --- --- --- --- --- ---  [ 384]
Astyanax mexicanus         --- --- --- --- --- --- --- --- --- --- --- --- --- --- --- --- ---  [ 384]

Danio rerio                --- --- --- --- --- --- --- --- --- --- --- --- --- --- --- --- ---  [ 432]
Xiphophorus maculatus      --- --- --- --- --- --- --- --- --- --- --- --- --- --- --- --- ---  [ 432]
Tetraodon nigroviridis     --- --- --- --- --- --- --- --- --- --- --- --- --- --- --- --- ---  [ 432]
Takifugu rubripes          --- --- --- --- --- --- --- --- --- --- --- --- --- --- --- --- ---  [ 432]
Takifugu obscurus          --- --- --- --- --- --- --- --- --- --- --- --- --- --- --- --- ---  [ 432]
Poecilia formosa           --- --- --- --- --- --- --- --- --- --- --- --- --- --- --- --- ---  [ 432]
Oryzias latipes            --- --- --- --- --- --- --- --- --- --- --- --- --- --- --- --- ---  [ 432]
Oreochromis niloticus      CCC GAA GCA CCG ACA GGA ACA CAG GCT TTG CAG ACG CAC GGC TGC ATG  [ 432]
Lepisosteus oculatus       --- --- --- --- --- --- --- --- --- --- --- --- --- --- --- --- ---  [ 432]
Latimeria chalumnae        --- --- --- --- --- --- --- --- --- --- --- --- --- --- --- --- ---  [ 432]
Gasterosteus aculeatus     --- --- --- --- --- --- --- --- --- --- --- --- --- --- --- --- ---  [ 432]
Gadus morhua               --- --- --- --- --- --- --- --- --- --- --- --- --- --- --- --- ---  [ 432]
Carassius auratus          --- --- --- --- --- --- --- --- --- --- --- --- --- --- --- --- ---  [ 432]
Astyanax mexicanus         --- --- --- --- --- --- --- --- --- --- --- --- --- --- --- --- ---  [ 432]
```

```
Danio rerio                --- --- --- --- --- --- --- --- --- --- --- --- --- --- --- --- ---  [ 480]
Xiphophorus maculatus      --- --- --- --- --- --- --- --- --- --- --- --- --- --- --- --- ---  [ 480]
Tetraodon nigroviridis     --- --- --- --- --- --- --- --- --- --- --- --- --- --- --- --- ---  [ 480]
Takifugu rubripes          --- --- --- --- --- --- --- --- --- --- --- --- --- --- --- --- ---  [ 480]
Takifugu obscurus          --- --- --- --- --- --- --- --- --- --- --- --- --- --- --- --- ---  [ 480]
Poecilia formosa           --- --- --- --- --- --- --- --- --- --- --- --- --- --- --- --- ---  [ 480]
Oryzias latipes            --- --- --- --- --- --- --- --- --- --- --- --- --- --- --- --- ---  [ 480]
Oreochromis niloticus      TGC CTC GCT GCA GGT TTT TTC CGG CAG AGT GTT TTT CTC TCA GTC TTT  [ 480]
Lepisosteus oculatus       --- --- --- --- --- --- --- --- --- --- --- --- --- --- --- --- ---  [ 480]
Latimeria chalumnae        --- --- --- --- --- --- --- --- --- --- --- --- --- --- --- --- ---  [ 480]
Gasterosteus aculeatus     --- --- --- --- --- --- --- --- --- --- --- --- --- --- --- --- ---  [ 480]
Gadus morhua               --- --- --- --- --- --- --- --- --- --- --- --- --- --- --- --- ---  [ 480]
Carassius auratus          --- --- --- --- --- --- --- --- --- --- --- --- --- --- --- --- ---  [ 480]
Astyanax mexicanus         --- --- --- --- --- --- --- --- --- --- --- --- --- --- --- --- ---  [ 480]

Danio rerio                --- --- --- --- --- --- --- --- --- --- --- --- --- --- --- --- ---  [ 528]
Xiphophorus maculatus      --- --- --- --- --- --- --- --- --- --- --- --- --- --- --- --- ---  [ 528]
Tetraodon nigroviridis     --- --- --- --- --- --- --- --- --- --- --- --- --- --- --- --- ---  [ 528]
Takifugu rubripes          --- --- --- --- --- --- --- --- --- --- --- --- --- --- --- --- ---  [ 528]
Takifugu obscurus          --- --- --- --- --- --- --- --- --- --- --- --- --- --- --- --- ---  [ 528]
Poecilia formosa           --- --- --- --- --- --- --- --- --- --- --- --- --- --- --- --- ---  [ 528]
Oryzias latipes            --- --- --- --- --- --- --- --- --- --- --- --- --- --- --- --- ---  [ 528]
Oreochromis niloticus      ATG ACC GAC CTC CAC ACC TTG TCG GCC TCT TTA ATG GGA TAA ATC AGT  [ 528]
Lepisosteus oculatus       --- --- --- --- --- --- --- --- --- --- --- --- --- --- --- --- ---  [ 528]
Latimeria chalumnae        --- --- --- --- --- --- --- --- --- --- --- --- --- --- --- --- ---  [ 528]
Gasterosteus aculeatus     --- --- --- --- --- --- --- --- --- --- --- --- --- --- --- --- ---  [ 528]
Gadus morhua               --- --- --- --- --- --- --- --- --- --- --- --- --- --- --- --- ---  [ 528]
Carassius auratus          --- --- --- --- --- --- --- --- --- --- --- --- --- --- --- --- ---  [ 528]
Astyanax mexicanus         --- --- --- --- --- --- --- --- --- --- --- --- --- --- --- --- ---  [ 528]

Danio rerio                --- --- --- --- --- --- --- --- --- --- --- --- --- --- --- --- ---  [ 576]
Xiphophorus maculatus      --- --- --- --- --- --- --- --- --- --- --- --- --- --- --- --- ---  [ 576]
Tetraodon nigroviridis     --- --- --- --- --- --- --- --- --- --- --- --- --- --- --- --- ---  [ 576]
Takifugu rubripes          --- --- --- --- --- --- --- --- --- --- --- --- --- --- --- --- ---  [ 576]
Takifugu obscurus          --- --- --- --- --- --- --- --- --- --- --- --- --- --- --- --- ---  [ 576]
Poecilia formosa           --- --- --- --- --- --- --- --- --- --- --- --- --- --- --- --- ---  [ 576]
Oryzias latipes            --- --- --- --- --- --- --- --- --- --- --- --- --- --- --- --- ---  [ 576]
Oreochromis niloticus      TGG ACT GAT CAG GTT CAA AAC CAG ATC CGG TGG TCA ATT CTG ACT TTT  [ 576]
Lepisosteus oculatus       --- --- --- --- --- --- --- --- --- --- --- --- --- --- --- --- ---  [ 576]
Latimeria chalumnae        --- --- --- --- --- --- --- --- --- --- --- --- --- --- --- --- ---  [ 576]
Gasterosteus aculeatus     --- --- --- --- --- --- --- --- --- --- --- --- --- --- --- --- ---  [ 576]
Gadus morhua               --- --- --- --- --- --- --- --- --- --- --- --- --- --- --- --- ---  [ 576]
Carassius auratus          --- --- --- --- --- --- --- --- --- --- --- --- --- --- --- --- ---  [ 576]
Astyanax mexicanus         --- --- --- --- --- --- --- --- --- --- --- --- --- --- --- --- ---  [ 576]
```

```
Danio rerio                --- --- --- --- --- --- --- --- --- --- --- --- --- --- --- --- --- ---  [ 624]
Xiphophorus maculatus      --- --- --- --- --- --- --- --- --- --- --- --- --- --- --- --- --- ---  [ 624]
Tetraodon nigroviridis     --- --- --- --- --- --- --- --- --- --- --- --- --- --- --- --- --- ---  [ 624]
Takifugu rubripes          --- --- --- --- --- --- --- --- --- --- --- --- --- --- --- --- --- ---  [ 624]
Takifugu obscurus          --- --- --- --- --- --- --- --- --- --- --- --- --- --- --- --- --- ---  [ 624]
Poecilia formosa           --- --- --- --- --- --- --- --- --- --- --- --- --- --- --- --- --- ---  [ 624]
Oryzias latipes            --- --- --- --- --- --- --- --- --- --- --- --- --- --- --- --- --- ---  [ 624]
Oreochromis niloticus      CCA CAA AAC TGT TAG GCT GAG GCA CGC TGA CCT TTT CTT ATC AAG CCC  [ 624]
Lepisosteus oculatus       --- --- --- --- --- --- --- --- --- --- --- --- --- --- --- --- --- ---  [ 624]
Latimeria chalumnae        --- --- --- --- --- --- --- --- --- --- --- --- --- --- --- --- --- ---  [ 624]
Gasterosteus aculeatus     --- --- --- --- --- --- --- --- --- --- --- --- --- --- --- --- --- ---  [ 624]
Gadus morhua               --- --- --- --- --- --- --- --- --- --- --- --- --- --- --- --- --- ---  [ 624]
Carassius auratus          --- --- --- --- --- --- --- --- --- --- --- --- --- --- --- --- --- ---  [ 624]
Astyanax mexicanus         --- --- --- --- --- --- --- --- --- --- --- --- --- --- --- --- --- ---  [ 624]

Danio rerio                --- --- --- --- --- --- --- ATG GTA CTC TGG TTG AAA GAT CAA GAC  [ 672]
Xiphophorus maculatus      --- --- --- --- --- --- --- --- --- --- --- --- --- --- --- --- --- ---  [ 672]
Tetraodon nigroviridis     --- --- --- --- --- --- --- --- --- --- --- --- --- --- --- --- --- ---  [ 672]
Takifugu rubripes          --- --- --- --- --- --- --- --- --- --- --- --- --- --- --- --- --- ---  [ 672]
Takifugu obscurus          --- --- --- --- --- --- --- ... ... ..T ... .C. ... ..A ... ...  [ 672]
Poecilia formosa           --- --- --- --- --- --- --- ... ... ..T ... .CA ... ..A ... ..T  [ 672]
Oryzias latipes            --- --- --- --- --- --- --- --- --- --- --- --- --- --- --- --- --- ---  [ 672]
Oreochromis niloticus      ACT GTC TTC AAA GGC TTC CGC ... ... ..T ... .C. ... ..A ... ..A  [ 672]
Lepisosteus oculatus       --- --- --- --- --- --- --- ... .A. ..T ... .C. G.G .C. ... ..A  [ 672]
Latimeria chalumnae        --- --- --- --- --- --- --- --- --- --- --- --- --- --- --- --- --- ---  [ 672]
Gasterosteus aculeatus     --- --- --- --- --- --- --- --- --- --- --- --- --- --- --- --- --- ---  [ 672]
Gadus morhua               --- --- --- --- --- --- --- --- --- --- --- --- --- --- --- --- --- ---  [ 672]
Carassius auratus          --- --- --- --- --- --- --- --- --- --- --- --- --- --- --- --- --- ---  [ 672]
Astyanax mexicanus         --- --- --- --- --- --- --- ... ... ... ... .C. ... ..G ... ...  [ 672]
                                                                                PCR Primer 1 >>>
Danio rerio                AAA CTG TCC --- --- GAC ATG TCC ACC GGG ACG GAA AGG ATA GAG ATG  [ 720]
Xiphophorus maculatus      --- --- --- --- --- --- --- --- --- --- --- --- --- --- --- --- --- ---  [ 720]
Tetraodon nigroviridis     --- --- --- --- --- --- --- --- --- --- --- --- --- --- --- --- --- ---  [ 720]
Takifugu rubripes          --- --- --- --- --- --- --- --- --- --- --- --- --- --- --- --- --- ---  [ 720]
Takifugu obscurus          ... G.C C.. GAC ATC ... ... ... T.. ... GAC ACT GAA ..G A.. .AA  [ 720]
Poecilia formosa           ... ..C C.T GAC ATC ..G ... ... T.G ... GAC ATT GA. ..G A.. .A.  [ 720]
Oryzias latipes            --- --- --- --- --- --- --- --- --- --- --- --- --- --- --- --- --- ---  [ 720]
Oreochromis niloticus      ..G ..C C.. GAC ATC ... ... ... T.T ... G.C ATT GA. ..G A.. .A.  [ 720]
Lepisosteus oculatus       ... .AA ..A --- --- A.A ... ... ... .TC G.T .G. GAA TCC A.A .AA  [ 720]
Latimeria chalumnae        --- --- --- --- --- --- --- --- --- --- --- --- --- --- --- --- --- ---  [ 720]
Gasterosteus aculeatus     --- --- --- --- --- --- --- --- --- --- --- --- --- --- --- --- --- ---  [ 720]
Gadus morhua               --- --- --- --- --- --- --- --- --- --- --- --- --- --- --- --- --- ---  [ 720]
Carassius auratus          --- --- --- --- --- --- --- --- --- --- --- --G ... .A. ... ...  [ 720]
Astyanax mexicanus         ... ... ... A-- -CC ... ... ... ... ... ... ..G ..A ... ... ...  [ 720]
```

```
Danio rerio                 AAG AAG GAG GGG GTG CCG CCG GCG TAC CAC CAC TCC AAT GGG TCG GTC  [ 768]
Xiphophorus maculatus       --- --- --- --- --- --- --- --- --- --- --- --- --- --- --- ---  [ 768]
Tetraodon nigroviridis      --- --- --- --- --- --- --- --- --- --- --- --- --- --- --- ---  [ 768]
Takifugu rubripes           --- --- --- --- --- --- --- --- --- --- --- --- --- --- --- ---  [ 768]
Takifugu obscurus           G.. GGC .GC CCC C.. A.C .A. ..C .T. .T. AC. ... ..C T.C ..T ...  [ 768]
Poecilia formosa            G.. GGA .GT CCC C.. A.C ..A A.C .T. .T. A.T ..T ..C T.C ..T ...  [ 768]
Oryzias latipes             --- --- --- --- --- --- --- --- --- --- --- --- --- --- --- ---  [ 768]
Oreochromis niloticus       G.. GGA .GC CCC C.C A.T T.. ..C .T. .T. A.. ... ..C T.C A.C ...  [ 768]
Lepisosteus oculatus        G.A G-- --- -C. TCT .TT ..C .TT .T. ... ... G.G ... ... A.A ..G  [ 768]
Latimeria chalumnae         --- --- --- --- --- --- --- --- --- --- --- --- --- --- --- ---  [ 768]
Gasterosteus aculeatus      --- --- --- --- --- --- --- --- --- --- --- --- --- --- --- ---  [ 768]
Gadus morhua                --- --- --- --- --- --- --- --- --- --- --- --- --- --- --- ---  [ 768]
Carassius auratus           C.. ..T ... ... .CT ..A ..A ..T .T. .G. ... ... ... ... ... ..T  [ 768]
Astyanax mexicanus          ... ... ... ..A .C. ... ... ..C ... ... ... ... ... ... ..C ...  [ 768]

Danio rerio                 CAT CCG GTT ATA CTA CCA GAC AGC CCA GAG GAG GTA CCC CAG ACC CCC  [ 816]
Xiphophorus maculatus       --- --- --- --- --- --- --- --- --- --- --- A.G AG. .CA CAA A.T  [ 816]
Tetraodon nigroviridis      --- --- --- --- --- --- --- --- --- --- --- --- --- --- --- ---  [ 816]
Takifugu rubripes           --- --- --- --- --- --- --- --- --- --- --- --- --- --- --- ---  [ 816]
Takifugu obscurus           ..C ..C ..C ..C ..C A.C A.G GCT ..C ... ... A.G AGT .CA GGG A.G  [ 816]
Poecilia formosa            ..C ... C.G ..C ..C A.C CGA G.. ... ..A ... A.G AG. .CA CAA A.T  [ 816]
Oryzias latipes             --- --- --- --- --- --- --- --- --- --- --- --- --- --- --- ---  [ 816]
Oreochromis niloticus       ..C ... ..G ..C ..G A.C A.G G.. ..T ..A ..A ..G AG. .C. GTG A..  [ 816]
Lepisosteus oculatus        ... ... ..C ... .GG ..C ... ... .A. ... ... C.T .GG .TA GAA G.T  [ 816]
Latimeria chalumnae         --- --- --- --- --- --- --- --- --- --- --- --- --- --- --- ---  [ 816]
Gasterosteus aculeatus      --- --- --- --- --- --- --- --- --- --- --- --- --- --- --- ---  [ 816]
Gadus morhua                --- --- --- --- --- --- --- --- --- --- --- --- --- --- --- ---  [ 816]
Carassius auratus           ... ... ... .A. T.. ..T CT. ..A ..T ... ... ..G ... ... G.. .TT  [ 816]
Astyanax mexicanus          ..C ... ..C ..C ..G ..C .G. GA. ..C ... ... AGG .AG .CC .A. G..  [ 816]

Danio rerio                 GGG --- GAG TAC GAA CTC ACA GAG GTG ACC TCC TTA CCG GAC T-- ---  [ 864]
Xiphophorus maculatus       ..A GGC ... .T. ..G ... ..C ... ..C ..G ..T ..C A.. ..A A-- -GG  [ 864]
Tetraodon nigroviridis      --- --- --- --- --- --- --- --- --- --- --- --- --- --- --- ---  [ 864]
Takifugu rubripes           --- --- --- --- --- --- --- --- --- --- --- --- --- --- --- ---  [ 864]
Takifugu obscurus           ... CCA ... .T. ..G ..G ... ... ... G.T ..A ..T GT. ..G ATG AGG  [ 864]
Poecilia formosa            ..A GGC ... .T. ..G ... ..T ... ..T ..G ..T ..C A.. ..A A-- -GG  [ 864]
Oryzias latipes             --- --- --- --- --- --- --- --- --- --- --- --- --- --- --- ---  [ 864]
Oreochromis niloticus       ... GAT ... .TT ..G ... ..C ... ..C ..A ..T ..C ..C ..G C-- -GA  [ 864]
Lepisosteus oculatus        ... --- .TC .G. ..G ..G ..G ... ..C C.G G.. ..T T.. ... C-- ---  [ 864]
Latimeria chalumnae         --- --- --- --- --- --- --- --- --- --- --- --- --- --- --- ---  [ 864]
Gasterosteus aculeatus      --- --- --- --- --- --- --- --- --- --- --- --- --- --- --- ---  [ 864]
Gadus morhua                --- --- --- --- --- --- --- --- --- --- --- --- --- --- --- ---  [ 864]
Carassius auratus           ... --- ... ... .C. ... ... ..A A.. T.. ... ACG T.. ..A C-- ---  [ 864]
Astyanax mexicanus          ..A --- ... ... ..G ... ... ... ..T ... ..T ..C T.. ... C-- ---  [ 864]
```

```
Danio rerio                --- --- -GC GGT GAT CAG GAG AAT GAG CGT CCG GA- --C ATG GTG GTC  [ 912]
Xiphophorus maculatus      ATC GGT GAG ACC .GG G.A A.C G.G ... A.G T.A ..G AT. G.. ... .CA  [ 912]
Tetraodon nigroviridis     --- --- --- --- --- --- --- --- --- --- --- --- ATT ... ... .CG  [ 912]
Takifugu rubripes          --- --- --- --- --- --- --- --- --- --- --- G.A ..G ATT G.. ... .CG  [ 912]
Takifugu obscurus          GTC AGC GAG ACC .GC G.. ..T G.G ... A.G G.A ..G ATT G.. ... .CG  [ 912]
Poecilia formosa           ATC GGT GAG ACC ..G G.A A.T G.G ... A.G T.. ..G ATT G.. ... .CA  [ 912]
Oryzias latipes            --- --- --- --- --- --- --- --- --- --- --- --- --- G.A ..A .CA  [ 912]
Oreochromis niloticus      GTG AAT GAG AC. .GG G.. A.C G.C ... A.G T.. ..G ATT G.. ... .C.  [ 912]
Lepisosteus oculatus       --- --- -.A .CC ..G .CT ..C CGC ..C A.G G.C ..- --A G.A ... ..G  [ 912]
Latimeria chalumnae        --- --- --- --- --- --- --- --- --- --- --- --- --- --- --- ---  [ 912]
Gasterosteus aculeatus     --- --- --- --- --- --- --- --- --- --- --- --- --- G.. ... .CG  [ 912]
Gadus morhua               --- --- --- --- --- --- --- --- --- --- --- --- --- G.. .CC A..  [ 912]
Carassius auratus          --- --- -A. A.. ... ..A ... ... ..A A.. ..A ..- --. ... ..T ...  [ 912]
Astyanax mexicanus         --- --- -.G .CC ..G ..A ... ..C ..C .A. T.C ..- --A ... ... ...  [ 912]

Danio rerio                CTC GAC TGT CGG GCC AAC GCG AAA GGC CAG AGG GAA GAG GAC GCG CTT  [ 960]
Xiphophorus maculatus      T.A ... ..C ... ... ... ..C ... ... ..A C.A ..G ... ..T ..T ..C  [ 960]
Tetraodon nigroviridis     A.G ... ..C ... ..A ..T ..C ... ..T ... C.. ..G ..A ..T ..T ..C  [ 960]
Takifugu rubripes          A.G ... ..C ... ..A ..T ..C ... ..T ... C.. ..G ..A ... ..T ..C  [ 960]
Takifugu obscurus          A.G ... ..C ... ..A ..T ..C ... ..T ... C.. ..G ..A ... ..T ..C  [ 960]
Poecilia formosa           T.A ... ... ... ... ..T ..C ... ..T ..A C.A ..G ... ..T ..T ..C  [ 960]
Oryzias latipes            A.A ... ... .TA .A. ... .TC ... ..T ... C.A ..G ... ..T ... ..C  [ 960]
Oreochromis niloticus      A.G ... ... ... ... ..T ..C ... ..T ... C.A ..G ... ..T ..T ..C  [ 960]
Lepisosteus oculatus       A.. ... ..C ... ... ... ..C ..G ..G ... ... ..G ... ... ... ..C  [ 960]
Latimeria chalumnae        --- --- --- --- --- --- --- --- --- --- --- --- --- --- --- ---  [ 960]
Gasterosteus aculeatus     A.G ... ..C ... ... ... ..C ... ..T ... ... ..G ... ... ..C ..G  [ 960]
Gadus morhua               G.G ... ..C ..C ... ... ..C ... ... ... C.C ..G ... ... ... ..G  [ 960]
Carassius auratus          ... AT. ... ... ... ... ..A ..G .A. ... ... .G. ... .G. A.. ..C  [ 960]
Astyanax mexicanus         A.T ... ... ... ... ..T ..C ..G ..G ... ... ..G ... ... ..T ..C  [ 960]
                               qPCR Primer 1>>>
Danio rerio                TTG GAG AAC GCT AGC CAA AGC AAT GAG AGT GAT GAC ACT AGT ACG GAC  [1008]
Xiphophorus maculatus      C.. ... ... ..A ... ..G ... ..C ... ... ..C ... .AC ..C .TC A.T  [1008]
Tetraodon nigroviridis     C.. ... ... ..A ..T ..G ... ..C ... ..C ... ... ..C ..C .TC A..  [1008]
Takifugu rubripes          C.. ... ... .GA ..T ..G ... ..C ... ..C ..C ... ..C ..C .TC A..  [1008]
Takifugu obscurus          C.. ... ... ..A ..T ..G ... ..C ... ..C ..C ... ..C ..C .TC A..  [1008]
Poecilia formosa           C.. ... ..T ..A ... ..G ... ..C ... ..C ..C ... .AC ..C .TC A.T  [1008]
Oryzias latipes            C.. ... ..T ..G ..T ..G ... ... ... ... ..C ... ..C ..C ..C A.T  [1008]
Oreochromis niloticus      C.. ... ..T ..A ... ..G ... ..C ... ... ... ... ..C ..C ..C ..T  [1008]
Lepisosteus oculatus       ... ... ... ..C ... ..G ... ..C ... ..- --C ... .TC ..C G.C ...  [1008]
Latimeria chalumnae        --- --- --- --- --- --- --- --- --- --- --- --- --- --- --- ---  [1008]
Gasterosteus aculeatus     C.. ... ... ..C ... ..G T.. ..C ... ..C ..C ... ..C ..C ..C ...  [1008]
Gadus morhua               C.. ... ... ... TC. ..G ... ..C ... ..C ..C ... ..C ..C GG. .G.  [1008]
Carassius auratus          C.. ... ... ..C ... ... ... ..C ... ... T.. .T. ... ... G.. ...  [1008]
Astyanax mexicanus         ... ... ... ..C ... ... ... ..C ..A ... ... ... ..A ..C ... ...  [1008]
```

```
Danio rerio                CAA AGC CCG GTG CCG CCG GCT CCA CTT AAG GAA ACG TCC TTC TCT ATT  [1056]
Xiphophorus maculatus      ..G ... ..T .A. ..A ..A ..G ..G ..C ... ..G ..C ... A.T ..C ..C  [1056]
Tetraodon nigroviridis     ..G ... ..A CA. ... ..A ... ..G ..C ..A ... ..C ... C.G AGC ..C  [1056]
Takifugu rubripes          ..G ... ..A .AA ..A ..A ... ..T ..C ..A ... .GC ... C.G A.C ...  [1056]
Takifugu obscurus          ..G ... ..A .AA ..A ..A ... ..T ..C ..A ... .GC ... C.G A.C ...  [1056]
Poecilia formosa           ..G ... ..T .AA ..A ..A ..G ..G ..C ... ..G ..C ... A.T ..C ..C  [1056]
Oryzias latipes            .GG ... ..T .AA ..A ... ..A ..C T.C ... ..G .GC ... ... ..C ..C  [1056]
Oreochromis niloticus      ..G ... ..C .AA ..A A.A ..A ..C ..C ... ..G ..C ... ..T ..C ..C  [1056]
Lepisosteus oculatus       ... ... ..C A.. ..C G.. ..G ..G ..G ... ..G ... ... ... ..C ..C  [1056]
Latimeria chalumnae        --- --- --- --- --- --- --- --- --- --- --- --- --- --- --- ---  [1056]
Gasterosteus aculeatus     ..G ... ... .A. ... ... C.C ..C ..C ... ..G ..C ... ... ..C ..C  [1056]
Gadus morhua               ..G ... ..C .A. ... ... C.C ..C ..C ... ..G ..C G.. ... ..C ..C  [1056]
Carassius auratus          ... .C. ... ..T ... T.. .T. ..T A.G ... ... ..A ... ..T ... ...  [1056]
Astyanax mexicanus         ... ... ..A ... ..A ... ... ..T ..G ... ..G ..A ... ... ..C ..C  [1056]

Danio rerio                GGA CTC CAG GTT TTG ATC CCT TTC CTG CTG GCA GGG TTT GGG ACG GTT  [1104]
Xiphophorus maculatus      ..T ..T ..A ..G G.T T.T ..C ..T ... ... ..T ..C ..C ..A ... ..G  [1104]
Tetraodon nigroviridis     ..G ... ... ..G G.C T.. ..C ... ... ... ..T ..C ... ... ... ..G  [1104]
Takifugu rubripes          ..G ... ... ..G G.C T.. ..C ... ... ... ..T ... ... ... ..A ..A  [1104]
Takifugu obscurus          ..G ... ... ..G G.C T.. ..C ... ... ... ..T ... ... ... ..A ..A  [1104]
Poecilia formosa           ..T ..T ..A ..G G.T T.T ..C ..T ... ... ..T ..C ..C ..A ... ..G  [1104]
Oryzias latipes            ..T ..G ..A ..G G.T T.T ..C ... ... ... ..C ... ..C ... ..A ..A  [1104]
Oreochromis niloticus      ... ..G ... ..G G.C T.. ..C ... T.. ... ..C ... ..C ... ... ..G  [1104]
Lepisosteus oculatus       ..G ..G ... ..C C.. T.. ..C ... ... ... ..G ... ..C ..A ..A ..A  [1104]
Latimeria chalumnae        --- --- --- --- --- --- --- --- --- --- --- --- --- --- --- ---  [1104]
Gasterosteus aculeatus     ..C ..A ... ..G G.C T.. ..C ... ... ... ..C ... ... ... ... ..G  [1104]
Gadus morhua               ..C ..G ... ..G G.C T.. ..C ... ... ... ..C ... ... ... ... ..G  [1104]
Carassius auratus          ... ... ... ... A.. ... ... ... T.. ... ... ... ... ... ..A ...  [1104]
Astyanax mexicanus         ... ... ... ..C G.. T.. ... ... ... ... ..G ... ... ..A ..A ..G  [1104]
                             <<<qPCR Primer 2
Danio rerio                GCT GCT GGC ATG GTA CTG GAC ATT GTT CAG CAC TGG ACA GTG TTC ACA  [1152]
Xiphophorus maculatus      ..A ..A ..A ... T.G ..A ... ... ..C ..A ... ... ..G ... ... ...  [1152]
Tetraodon nigroviridis     ..G ... ..G ... ..T ..C ... ... ..G ... ... ... C.T ... ... .AG  [1152]
Takifugu rubripes          ... ... ..A ... ..T ... ... ..C ..C ... ... ... C.C ... ..T .AG  [1152]
Takifugu obscurus          ... ... ..A ... ..T ... ... ... ..C ... ... ... C.C ... ..T .AG  [1152]
Poecilia formosa           ..A ..A ..A ... T.G ..A ... ... ..C ..A ... ... ..G ... ... ...  [1152]
Oryzias latipes            ... ..G ..A ... ..G T.. ... ..C ..C ... ... ... ..G ... ..T .TT  [1152]
Oreochromis niloticus      ..A ..A ..G ... ..G ..A ... ..C ..C ... ... ... ..G ... ... ..C  [1152]
Lepisosteus oculatus       ..C ..C ... ... ..C ... ... ..C ..G ... ... ... ..G ... ... .AG  [1152]
Latimeria chalumnae        ATG C.. TTT T.T ..T T.- --T TCC CCA ... ... ... GA. ..C ..T .AG  [1152]
Gasterosteus aculeatus     ..G ..C ..A ... ..G ..C ... ... ... ... ... ... ..G ... ... ..G  [1152]
Gadus morhua               ..G ..G ..G ... ..G ... ... ... ..G ... ... ... .TC ... ... ...  [1152]
Carassius auratus          ..A ... CA. ... ..T .C. ... ... ..A ... ..A ... T.G ..A ... ...  [1152]
Astyanax mexicanus         ..C ... ... ... ..C ..C ... ..A ... ..A ..T ... .A. ... ... G.T  [1152]
```

```
Danio rerio                GAG GTG ACT GAA GTC TTT ATC CTT GTG CCT GCT CTC CTG GGC CTG AAA  [1200]
Xiphophorus maculatus      A.. ... T.G ... ... ..C ... ... ..T ... ..G T.G T.. ..G ..A ...  [1200]
Tetraodon nigroviridis     ... ... ..G ..G ..G ..C ... ..G ..T ..A ..A ..T ... ..T ..C ...  [1200]
Takifugu rubripes          ... ... ..G ..G ..G ..C ... ..G ..T ..G ..A ..G ... ..T ..C ...  [1200]
Takifugu obscurus          ..C ... ..G ..G ..G ..C ... ..G ..T ..G ..A ..G ... ..T ..C ...  [1200]
Poecilia formosa           ... ... T.G ... ... ..C ... ... ..T ... ..A T.G T.. ..G ..A ...  [1200]
Oryzias latipes            ... ... T.G ..G ..G ..C ..T ..G ..T ... ..A T.G T.. ..G ..C ...  [1200]
Oreochromis niloticus      ..T ... T.. ..G ..G ..C ... ... ..T ... ..A ..G ... ..G ..T ...  [1200]
Lepisosteus oculatus       ... ... ..G ..G ..G ... ..T ..A ..T ... ..C ... ... ..G ..C ..G  [1200]
Latimeria chalumnae        C.. ... .A. ... ..A ... ... T.A ..C ... ... ... ... ..A ... ..G  [1200]
Gasterosteus aculeatus     ... ... T.A ..G ..T ..C ... ..G ... ..G ..G ..G ... ..A ..C ...  [1200]
Gadus morhua               ... ... ..C ..G ..G ..C ... ..G ..C ..C ... ..T ... ..A ..C ...  [1200]
Carassius auratus          ... ... T.C ... ... ... ... ..- ... ... ... ... T.. ... .C. ...  [1200]
Astyanax mexicanus         ... ... .A. ..G ... ..C ... ..G ... ... ... ... T.. ..T ..C ..G  [1200]

Danio rerio                GGG AAC TTG GAG ATG ACC CTT GCA TCC AGA CTG TCT ACC GCG GCT AAT  [1248]
Xiphophorus maculatus      ... ... ..A ... ... ..G ..G ..C ..T ..G ..T ..A ..A ... ... ...  [1248]
Tetraodon nigroviridis     ..C ... C.. ... ... ... ..G ..C ... ... ... ..A ..A ... ... ...  [1248]
Takifugu rubripes          ..C ... C.. ... ... ..G ..G ..C ... ... ... ..A ..A ... ... ...  [1248]
Takifugu obscurus          ..C ... C.. ... ... ..G ..G ..C ... ... ... ..A ..A ... ... ...  [1248]
Poecilia formosa           ... ... ... ... ... ..G ..G ..C ... ..G ..T ..A ..A ... ... ...  [1248]
Oryzias latipes            ..C ... ... ... ... ..A ..G ..C ... ..G ..T ..C ..A ... ... ...  [1248]
Oreochromis niloticus      ..C ... ... ... ... ..G ..G ..C ..T ... ..T ... ..A ... ... ...  [1248]
Lepisosteus oculatus       ... ..T C.. ..A ... ..T ..G ..T ... C.G ..C ..C ... ..A ..C ..C  [1248]
Latimeria chalumnae        ... ... C.. ..A ... ..T T.A ..T ... C.G ..C ..C ..T ..T ... ..C  [1248]
Gasterosteus aculeatus     ..C ... C.. ... ... ..G T.G ..C ... ... ..T ..C ... ... ..G ...  [1248]
Gadus morhua               ..C ... C.. ... ... ... ..A ..T ..A ... ..C ..C ... ... ..G ..C  [1248]
Carassius auratus          ... ... ... ... ... .T. ..G ... ... ... ... ... ..T ..A ... ...  [1248]
Astyanax mexicanus         ... ... C.. ... ... ..A ..G ..C ..T ... ..T ..A ..T ..A ... ...  [1248]

Danio rerio                ATT GGA CAA ATG GAC ACA GCC AAG GAT ATG TGG AAA ATG ATC ATG GGA  [1296]
Xiphophorus maculatus      ... ..T ..G ... ... ... ... ... ..C ... ... ..G ... ... G.A ..G  [1296]
Tetraodon nigroviridis     ... ..T ... ... ... ..G ... ... ... ... ... ... ... ... ... ..G  [1296]
Takifugu rubripes          ... ..T ... ... ... ..G ... ... ..C ... ... ..G ... ... ... ..G  [1296]
Takifugu obscurus          ... ..T ... ... ... ..G ... ... ..C ... ... ..G ... ... ... ..G  [1296]
Poecilia formosa           ... ..T ..G ... ... ... ... ... ..C ... ... ..G ... ... ... ..G  [1296]
Oryzias latipes            ... ..T ... ... ..T ... ... ... ..C ... ... ... ... G.T ... ...  [1296]
Oreochromis niloticus      ... ..G ..C ... ... ... ... ... ..C ... ... ..G ... ... ... ..G  [1296]
Lepisosteus oculatus       ... ..G ..G ... ... ..T ... ... ..A ... ... ... ... ... ..A ...  [1296]
Latimeria chalumnae        ... ..G ..G ... ... ... ... .CA .GA C.. ... ..G ... ... .CA ..G  [1296]
Gasterosteus aculeatus     ... ..T ..G ... ... ... ... ... A.C ... ... ..G ... ..A ... ..G  [1296]
Gadus morhua               ..C ..G ..G ... ... ... C.G ... ..C ... ... ..G ... ... G.. ..G  [1296]
Carassius auratus          ... ... ... ... ..T ..G ..G ... ... ... ... ..G ... ... ... ..G  [1296]
Astyanax mexicanus         ... ..G ..G ... ... ..C ... ... ..G ... ... ... ... ..A ... ...  [1296]
```

```
Danio rerio                AAC CTC GCG CTA ATT CAG GTT CAG GCC ACC GTG GTC GGA TTT CTG GCT  [1344]
Xiphophorus maculatus      ... T.G ..C ..C ..C ... ..C ... ... ..A ..T ..G ..G ..C ... ...  [1344]
Tetraodon nigroviridis     ... T.G ..T ..C ... ... ..C ... ..T ..A ... ..G ..G ..C ... ..C  [1344]
Takifugu rubripes          ... T.G ..T ..C ... ... ..C ... ..T ..A ... ..G ..G ..C ..T ..C  [1344]
Takifugu obscurus          ... T.G ..T ..C ... ... ..C ... ..T ..A ... ..G ..G ..C ..T ..C  [1344]
Poecilia formosa           ... T.G ..C ..C ..C ... ..C ... ... ..A ..T ..G ..G ..C ... ...  [1344]
Oryzias latipes            ... T.G ..C ... ..C ... ..C ... ..G ..A ... ..G ..G ..C ... ...  [1344]
Oreochromis niloticus      ... T.G ..C ..C ..C ... ..C ..A ... ..A ... ..G ..G ..C ... ..C  [1344]
Lepisosteus oculatus       ... T.G ..T ..T ... ... ... ... ... ..G ..A ..G ... ..C ... ..C  [1344]
Latimeria chalumnae        ... A.G ..C ..C ..A ... ..C ... ..A ..A ... ..G ..C ... ..T ..C  [1344]
Gasterosteus aculeatus     ... T.G ..T ..C ..C ... ... G.A A.. ..A ... ..G ..C ..C ... ..C  [1344]
Gadus morhua               ..T ..G ..C ... ..C ... --- --- --- ..A ... ..G ..C ..C ... ..C  [1344]
Carassius auratus          ... ... ..A ... ... ... ... ... ... ..A ..A ... ..C ..C ... ...  [1344]
Astyanax mexicanus         ... ..T ... ..G ... ... ..A ... ... ... ... ..T ..C ..C ... ..C  [1344]

Danio rerio                TCC ATC GCC GCC GTC ATC TTT GGC TGG ATC CCA GAG GGC AAC TTT AGG  [1392]
Xiphophorus maculatus      ... ..A ..T ..T ..A ... ... ... ... C.. ... ... ..A C.G ..C CA.  [1392]
Tetraodon nigroviridis     ... ..T ..A ..T ..G ... ..C A.. ... ..T ... ... ... C.. ..C ...  [1392]
Takifugu rubripes          ... ... ..G ..T ..G ... ..C A.. ... ..T ... ... ..A C.. ..C C..  [1392]
Takifugu obscurus          ... ... ..G ..T ..G .C. ..C A.. ... ..T ... ... ..A C.. ..C C..  [1392]
Poecilia formosa           ... ..A ..T ..T ..A ... ... ... ... C.. ... ... ..A G.G ..C .A.  [1392]
Oryzias latipes            ... ..A ..T ..T ..G ... ... ... ... ... ... ... ..A C.. A.C ...  [1392]
Oreochromis niloticus      ... ..A ..T ..T ..G ... ... ... ... ... ... ... ..A C.. ..C .A.  [1392]
Lepisosteus oculatus       ... ..T ..T ... ... ... ... ... ... ... ... ... ..G C.T ..C .A.  [1392]
Latimeria chalumnae        ..T ..T ..T ..G ..G G.G ... ... ... ... ... ..T ..A C.. ... GAT  [1392]
Gasterosteus aculeatus     ... ..A ..T ..T ..G ... ..C ... ... ... ..T ... ..A C.. ... C..  [1392]
Gadus morhua               ... ..A ..G ..T ..G ... ..C ... ... ... ... ... ..T C.G ..C ...  [1392]
Carassius auratus          ... ... ..T ..A ... ..T ... ... ... ..T ... ... ..T ..T ... .A.  [1392]
Astyanax mexicanus         ... ..T ..T ..A ... ..T ... ... ... ..T ... ... ... ..T ..C .A.  [1392]

Danio rerio                ATG GGT CAT GCC ATC CTG CTC TGT GCC AGC AGC GTG GCC ACC GCA TTC  [1440]
Xiphophorus maculatus      C.. ..C ... ..A G.G ... ..G ... ... TC. ... A.. ... ..T ..C ...  [1440]
Tetraodon nigroviridis     C.. A.C ... ... G.G ... ..G ..C ... TC. ..T ..T ..T ..T ..C ...  [1440]
Takifugu rubripes          C.. ..C ... ..T G.G ... ..G ... ... TCT ..T ..T ..T ..T ... ..T  [1440]
Takifugu obscurus          C.. ..C ... ..T G.G ... ..G ... ... TCT ..T ..C ..T ..T ... ..T  [1440]
Poecilia formosa           C.. ..C ... ..G G.G ... ..G ... ... TC. ... A.. ... ..A ..C ...  [1440]
Oryzias latipes            C.. ... ..C ... G.G ... ..G ..C ... TC. ... ..T ... ... ..C ...  [1440]
Oreochromis niloticus      C.. ..C ... ..A G.G ... T.G ... ... TCT ..T ... ... ..T ..C ...  [1440]
Lepisosteus oculatus       ..T ..C ... ..A ..A ... ..G ... ... ... ..T ... ... ..A ..C ...  [1440]
Latimeria chalumnae        C.T ..A ... ..T G.T ..C ..G ... ... ..T ..T ..A ... ..T ..G ...  [1440]
Gasterosteus aculeatus     C.C ..C ..C ... G.G ... ..G ... ... TC. ..T ... ..G ... ..C ...  [1440]
Gadus morhua               C.. ..C ... ... G.G G.. ..G ... ... TC. ... ... ... ..G ..C ...  [1440]
Carassius auratus          ... ..C ... ... G.. ... ... ... ... ... ... ... ... ..T ... ...  [1440]
Astyanax mexicanus         ... ..C ... ..A G.T ..T ..T ... ... ... ... ..A ... ..A ..C ...  [1440]
```

```
Danio rerio                ATC GCC TCT TTG GCT TTA GGT CTT ATC ATG ATC GGG GTT ATC ATC GCA  [1488]
Xiphophorus maculatus      ... ..A ..G C.A CTC C.G ... ..C ... ... ... ..C ..G ..T G.T ..G  [1488]
Tetraodon nigroviridis     ... ... ... C.. CTG C.. ..A ..C ... ... ... ..C ..G ..T G.G ...  [1488]
Takifugu rubripes          ..T ... ... C.. CTG C.. ..A ..C ... ... ... ..C ..G ..T ... ...  [1488]
Takifugu obscurus          ..T ... ... C.. CTG C.. ..A ..C ... ... ... ..C ..G ..T ... ...  [1488]
Poecilia formosa           ... ..A ..G C.. CTC C.G ... ..C ... ... ... ..C ..G ..T G.. ..G  [1488]
Oryzias latipes            ..T ..T ..C C.C ATC C.C ... ..C ... ... ..T ..C ... ... ... ...  [1488]
Oreochromis niloticus      ... ..T ... ... CT. C.. ... ..C ... ... ... ..C ..C ..T G.T ...  [1488]
Lepisosteus oculatus       ... ... ..C C.C CTG C.G ... ..G ... ... ..T ..A ..G ... ..T .GC  [1488]
Latimeria chalumnae        ..A ..T ..G C.C ATA ..G ... A.G ... ... ..T ... ... ..T ..T .GC  [1488]
Gasterosteus aculeatus     ... ... ... C.. CTG C.T ..G G.C ... ... ... ..C ..G ... ... ..G  [1488]
Gadus morhua               ..A ... ..C C.. CTG C.. ... ..C ... ... ... ..T ..G ... C.G TTG  [1488]
Carassius auratus          ... ..T ... ... ..G C.. ... ... ... ... ..T ..A ..C ... ..T ...  [1488]
Astyanax mexicanus         ..A ... ..C ... CTG C.. ..C ..C G.. ... ..T ... ..G ... ..A ..T  [1488]

Danio rerio                TCC AGG AAG GTT GGC ATA AAC CCA GAC AAC GTG GCC ACC CCT ATT GCT  [1536]
Xiphophorus maculatus      ..G ..A ..A ..C ... ..C ... ... ... ... ... ... ..A ..C ..C ..C  [1536]
Tetraodon nigroviridis     ... ..A ..A A.C ..G ..C ... ..T ... ... ... ... ..A ..C ..C ...  [1536]
Takifugu rubripes          ... ..A ..A A.C ... ..C ... ..T ... ... ... ... ..G ..C ..C ...  [1536]
Takifugu obscurus          ... ..A ..A A.C ... ..C ... ..T ... ... ... ... ..G ..C ..C ...  [1536]
Poecilia formosa           ..G ..A ..A ..C ... ..C ..T ... ... ... ... ... ..A ..C ..C ...  [1536]
Oryzias latipes            ... ... ..A ... ... ..C ... ..T ... ..T ... ... ..A ..C ..C ...  [1536]
Oreochromis niloticus      ... ..A ..A ..C ... ..C ... ..T ... ..T ... ... ..A ... ... ...  [1536]
Lepisosteus oculatus       ..T ... ... A.A ... ... ... ..G ... ..T ..T ..A ..A ..C ..C ..G  [1536]
Latimeria chalumnae        ..G ... ... A.C ..T ..C ... ..C ..T ..T ..C ..G ..T ..A ... ...  [1536]
Gasterosteus aculeatus     ... ... ..A ..C ... ..C ... ..T ... ... ... ... ..G ..C ..C ..C  [1536]
Gadus morhua               ... ... ... ..G ..T ..C ... ..G ... ... ... ... ..G ..C ... ...  [1536]
Carassius auratus          ... ... ... ... ... ..C ... ... ... ..T ... ... ... ..C ... ..A  [1536]
Astyanax mexicanus         ... ..A ... ... ... ..T ..T ... ... ... ... ... ... ... ... ...  [1536]

Danio rerio                GCC AGC CTG GGT GAC CTG ATC ACG CTG TCG CTG CTG GCT GGC ATC AGC  [1584]
Xiphophorus maculatus      ..T ... ..C ..A ... ... ..T ..C T.. ..C ... ... ..A ... ... TCA  [1584]
Tetraodon nigroviridis     ... ... ... ..A ... T.. ... ..C ... ..C ..C ..C ..A ... ... TC.  [1584]
Takifugu rubripes          ... ... ... ..A ... T.. ... ..C ... ..C ..C ..C ..A ... ... TC.  [1584]
Takifugu obscurus          ... ... ... ..A ... T.. ... ..C ... ..C ..C ..C ..A ... ... TC.  [1584]
Poecilia formosa           ..T ... ..C ..A ... ... ..T ..C T.. ..C ... ... ..A ... ... TCA  [1584]
Oryzias latipes            ..A ... ..C ..G ... ..A ... ..C ..T ..C ..A ... ..A ... ... TC.  [1584]
Oreochromis niloticus      ..T ... ..A ..A ..T ... ... ... ... ..C ... ... ..A ... ... TCA  [1584]
Lepisosteus oculatus       ..T ... ... ..C ... ..T ..T ... ... G.. ..C ... ... A.. ... ...  [1584]
Latimeria chalumnae        ... ... ... ..G ... ..C ... ..T ... G.A ... ... T.. ..G ... ...  [1584]
Gasterosteus aculeatus     ... ... ... ..A ... ... ... ..C ... ..C G.. ... ..A ... ... TCA  [1584]
Gadus morhua               ... ..T ... ..C ... ..C ... ..T ... ..T ..C T.. ..G ... ... TCT  [1584]
Carassius auratus          ... ... ..C ... ... ... ... ..C ... G.. ... T.. ... ... ... ..T  [1584]
Astyanax mexicanus         ... ... ..T ..A ... ... ..T ..C ... ..C T.. ... ... ... ... ...  [1584]
```

```
Danio rerio                ACA GGC CTG TAT AAG GAG CTT GAA TTC AAC AAT TAT GCC AAC CCG ATG  [1632]
Xiphophorus maculatus      ... ..G ..C ..C ... A.. ..A ..G .A. ..T G.C ..C ... ... ... C..  [1632]
Tetraodon nigroviridis     ... ... ... ..C .G. ..A ..A ... .A. ..T G.C ..C ... .G. ... C..  [1632]
Takifugu rubripes          ... ... ... ..C ... ..A ..A ... .AT ..T G.C ... ... .G. ..A C..  [1632]
Takifugu obscurus          ... ... ... ..C ... ..A ..A ... .AT ..T G.C ... ... .G. ..A C..  [1632]
Poecilia formosa           ... ..G ..C ..C ... A.. ..A ..G .A. ... G.C ... ... ... ... C..  [1632]
Oryzias latipes            ..T ..G ..C ..C ... ... ..A ..G .A. ... G.C ..C ... ... ... C..  [1632]
Oreochromis niloticus      ... ..A ..C ..C ..A ... ..A ..G .A. ..T G.. ... ... ... ..T C.A  [1632]
Lepisosteus oculatus       ..G ... ... ..C C.A C.. ..A ..G C.G ..T G.C ..C A.. ..T ..C C..  [1632]
Latimeria chalumnae        TGG ..A ..C ..C ... ... ..G A.G AC. ..T ..C ... ..A ..T ..A C..  [1632]
Gasterosteus aculeatus     ..C ... ..C ..C ... ... ..C ..G ... ... G.C ..C ... ... ... C..  [1632]
Gadus morhua               ... ..A ... ..C ... ... ..A ..G CA. ... G.C .GG ... .G. ..C C..  [1632]
Carassius auratus          ..G ... ... ... .G. ... ..C ... .A. ..T G.C ... ... ... ... T..  [1632]
Astyanax mexicanus         ..G ..G ..T ..C ... ... ..G ..T .AT ..T G.A ..C ... ... ... G..  [1632]

Danio rerio                GTT TGT GCC TTC TTC GTG GCT CTG ACG CCC ATC TGG GTC CTC ATC GCC  [1680]
Xiphophorus maculatus      ..G ... ..G G.G ..T ... ..G A.. TGT ..T T.G ... ... ..G ..A ...  [1680]
Tetraodon nigroviridis     ..G ... ..G G.T ..T ... ..C T.. TGT ... C.G ... ..G ..G ..T ...  [1680]
Takifugu rubripes          ..G ... ..G G.T ..T ... ..G T.A TGC ... C.G ... ..G ..G ..A ...  [1680]
Takifugu obscurus          ..G ... ..G G.T .-- --- --- --- --- --- --- --- --- --- --- ---  [1680]
Poecilia formosa           ..G ... ..G G.G ..T ... ..C A.. TGT ..T T.G ... ... ..G ..A ...  [1680]
Oryzias latipes            ..G ... ..A GCG ... ... ..A A.. TGC ..T C.G ... ..G ..G ... ...  [1680]
Oreochromis niloticus      ..G ... ..A G.A ..T ... ..G A.. TGC ..A C.A ... ..G ..G ..A ...  [1680]
Lepisosteus oculatus       ..G ... ... ... ..T ... ..G ... ..C ... C.G ... A.. G.. ... ..A  [1680]
Latimeria chalumnae        ..A ..C ..A ... ..T ... ..C T.A ..A ..T T.G ... ..T G.T ..T ..A  [1680]
Gasterosteus aculeatus     ..G ..C ... G.G ..T ... ..C ... TGC ... C.A ... ..G ..G ..A ...  [1680]
Gadus morhua               ..G ... ..T G.G ... ... ..C ..C TGT ... ..A ... ... ..G ... ..T  [1680]
Carassius auratus          .G. ... ... ... ..T ..C ..C ... ..A ... T.. ... ... ... ... ...  [1680]
Astyanax mexicanus         ..A ... .T. ... ..T A.C ..A ... ... ..T G.. ... ... ..G ..T ...  [1680]

Danio rerio                CGG CGG ATT CCC TCC ACC CGG GAA GTG CTG TAC TCA GGC TGG GAG CCT  [1728]
Xiphophorus maculatus      A.. AA. ..C ..A G.T ... A.A ... ..C ..C ..T ... ... ... ..A ...  [1728]
Tetraodon nigroviridis     A.. AA. ..C ... ... ... A.A ... C.C ..T ..T ..G ... ... ... ..G  [1728]
Takifugu rubripes          A.. AA. ..C ... ... ... A.A ... C.C ..C ..T ..T ... ... ... ...  [1728]
Takifugu obscurus          --- --- --- --- --- --- --- --- --- --- --- --- --- --- --- ---  [1728]
Poecilia formosa           A.. AA. ..C ..A G.T ... A.. ... ..C ..C ..T ... ... ... ... ..G  [1728]
Oryzias latipes            A.. AA. .CC ... ... ... A.. ..G ..C ..C ..T ..T ... ... ... ..G  [1728]
Oreochromis niloticus      A.. AA. ..C ..A ... ... A.A ..G ..C ..T ... ..C ... ... ... ..A  [1728]
Lepisosteus oculatus       ..C ..C ..C ... ... ... ..C ..G ... ... ... ..G ... ... ... ..C  [1728]
Latimeria chalumnae        AAA A.. .AC ..T G.A ..T ... ... ... T.. ... ... ..A ... ..A ...  [1728]
Gasterosteus aculeatus     A.. A.. ..C ..A ... ... ..A ... C.. ... ... ..C ... ... ... ..G  [1728]
Gadus morhua               ..C AA. ..C ..G ... ... ..A ..G ... ..T ... ..G ... ... ... ..C  [1728]
Carassius auratus          ... GC. ... .A. .T. ..T ... ... ... ..C ... ... ..T G.A ... ...  [1728]
Astyanax mexicanus         A.A AAA ..C ..A ... ..G A.A ... ... ..C ..T ..T ..G ... ..A ..A  [1728]
```

```
Danio rerio                GTC ATC ATC GCC ATG GCC ATC AGC AGT GTC GGA GGC CTC ATT CTG GAT  [1776]
Xiphophorus maculatus      ... ... ... ... ... ... ... ... ... ..T ... ..T ..G ..C ..T ..C  [1776]
Tetraodon nigroviridis     ... ... ... ... ... ... ... ... ... ... ..T ..T T.G ..C ... ..C  [1776]
Takifugu rubripes          ... ... ..T ... ... ... ... ... ... ... ..T ..T ..T T.A ..C ..C ..C  [1776]
Takifugu obscurus          --- --- --- --- --- --- --- --- --- --- --- --- --- --- --- --- ---  [1776]
Poecilia formosa           ... ... ... ... ... ... ... ... ... ..T ... ..T ..G ..C ..T ..C  [1776]
Oryzias latipes            ... ..T ... ..A ... ..G ... ..T ... ..G ... ..T T.G ..C ..C ..C  [1776]
Oreochromis niloticus      ... ... ... ... ... ... ... ... ... ... ..T ..T ..G ..C ..T ..C  [1776]
Lepisosteus oculatus       ... ..T ... ... ... ..G ..A ... ... ... ..G ..G ..G ..C ... ...  [1776]
Latimeria chalumnae        ..T ... ... ... ... ..A ... ... ... ... ..G ..T T.G ..A ... ...  [1776]
Gasterosteus aculeatus     ... ... ... ... ... ..A ... ... ... ..T ..T ..T T.G ..C ..C ..C  [1776]
Gadus morhua               ... ... ... ... ... ..G ... ... ... ..T ..C ... ..G ..C ... ..C  [1776]
Carassius auratus          ... ... ... ... ... ... ... ... .A. ..T ..C ..T T.T ... ... ...  [1776]
Astyanax mexicanus         ..T ..A ..T ... ... ..A ... ... ... ..T ..G ..A ..T ..C ... ...  [1776]

Danio rerio                AAG ACC GTA TCA AAC CCC AAC TTC GCA GGA ATG GCC GTT TTC ACT CCG  [1824]
Xiphophorus maculatus      ... ..T ..T AGC G.. ..A ..T ... ..T ..C ... ..T ... ... ... ..A  [1824]
Tetraodon nigroviridis     ... ... ..C A.C ... ..A ... ..T CGT ..C ... ..T ..G ... ..A ...  [1824]
Takifugu rubripes          ... ... ..C A.C ... ..G ... ..T .TT ..C ... ..T ..C ..T ..A ..A  [1824]
Takifugu obscurus          --- --- --- --- --- --- --- --- --- --- --- --- --- --- --- --- ---  [1824]
Poecilia formosa           ... ... ... AGC G.. ..A ... ... T.T ... ... ..T ... ... ... ..A  [1824]
Oryzias latipes            ..A ..T ..C A.C ... ... ... ..T ..T ... ..T ... ..C ... ..A ..A  [1824]
Oreochromis niloticus      ..A ..T ..C A.C ... ..A ... ..T ..T ..C ... ..T ..C ... ... ..A  [1824]
Lepisosteus oculatus       ... ... ..G ..C G.T ... ... ... ..C ..G ... ..G ..G ... ... ...  [1824]
Latimeria chalumnae        ..A ... ... ..G G.T ..A ... ..T ... ... ... ..A ... ..T ..A ..A  [1824]
Gasterosteus aculeatus     ... ... ..C A.C ... ..A ... ..T ..T ..C ... ..G ..C ... ..C ...  [1824]
Gadus morhua               ... ..G ..G ..C ... ..A ... ..T ..G ..C ... ..T ... ... ... ..T  [1824]
Carassius auratus          ... ..A ... ..T ... ..T ... ..T ..T ... ... ..G ..G ... ... ..T  [1824]
Astyanax mexicanus         ... ..T ..G A.G G.T ... ... ..T ..T ... ... ..A ... ... ..A ..A  [1824]

Danio rerio                GTC ATT AAC GGT G-- --- --- -TG GGT GGT AAT CTG GTG GCG GTT CAA  [1872]
Xiphophorus maculatus      ... ..C ... ... .-- --- --- -.A ..A ..C ..C ... ... ..A ... ..G  [1872]
Tetraodon nigroviridis     ... ..C ... ... .-- --- --- -.T ..A ... ..C T.. ..T ..T ... ...  [1872]
Takifugu rubripes          ... ..C ..T ... .-- --- --- -.T ..A ..G ..C T.. ..T ..A ... ...  [1872]
Takifugu obscurus          --- --- --- --- --- --- --- --- --- --- --- --- --- --- --- --- ---  [1872]
Poecilia formosa           ... ..C ... ... .GA ACA GGT G.A ..A ..C ..C ... ... ..A ... ..G  [1872]
Oryzias latipes            ... ..C ... ... .-- --- --- -.T ..G ... ... ... ... ..A ... ..G  [1872]
Oreochromis niloticus      ... ..C ... ... .-- --- --- -.. ..A ... ..C ... ..A ..A ... ..G  [1872]
Lepisosteus oculatus       ... ..C ... ... .-- --- --- -.T ..C ..G ..C ... ... ... ..G ..G  [1872]
Latimeria chalumnae        ..T ..C ..T ... .-- --- --- -.C .C. ..G ..C ..A ..A ..T ..C ...  [1872]
Gasterosteus aculeatus     ... ..C ..T ..G .-- --- --- -.. ..A ... ..C ... ..C ..A ..G ..G  [1872]
Gadus morhua               ... ..C ... ..C .-- --- --- -.T ..C ..G ..C ... ... ... ..A ..G  [1872]
Carassius auratus          ... ..C ... ... .-- --- --- -.. ..C ..C ... T.. ... ... ... ...  [1872]
Astyanax mexicanus         ... ..C ... ..C .-- --- --- -.. .C. ... ..C T.. ... ..A ..G ..G  [1872]
```

```
Danio rerio                GCC AGT CGT ATC TCC ACC TAC CTG CAC ATG AAC GCC CTG CCC ATT GTA  [1920]
Xiphophorus maculatus      ... ... ..G ... ... ... ..T ..C ... ... ... .GG ... ... C.G .GG  [1920]
Tetraodon nigroviridis     ..T ... ..A ... ... ... ..T ... ... ..C ..T .G. G.C ... ..G .GG  [1920]
Takifugu rubripes          ... ... ..A ... ... ... ..T ... ... ..C ... .GT G.C ... ..G .GG  [1920]
Takifugu obscurus          --- --- --- --- --- --- --- --- --- --- --- --- --- --- --- ---  [1920]
Poecilia formosa           ... ... ..G ... ... ... ..T ..C ... ... ... .GA ... ... C.G .GG  [1920]
Oryzias latipes            ... ... ..A ..T ... ... ..T ..C ... ... .GT .GT ..T ... ..G .G.  [1920]
Oreochromis niloticus      ..A ... ..A ... ... ... ..T ..C ... ... ... .GT A.A ... ..G .GG  [1920]
Lepisosteus oculatus       ... ..C ..G ... ... ... ... ... ... ... .GT .G. A.. ..A GGC C.G  [1920]
Latimeria chalumnae        ..T ... ..G ... ..T ... .T. ..T ... ..T ..T .GG A.. ..A GGG .AG  [1920]
Gasterosteus aculeatus     ... ... ..A ... ... ... ... ... ... ... ... .G. ..C ... ..G .GG  [1920]
Gadus morhua               ... ..C A.G ... ... ... ... ... ... ... ..T .G. ..T ... T.A .GG  [1920]
Carassius auratus          ... ... ..A ... ... ..A ... ... ... ... ... ... T.. ... ..A .C.  [1920]
Astyanax mexicanus         ... ... ..G ... ... ..G ... T.. ... ... ..T .G. ... ... ... .CC  [1920]

Danio rerio                GAG CCA AAC CCG GCC CCT CGC AAA TGC CCT ACT CCA TGG GGC ACC TTC  [1968]
Xiphophorus maculatus      ..C ..C ... .T. ..G ..C A.G ..G ..T ..C ..A ..C ..C TCT T.. ..T  [1968]
Tetraodon nigroviridis     ..C ..C .C. ..C A.. T.C A.G ..G ... ..C ..A ..C ..T AC. ... ...  [1968]
Takifugu rubripes          ..C ..C ... ..C A.. T.C A.G ..G ... ..C ..A ..C ..C AC. T.. ...  [1968]
Takifugu obscurus          --- --- --- --- --- --- --- --- --- --- --- --- --- --- --- ---  [1968]
Poecilia formosa           ..C ..C ... .T. ..G ..C A.G ..G ..T ..C ..A ..C ..C TCT T.. ..T  [1968]
Oryzias latipes            ..A ..T .G. ..C T.. ..C A.G ..G ... ..A ..A ..C ..C ATG G.T ...  [1968]
Oreochromis niloticus      ..T ..C ... ..A ... ..C A.G ..G ..T ..C ..A ..C ..C AC. T.. ...  [1968]
Lepisosteus oculatus       ... ..C .G. GTC C.G .AG ... .GG ... ..C ..G ..C ..C A.. ... ...  [1968]
Latimeria chalumnae        .G. T.T G.G ATC ATT .AC ..G ..G ... ..A .G. ..C ..C A.. ..G ...  [1968]
Gasterosteus aculeatus     ..C ..C ... .AC AT. ..C A.G ..G ... ..C ..C ..C ..C .C. T.. ...  [1968]
Gadus morhua               ..C ..C ... TAC C.. ..C A.G ..G ... ..C ..A ..C ..C AT. T.A ...  [1968]
Carassius auratus          ... ..C .G. ..A ... ..G .AG ... ..T ..A ... ..C ... A.. T.G ...  [1968]
Astyanax mexicanus         ..A ..C ... ..T T.T ..G .AA ... ... ..C ..A ..C ..C A.. ..A ...  [1968]

Danio rerio                TTT GGG TCT GGT GTG AAT TCT CGA TCT GCC AAA GTG CTG TTT CTG CTG  [2016]
Xiphophorus maculatus      ..C ..C ..C AC. ... ..C ... ... ... ... CGT ..T ..C ..C T.C ...  [2016]
Tetraodon nigroviridis     ..C A.C ..C TCC C.. ... G.G ..T ..A ..T CGT ... ..T ..C ... ...  [2016]
Takifugu rubripes          ... ..C ..C TC. C.. ..C G.A ..G ..G ... CGG ... ... ..C ... ...  [2016]
Takifugu obscurus          --- --- --- --- --- --- --- --- --- --- --- --- --- --- --- ---  [2016]
Poecilia formosa           ..C ..C ..C AC. ... ..C ... ..C ... ... CGT ..T ... ..C T.C ...  [2016]
Oryzias latipes            ..C A.C ..C ACG ..T ..C ... ..T ..G ... CGT ... ..C ..C ..C T..  [2016]
Oreochromis niloticus      ... ..T ..C AC. ... ..C ... ..T ..A ... CGT ..A ..T ..C ..C ...  [2016]
Lepisosteus oculatus       ..C ..A ..C A.C ... ..C ..G ... ... ..G CGG ... ..C ..C ..C ...  [2016]
Latimeria chalumnae        ... ..T ..A .A. ... ..C ..C A.G ... ..T CG. ... ... ... T.A ..T  [2016]
Gasterosteus aculeatus     ..C ..C ..C TC. ... ..C ..C ..C ..G ... CG. ... ..C ..C ..C ...  [2016]
Gadus morhua               ..C ..T ..C TCG C.. ..C G.G ..C ..C ... CGC ..T ..C ..C A.. ...  [2016]
Carassius auratus          ... ..C ..A .C. C.C ..C ..A ..T ... ... .G. ... ..C ..C ..C ...  [2016]
Astyanax mexicanus         ... ..C ..A ..A ... ... ..C ..T ..A ... CG. ... ..C ..C ..C ...  [2016]
```

```
Danio rerio                GTC GCT CCT GGT CAT CTG GTC TTC CTC TAC ACT ATT AAC TCT ATG CGG  [2064]
Xiphophorus maculatus      ..T ..C ..G ... ..C A.C A.. ... ... ... ..C ... ... ..C C.. A.A  [2064]
Tetraodon nigroviridis     ..T ..G ..A ..A ..C ..C A.. ... ... ... ..C ..C ... ..C C.. A..  [2064]
Takifugu rubripes          ..T ..C ..G ..A ..C ..C A.. ... ... ... ..C ..C ... ..C C.. A.A  [2064]
Takifugu obscurus          --- --- --- --- --- --- --- --- --- --- --- --- --- --- --- ---  [2064]
Poecilia formosa           ..T ..C ..G ... ..C A.C A.. ... ... ... ..C ... ... ..C C.. A.A  [2064]
Oryzias latipes            ..T ... ... ... ..C ..C ... ... ... ..T ..C ..C ... ... C.. A..  [2064]
Oreochromis niloticus      ..T ..C ..A ..G ..C ..C ... ... ... ... ..C ..C ... ..C C.. A..  [2064]
Lepisosteus oculatus       ..G .TG ..C ..G ... ... ... ... ... ... ..C ..C ... ..C ... .A.  [2064]
Latimeria chalumnae        ..G .TG ... ..A ..C ... ..T ... ..A ... ..C ..A ... ..A ... .AA  [2064]
Gasterosteus aculeatus     ... ..C ..G ... ..C ..C .C. ... ... ... ..C ..C ... ... C.. A..  [2064]
Gadus morhua               ..G ..G ..C ..C ..C ..C ... ... ... ... ..C ..C ... ..C ... ..A  [2064]
Carassius auratus          ... ... ... ... ... ... ... ... ..G ... ... ... ... ... ... .A.  [2064]
Astyanax mexicanus         ..G ... ... ... ... ... ... ..T ..G ... ... ... ... ..C ... A..  [2064]

Danio rerio                GGA GGA CAC ACC ACT CTC ACT TAC ATC TTC ATT GCT TTT TAC CTG GCT  [2112]
Xiphophorus maculatus      ..G ..T ... ... ... ..G ..C CC. ... ... G.C A.C ..C ... ... .TA  [2112]
Tetraodon nigroviridis     .CG ..C ... ... ..C ..G ..A CC. ... ... ... AGC ..C ... ... ...  [2112]
Takifugu rubripes          ..G ..C ... ... ..C ..G ..A CC. G.. ... ... AGC ..C ... ... ...  [2112]
Takifugu obscurus          --- --- --- --- --- --- --- --- --- --- --- --- --- --- --- ---  [2112]
Poecilia formosa           ..G ..T ... ... ..C ..G ..C CC. ... ... ..C T.C ..C ... ... .TA  [2112]
Oryzias latipes            ... ..G ... ... ..C ..G ..A CC. ... ... ..C A.C ... ..T ... ..A  [2112]
Oreochromis niloticus      ..G ..G ... ... ..C ... ..A CC. ... ... ... A.C ..C ..T ... TT.  [2112]
Lepisosteus oculatus       .CG ... ... ... ..C ... ..C .C. ..T ..T G.. ..C ... ... A.. A..  [2112]
Latimeria chalumnae        ... ..G ..T ... ..A ..G ... CCT ..A ..T G.A ... ..C ... A.. A..  [2112]
Gasterosteus aculeatus     ..G ..G ... ... ..C ..G ..G GCG C.. ..T G.. T.C ..C ... A.. .TC  [2112]
Gadus morhua               ..C ... ... ... ..C ..G ..G .C. ... ... G.. ..C ..C ... ... .GC  [2112]
Carassius auratus          ..T ... ... ... ... ... ..C .C. C.. ... ... ..A ... ..T ... ..C  [2112]
Astyanax mexicanus         ..T ... ... ... ... ... ..C ... ... ... ... ... ... ... T.. ...  [2112]

Danio rerio                GCT GCT CTA CTA CAG GTC ATT ATC CTG CTG TAT CTG GCA GAC TGG ATG  [2160]
Xiphophorus maculatus      ... ... ... ..G ... ... GCA ... ..C ... ..C ... ..T ... ... ...  [2160]
Tetraodon nigroviridis     ... ..A ... ..G ... ..G ..G ..T ..T ..C ..C A.. ..G ... ... ...  [2160]
Takifugu rubripes          ... ..A ... ..G ... ..G ..G ... ..T ..C ..C A.. ..G ... ... ...  [2160]
Takifugu obscurus          --- --- --- --- --- --- --- --- --- --- --- --- --- --- --- ---  [2160]
Poecilia formosa           ... ... ..T ..G ... ..T GCA ... ..C ... ..C ... ..T ... ... ...  [2160]
Oryzias latipes            ... ..A ... ..G ... ..T ..G ... ..C ..C ..C ... ... ... ... ...  [2160]
Oreochromis niloticus      ... ..A ... ..C ... ... ..G ... ..C ..C ..C ... ... ... ... ...  [2160]
Lepisosteus oculatus       ... ..A ..G ... ... ..G C.G ... ... ... ..C T.T T.T ... ... ...  [2160]
Latimeria chalumnae        ... ... ..T ... ... ..G C.A ..T ..T ..C ..C A.T ..T ..T ... ...  [2160]
Gasterosteus aculeatus     ..C ... ... ... ... ..G T.A ... ..C ..C ..C ... ... ... ... ...  [2160]
Gadus morhua               ..C ..C ..T ..G ... ..G C.G ... ... ... ..C ... ..C ... ... ...  [2160]
Carassius auratus          ..G ... ..G ..T ... ..T G.G ... ... ... ..C ..T ... ... ... ...  [2160]
Astyanax mexicanus         ... ..A T.. ..T ... ..G ..G ... ..A ... ... ... ..T ... ... ...  [2160]
```

```
Danio rerio                GTG AAC TGG ATG TGG CGT CGA GGG ATG GAT CCT GAC AAC TTC TCC ATC  [2208]
Xiphophorus maculatus      ..T C.. ... ... ... G.C ... ..C ... ..C ..C ... ... ... ... ...  [2208]
Tetraodon nigroviridis     ..T C.. ... ... ... G.C ... ..C ... ..C ... ... ... ... ... ...  [2208]
Takifugu rubripes          ..T C.. ... ... ... G.C ... ..C ... ..C ..C ... ... ... ... ...  [2208]
Takifugu obscurus          --- --- --- --- --- --- --- --- --- --- --- --- --- --- --- ---  [2208]
Poecilia formosa           ..T C.. ... ... ... G.C ... ..C ... ..C ..C ... ... ... ... ...  [2208]
Oryzias latipes            ..T ... ... ... ... G.G A.G ..C ... ... ..A ... ... ... ... ...  [2208]
Oreochromis niloticus      ..C C.. ... ... ... G.. ..G ..C ... ..C ... ... ... ..T ... ...  [2208]
Lepisosteus oculatus       ... C.. ... ... ... G.G A.G ..C ... ..C ... ..T ... ... ... ...  [2208]
Latimeria chalumnae        ..C ... ... ... ... G.G ..G ..A ... ..C ..A ..T ... ... ... ...  [2208]
Gasterosteus aculeatus     ... C.. ... ... ... G.G ..C ..C ... ..C ..C ... ... ... ... ...  [2208]
Gadus morhua               ... C.. ... ... ... G.G ..G ..C ... ..C ..G ... ... ... ... ...  [2208]
Carassius auratus          ..T ..T ... ... ... .A. ... ... ... A.. ... ... ... ... ... ..T  [2208]
Astyanax mexicanus         ... C.G ... ... ... AAA ... ... ... ..C ..C ..T ... ... ... ..T  [2208]
                                                                          <<<PCR Primer 2

Danio rerio                CCC TAC TTG ACG GCG CTG GGA GAC CTG CTG GGG ACA GGC TTC CTG GCT  [2256]
Xiphophorus maculatus      ..G ... C.. ..C ..T ... ..C ... ..C ... ..A ..C ... ... ..C ..C  [2256]
Tetraodon nigroviridis     ... ... C.. ..C ..C ... ..C ... ... ... ... ..C ... ... ..C ...  [2256]
Takifugu rubripes          ... ... C.. ..C ..T ... ..T ... ... ... ... ..C ... .A. ..C ..C  [2256]
Takifugu obscurus          --- --- --- --- --- --- --- --- --- --- --- --- --- --- --- ---  [2256]
Poecilia formosa           ..G ... C.. ..C ..T ... ..C ... ..C ... ..A ... ... ... ..C ..C  [2256]
Oryzias latipes            ..G ... C.. ..C ..C ... ..C ... ..C ... ... ..G ... ... ..C ..C  [2256]
Oreochromis niloticus      ..G ... C.. ..C ... ... ..T ... ... ... ... ..T ... ... ..A ..C  [2256]
Lepisosteus oculatus       ..T ... C.. ... ..C ... ..G ... ... ... ..A ..T ... ... ... ...  [2256]
Latimeria chalumnae        ..A ... C.A ... ..T ... ..C ... ..C ..T ..A ... ... ... ..A ...  [2256]
Gasterosteus aculeatus     ... ... C.. ..C ..T ... ..C ... ... ... ..C ..C ... ... ..C ..C  [2256]
Gadus morhua               ... ... C.. ... ..C ... ... ... ... ... ..C ..G ... ... ... ..A  [2256]
Carassius auratus          ... ... ... ..T ..C ... ... ... ... ... ... ..G ... ... ... ...  [2256]
Astyanax mexicanus         ... ... C.. ..T ..C ... ..T ... ... ... ... ..G ... ... ... ...  [2256]

Danio rerio                CTG TGT TTC CAC ATC CTG TGG CTA ATT GGA GAT CGG GAC ACA GAT GTG  [2304]
Xiphophorus maculatus      ..C ..C ... ... ..G .GT ... T.C ..C ..G ..C A.A ... T.C A.. T.A  [2304]
Tetraodon nigroviridis     ..C ..C ... ... ..G .GC ... T.T ..C ..G ..C A.A ... ..T .TC CC.  [2304]
Takifugu rubripes          ..C ..C ... ... ..G TGC ... T.T ..C ... ..C A.A ... C.G ATC CC.  [2304]
Takifugu obscurus          --- --- --- --- --- --- --- --- --- --- --- --- --- --- --- ---  [2304]
Poecilia formosa           ..C ..C ... ... ..G .GT ... T.C ..C ..G ..C A.A ... T.C A.. T.A  [2304]
Oryzias latipes            ..C ..C ..T ... ..G .GC ... T.C ... ..G ..C A.A ... .TG A.. ...  [2304]
Oreochromis niloticus      ... ..C ... ... T.G .GC ... T.C ..C ... ..C A.A ... ..T A.. ...  [2304]
Lepisosteus oculatus       T.. A.C ..T ... ... ... ... ..C ..C ..G ..C ..C ... ..C ..C ..C  [2304]
Latimeria chalumnae        ... A.C ..T ... ..T ... ... ..T ... ... ..C ... ... ... ..T ..T  [2304]
Gasterosteus aculeatus     ..C ..C ... ... ..G .GC ... T.C ..C ..C ..C TCT ... T.T A.C .C.  [2304]
Gadus morhua               ..C ..C ... ... G.G ..T ... ..C ..C ..G ..C ..A ... ..G ..C ...  [2304]
Carassius auratus          ... ... ... A-- --- --- --- --- --- --- --- --- --- --- --- ---  [2304]
Astyanax mexicanus         ... ..C ... ... ... ... ... ..G ... ... ..C ..A ... ..G ..C ...  [2304]
```

```
Danio rerio                GGT GAT TGA  [2313]
Xiphophorus maculatus      ..C A.C ...  [2313]
Tetraodon nigroviridis     ..A A.C ...  [2313]
Takifugu rubripes          ..A A.C ...  [2313]
Takifugu obscurus          --- --- ---  [2313]
Poecilia formosa           ..C A.C ...  [2313]
Oryzias latipes            ..C ... ...  [2313]
Oreochromis niloticus      ..C A.C ...  [2313]
Lepisosteus oculatus       ..C ... ...  [2313]
Latimeria chalumnae        ..A ..C ...  [2313]
Gasterosteus aculeatus     ..G A.C ...  [2313]
Gadus morhua               ... ..C ...  [2313]
Carassius auratus          --- --- ---  [2313]
Astyanax mexicanus         ..C ..C ...  [2313]
```

Figure 29: SLC41a1 nucleotide alignment. Alignment of the coding sequences for *Oreochromis niloticus (*ENSONIG00000003282), *Gadus morhua (*ENSGMOG00000004376), *Danio rerio (*ENSDARG00000070214), *Poecilia formosa (*ENSPFOG00000005128), *Astyanax mexicanus (*ENSAMXG00000003381), *Latimeria chalumnae (*ENSLACG00000001579), *Oryzias latipes (*ENSORLG00000012106), *Lepisosteus oculatus (*ENSLOCG00000011890), *Gasterosteus aculeatus (*ENSGACG00000010942) and *Takifugu rubripes* (ENSTRUG00000000115) *and Takifugu obscurus (*AB700626*)* and the obtained *Carassius auratus* sequence. The primers used for the initial sequencing (PCR primers 1 and 2) are highlighted in yellow on the used *D. rerio* sequence, while the qPCR primers designed and used for the expression studies are highlighted in light blue on the obtained *C. auratus* sequence; >>> signifies forward primers, <<< signifies reverse primer.

```
Danio rerio                ---------- ---------- ---------- ---------- ----------  [ 50]
Xiphophorus maculatus      ---------- ---------- ---------- ---------- ----------  [ 50]
Tetraodon nigroviridis     ---------- ---------- ---------- ---------- ----------  [ 50]
Takifugu rubripes          ---------- ---------- ---------- ---------- ----------  [ 50]
Takifugu obscurus          ---------- ---------- ---------- ---------- ----------  [ 50]
Poecilia formosa           ---------- ---------- ---------- ---------- ----------  [ 50]
Oryzias latipes            ---------- ---------- ---------- ---------- ----------  [ 50]
Oreochromis niloticus      VTVHSGWRDT FPQLVIQSSY *DL*ISHLKT VQRPRGVK*D V*SPVQRPVS  [ 50]
Lepisosteus oculatus       ---------- ---------- ---------- ---------- ----------  [ 50]
Latimeria chalumnae        ---------- ---------- ---------- ---------- ----------  [ 50]
Gasterosteus aculeatus     ---------- ---------- ---------- ---------- ----------  [ 50]
Gadus morhua               ---------- ---------- ---------- ---------- ----------  [ 50]
Carassius auratus          ---------- ---------- ---------- ---------- ----------  [ 50]
Astyanax mexicanus         ---------- ---------- ---------- ---------- ----------  [ 50]

Danio rerio                ---------- ---------- ---------- ---------- ----------  [100]
Xiphophorus maculatus      ---------- ---------- ---------- ---------- ----------  [100]
Tetraodon nigroviridis     ---------- ---------- ---------- ---------- ----------  [100]
Takifugu rubripes          ---------- ---------- ---------- ---------- ----------  [100]
Takifugu obscurus          ---------- ---------- ---------- ---------- ----------  [100]
Poecilia formosa           ---------- ---------- ---------- ---------- ----------  [100]
Oryzias latipes            ---------- ---------- ---------- ---------- ----------  [100]
Oreochromis niloticus      HGQQTDSMTG ATAGL*FTYF SSLY*TAKDC LQLNAGEFCG ESPPCCFLSF  [100]
Lepisosteus oculatus       ---------- ---------- ---------- ---------- ----------  [100]
Latimeria chalumnae        ---------- ---------- ---------- ---------- ----------  [100]
Gasterosteus aculeatus     ---------- ---------- ---------- ---------- ----------  [100]
Gadus morhua               ---------- ---------- ---------- ---------- ----------  [100]
Carassius auratus          ---------- ---------- ---------- ---------- ----------  [100]
Astyanax mexicanus         ---------- ---------- ---------- ---------- ----------  [100]

Danio rerio                ---------- ---------- ---------- ---------- ----------  [150]
Xiphophorus maculatus      ---------- ---------- ---------- ---------- ----------  [150]
Tetraodon nigroviridis     ---------- ---------- ---------- ---------- ----------  [150]
Takifugu rubripes          ---------- ---------- ---------- ---------- ----------  [150]
Takifugu obscurus          ---------- ---------- ---------- ---------- ----------  [150]
Poecilia formosa           ---------- ---------- ---------- ---------- ----------  [150]
Oryzias latipes            ---------- ---------- ---------- ---------- ----------  [150]
Oreochromis niloticus      SVLNQYAFCF LPA*PEHLAV NGEHTGSAPE APTGTQALQT HGCMCLAAGF  [150]
Lepisosteus oculatus       ---------- ---------- ---------- ---------- ----------  [150]
Latimeria chalumnae        ---------- ---------- ---------- ---------- ----------  [150]
Gasterosteus aculeatus     ---------- ---------- ---------- ---------- ----------  [150]
Gadus morhua               ---------- ---------- ---------- ---------- ----------  [150]
Carassius auratus          ---------- ---------- ---------- ---------- ----------  [150]
Astyanax mexicanus         ---------- ---------- ---------- ---------- ----------  [150]
```

```
Danio rerio                ---------- ---------- ---------- ---------- ----------  [200]
Xiphophorus maculatus      ---------- ---------- ---------- ---------- ----------  [200]
Tetraodon nigroviridis     ---------- ---------- ---------- ---------- ----------  [200]
Takifugu rubripes          ---------- ---------- ---------- ---------- ----------  [200]
Takifugu obscurus          ---------- ---------- ---------- ---------- ----------  [200]
Poecilia formosa           ---------- ---------- ---------- ---------- ----------  [200]
Oryzias latipes            ---------- ---------- ---------- ---------- ----------  [200]
Oreochromis niloticus      FRQSVFLSVF MTDLHTLSAS LMG*ISWTDQ VQNQIRWSIL TFPQNC*AEA  [200]
Lepisosteus oculatus       ---------- ---------- ---------- ---------- ----------  [200]
Latimeria chalumnae        ---------- ---------- ---------- ---------- ----------  [200]
Gasterosteus aculeatus     ---------- ---------- ---------- ---------- ----------  [200]
Gadus morhua               ---------- ---------- ---------- ---------- ----------  [200]
Carassius auratus          ---------- ---------- ---------- ---------- ----------  [200]
Astyanax mexicanus         ---------- ---------- ---------- ---------- ----------  [200]

Danio rerio                ---------- -----MVLWL KDQDKLS--D MSTGTERIEM KKEGVPPAYH  [250]
Xiphophorus maculatus      ---------- ---------- ---------- ---------- ----------  [250]
Tetraodon nigroviridis     ---------- ---------- ---------- ---------- ----------  [250]
Takifugu rubripes          ---------- ---------- ---------- ---------- ----------  [250]
Takifugu obscurus          ---------- -----....S .E...VPDI. ..S.DTEMKK EGGPLTQ.FL  [250]
Poecilia formosa           ---------- -----....S .E....PDIE ..S.DIEMKK EGGPLT.TFL  [250]
Oryzias latipes            ---------- ---------- ---------- ---------- ----------  [250]
Oreochromis niloticus      R*PFLIKPTV FKGFR....S .E.E..PDI. ..S.AIEMKK EGGPLTS.FL  [250]
Lepisosteus oculatus       ---------- -----.E..S EA.E.Q.--K ...VAGESKK E---SL.VF.  [250]
Latimeria chalumnae        ---------- ---------- ---------- ---------- ----------  [250]
Gasterosteus aculeatus     ---------- ---------- ---------- ---------- ----------  [250]
Gadus morhua               ---------- ---------- ---------- ---------- ----------  [250]
Carassius auratus          ---------- ---------- ---------- ------.K.. QN..A...FR  [250]
Astyanax mexicanus         ---------- -----....S .E.....--. .......... ....A.....  [250]

Danio rerio                HSNGSVHPVI LPDSPEEVPQ TPG-EYELTE VTSLPD---- -GDQENERP-  [300]
Xiphophorus maculatus      ---------- -------MSP QT.G.F.... ...FTE--IG ETGENE..SE  [300]
Tetraodon nigroviridis     ---------- ---------- ---------- ---------- ----------  [300]
Takifugu rubripes          ---------- ---------- ---------- ---------- --------AE  [300]
Takifugu obscurus          T..C...... .TKA...MSP GT.P.F.... .A.FVEMRVS ETGEDE..AE  [300]
Poecilia formosa           N..C....L. .TRG...MSP QT.G.F.... ...FTE--IG ETEENE..SE  [300]
Oryzias latipes            ---------- ---------- ---------- ---------- ----------  [300]
Oreochromis niloticus      N..CT..... .TKG....SP VT.D.F.... ...F.E--VN ETGEND..SE  [300]
Lepisosteus oculatus       .A..T..... R...Q..LRL EA.-VC.... .PAFS.---- -AEPDRD.A-  [300]
Latimeria chalumnae        ---------- ---------- ---------- ---------- ----------  [300]
Gasterosteus aculeatus     ---------- ---------- ---------- ---------- ----------  [300]
Gadus morhua               ---------- ---------- ---------- ---------- ----------  [300]
Carassius auratus          .........K ..LR...... AL.-..A... MS.TSE---- -S.....S.-  [300]
Astyanax mexicanus         .......... ..GD...RQP NA.-...... ...FS.---- -AE...DHS-  [300]
```

```
Danio rerio                -MVVLDCRAN AKGQREEDAL LENASQSNES DDTSTDQSPV PPAPLKETSF  [350]
Xiphophorus maculatus      IV.A..... .......... .......... ..N.IN...E .........I  [350]
Tetraodon nigroviridis     I..AM..... .......... .......... ....IN...Q .........L  [350]
Takifugu rubripes          IV.AM..... .......... ...G...... ....IN...E .......S.L  [350]
Takifugu obscurus          IV.AM..... .......... .......... ....IN...E .......S.L  [350]
Poecilia formosa           IV.A..... .......... .......... ..N.IN...E .........I  [350]
Oryzias latipes            -V.AI..LD. V......... .......... .....NR..E ....F..S..  [350]
Oreochromis niloticus      IV.AM..... .......... .......... .........E .T........  [350]
Lepisosteus oculatus       -V..I..... .......... ..........- -.I.A....M .A........  [350]
Latimeria chalumnae        ---------- ---------- ---------- ---------- ----------  [350]
Gasterosteus aculeatus     -V.AM..... .......... ......C... .........E ..P.......  [350]
Gadus morhua               -VAIV..... .......... .......... ....GG...E ..P.....A.  [350]
Carassius auratus          -....I.... ..D..G.GT. .......... YV..A..T.. .SV.M.....  [350]
Astyanax mexicanus         -...I..... .......... .......... .......... ..........  [350]
                                                                    D1 >>>

Danio rerio                SIGLQVLIPF LLAGFGTVAA GMVLDIVQHW TVFTEVTEVF ILVPALLGLK  [400]
Xiphophorus maculatus      ......VF.. .......... ..L....... ....K.S... ..........  [400]
Tetraodon nigroviridis     ......VF.. .......... .......... P..K...... ..........  [400]
Takifugu rubripes          T.....VF.. .......... .......... P..K...... ..........  [400]
Takifugu obscurus          T.....VF.. .......... .......... P..KD..... ..........  [400]
Poecilia formosa           ......VF.. .......... ..L....... .......S... ..........  [400]
Oryzias latipes            ......VF.. .......... .......... ...I..S... ..........  [400]
Oreochromis niloticus      ......VF.. .......... .......... ....D.S... ..........  [400]
Lepisosteus oculatus       .......F.. .......... .......... ...K...... ..........  [400]
Latimeria chalumnae        ---------- --------MP FF.--SP... E..KQ.N... ..........  [400]
Gasterosteus aculeatus     ......VF.. .......... .......... .......S... ..........  [400]
Gadus morhua               ......VF.. .......... .......... I......... ..........  [400]
Carassius auratus          ......M... .......... H..P....Q. S.....S... .-......P.  [400]
Astyanax mexicanus         ......VF.. .......... .......... K..A..N... ..........  [400]

Danio rerio                GNLEMTLASR LSTAANIGQM DTAKDMWKMI MGNLALIQVQ ATVVGFLASI  [450]
Xiphophorus maculatus      .......... .......... .......... V......... ..........  [450]
Tetraodon nigroviridis     .......... .......... .......... .......... ..........  [450]
Takifugu rubripes          .......... .......... .......... .......... ..........  [450]
Takifugu obscurus          .......... .......... .......... .......... ..........  [450]
Poecilia formosa           .......... .......... .......... .......... ..........  [450]
Oryzias latipes            .......... .......... .........V .......... ..........  [450]
Oreochromis niloticus      .......... ........H. .......... .......... ..........  [450]
Lepisosteus oculatus       .......... .......... ....E..... I......... ..........  [450]
Latimeria chalumnae        .......... .......... ...TGL.... T..M...... ..........  [450]
Gasterosteus aculeatus     .......... .......... ....N..... .........E T.........  [450]
Gadus morhua               .......... .......... ..P....... V.......-- -.........  [450]
Carassius auratus          .....I.... .......... .......... .......... ..........  [450]
Astyanax mexicanus         .......... .......... ....E..... .......... ..........  [450]
```

```
Danio rerio                AAVIFGWIPE GNFRMGHAIL LCASSVATAF IASLALGLIM IGVIIASRKV  [500]
Xiphophorus maculatus      .......L.. .Q.QL...V. .....M.... ....L..... ....V.....  [500]
Tetraodon nigroviridis     .....S.... .H..LS..V. .......... ....L..... ....V....I  [500]
Takifugu rubripes          .....S.... .H..L...V. .......... ....L..... .........I  [500]
Takifugu obscurus          ...T.S.... .H..L...V. .......... ....L..... .........I  [500]
Poecilia formosa           .......L.. .E.KL...V. .....M.... ....L..... ....V.....  [500]
Oryzias latipes            .......... .HI.L...V. .......... ....I..... ..........  [500]
Oreochromis niloticus      .......... .H.KL...V. .......... ....L..... ....V.....  [500]
Lepisosteus oculatus       .......... .H.KI..... .......... ....L..... .....G...I  [500]
Latimeria chalumnae        ...V.....D .H.DL...V. .......... ....I..M.. .....G...I  [500]
Gasterosteus aculeatus     .......... .H..L...V. .......... ....L..V.. ..........  [500]
Gadus morhua               .......... .Q..L...VV .......... ....L..... ....LL....  [500]
Carassius auratus          .......... ...K....V. .......... .......... ..........  [500]
Astyanax mexicanus         .......... ...K....V. .......... ....L...V. ..........  [500]
                                                  <<< D1

Danio rerio                GINPDNVATP IAASLGDLIT LSLLAGISTG LYKELEFNNY ANPMVCAFFV  [550]
Xiphophorus maculatus      .......... .......... .......... ...K..Y.D. ...L...V..  [550]
Tetraodon nigroviridis     .......... .......... .......... ..R...Y.D. .S.L...V..  [550]
Takifugu rubripes          .......... .......... .......... ......Y.D. .S.L...V..  [550]
Takifugu obscurus          .......... .......... .......... ......Y.D. .S.L...V--  [550]
Poecilia formosa           .......... .......... .......... ...K..Y.D. ...L...V..  [550]
Oryzias latipes            .......... .......... .......... ......Y.D. ...L...A..  [550]
Oreochromis niloticus      .......... .......... .......... ......Y.D. ...L...V..  [550]
Lepisosteus oculatus       .......... .......... .A...S.... ..QQ..L.D. T..L......  [550]
Latimeria chalumnae        .......... .......... .A..S...W. .....KT... ...L......  [550]
Gasterosteus aculeatus     .......... .......... ..V....... .........D. ...L...V..  [550]
Gadus morhua               .......... .......... .......... ......H.DW .S.L...V..  [550]
Carassius auratus          .......... .......... .A.....ii. ..R...Y.D. ...LG.....  [550]
Astyanax mexicanus         .......... .......... .......... .....DY.E. ...V..V..I  [550]

Danio rerio                ALTPIWVLIA RRIPSTREVL YSGWEPVIIA MAISSVGGLI LDKTVSNPNF  [600]
Xiphophorus maculatus      .MC.L..... .K..A..... .......... .......... ......D...  [600]
Tetraodon nigroviridis     ..C.L..... .K......L. .......... .......... .....T....  [600]
Takifugu rubripes          ..C.L..... .K......L. .......... .......... .....T....  [600]
Takifugu obscurus          ---------- ---------- ---------- ---------- ----------  [600]
Poecilia formosa           .MC.L..... .K..A..... .......... .......... ......D...  [600]
Oryzias latipes            .MC.L..... .KT....... .......... .......... .....T....  [600]
Oreochromis niloticus      .MC.L..... .K........ .......... .......... .....T....  [600]
Lepisosteus oculatus       ....L.IV.. .......... .......... .......... ......D...  [600]
Latimeria chalumnae        ....L..V.. K.N.A..... .......... .......... ......D...  [600]
Gasterosteus aculeatus     ..C.L..... ........L. .......... .......... .....T....  [600]
Gadus morhua               ..C.....i. .K........ .......... .......... ..........  [600]
Carassius auratus          ....F..... .A.HF..... ...G...... ....N...F. ..........  [600]
Astyanax mexicanus         ....V..... .K........ .......... .......... .....TD...  [600]
```

```
                                  D2 >>>
Danio rerio                AGMAVFTPVI NG----GGNL VAVQASRIST YLHMNALPIV EPNPAPRKCP  [650]
Xiphophorus maculatus      .......... ..----.... .......... .....G..LG D..L......  [650]
Tetraodon nigroviridis     R......... ..----.... .......... ...I.GV.MG D.T.TS....  [650]
Takifugu rubripes          V......... ..----.... .......... ...I.GV.MG D...TS....  [650]
Takifugu obscurus          ---------- ---------- ---------- ---------- ----------  [650]
Poecilia formosa           S......... ..GTGV.... .......... .....G..LG D..L......  [650]
Oryzias latipes            ..I....... ..----.... .......... ....SG..MG ..S.S.....  [650]
Oreochromis niloticus      .......... ..----.... .......... .....GI.MG D.........  [650]
Lepisosteus oculatus       .......... ..----.... .......... ....SGM.GL ..SVPQ.R..  [650]
Latimeria chalumnae        .......... ..----A... .......... F..I.GM.GE GSEIIH....  [650]
Gasterosteus aculeatus     .......... ..----.... .......... .....G..MG D..HI.....  [650]
Gadus morhua               .......... ..----.... .......... .....G..LG D..YP.....  [650]
Carassius auratus          ..........  ..----.... .......... .........A ..S...Q...  [650]
Astyanax mexicanus         .......... ..----A... .......... .....G...A ....S.Q...  [650]

Danio rerio                TPWGTFFGSG VNSRSAKVLF LLVAPGHLVF LYTINSMRGG HTTLTYIFIA  [700]
Xiphophorus maculatus      ..CSS....T ......R... F......II. ......L... .....P..VT  [700]
Tetraodon nigroviridis     ..CT...S.S L.A...R... ........I. ......L.A. .....P...S  [700]
Takifugu rubripes          ..CTS....S L.A...R... ........I. ......L... .....PV..S  [700]
Takifugu obscurus          ---------- ---------- ---------- ---------- ----------  [700]
Poecilia formosa           ..CSS....T ......R... F......II. ......L... .....P...S  [700]
Oryzias latipes            ..CMA..S.T ......R... .......... ......L... .....P...T  [700]
Oreochromis niloticus      ..CTS....T ......R... .......... ......L... .....P...T  [700]
Lepisosteus oculatus       ..CS.....S ......R... ...V...... ........QA. .....S..V.  [700]
Latimeria chalumnae        S.CS.....D ......R... ...V...... ........Q.. .....P..V.  [700]
Gasterosteus aculeatus     ..CAS....S ......R... .........A. ......L... .....AL.VS  [700]
Gadus morhua               ..CIS....S L.A...R... M......... .......... .....S..V.  [700]
Carassius auratus          ...SS....A L.....R... .......... .......Q.. .....SL...  [700]
Astyanax mexicanus         ..CS...... ......R... .......... .......... ..........  [700]

Danio rerio                FYLAAALLQV IILLYLADWM VNWMWRRGMD PDNFSIPYLT ALGDLLGTGF  [750]
Xiphophorus maculatus      ...V...... A......... .H...G.... .......... ..........  [750]
Tetraodon nigroviridis     .......... M....M.... .H...G.... .......... ..........  [750]
Takifugu rubripes          .......... M....M.... .H...G.... .......... .........Y  [750]
Takifugu obscurus          ---------- ---------- ---------- ---------- ----------  [750]
Poecilia formosa           ...V...... A......... .H...G.... .......... ..........  [750]
Oryzias latipes            .......... M......... .....G.... .......... ..........  [750]
Oreochromis niloticus      ...F...... M......... .H...G.... .......... ..........  [750]
Lepisosteus oculatus       ..MT...... L....FS... .H...G.... .......... ..........  [750]
Latimeria chalumnae        ..MT...... L....I.... .....G.... .......... ..........  [750]
Gasterosteus aculeatus     ..MV...... L......... .H...G.... .......... ..........  [750]
Gadus morhua               ...G...... L......... .H...G.... .......... ..........  [750]
Carassius auratus          .......... V......... .....H...N .......... ..........  [750]
Astyanax mexicanus         .......... M......... .Q...K.... .......... ..........  [750]
```

```
                          <<< D2
Danio rerio               LALCFHILWL IGDRDTDVGD * [771]
Xiphophorus maculatus     ......MR.F .....SNL.N . [771]
Tetraodon nigroviridis    ......MR.F ......VP.N . [771]
Takifugu rubripes         ......MC.F .....PIP.N . [771]
Takifugu obscurus         ---------- ---------- - [771]
Poecilia formosa          ......MR.F .....SNL.N . [771]
Oryzias latipes           ......MR.F .....MN... . [771]
Oreochromis niloticus     ......LR.F ......N..N . [771]
Lepisosteus oculatus      ...S...... .......... . [771]
Latimeria chalumnae       ...S...... .......... . [771]
Gasterosteus aculeatus    ......MR.F ...S.SNA.N . [771]
Gadus morhua              ......V... .......... . [771]
Carassius auratus         .....----- ---------- - [771]
Astyanax mexicanus        .......... .......... . [771]
```

Figure 30: SLC41a1 amino acid alignment. Peptide alignment of the obtained *C. auratus* SLC41a1 sequence with *Oreochromis niloticus (*ENSONIG00000003282), *Gadus morhua (*ENSGMOG00000004376), *Danio rerio (*ENSDARG00000070214), *Poecilia formosa (*ENSPFOG00000005128), *Astyanax mexicanus (*ENSAMXG00000003381), *Latimeria chalumnae (*ENSLACG00000001579), *Oryzias latipes (*ENSORLG00000012106), *Lepisosteus oculatus (*ENSLOCG00000011890), *Gasterosteus aculeatus (*ENSGACG00000010942) and *Takifugu rubripes* (ENSTRUG00000000115) *and Takifugu obscurus* **(**AB700626**).** Transmembrane domain D1 is contained within the D1 >>>> and <<< D1 markers and is higlited yellow. Transmembrane domain D2 is contained within the D2 >>> and <<<D2 markers and highlited yellow.

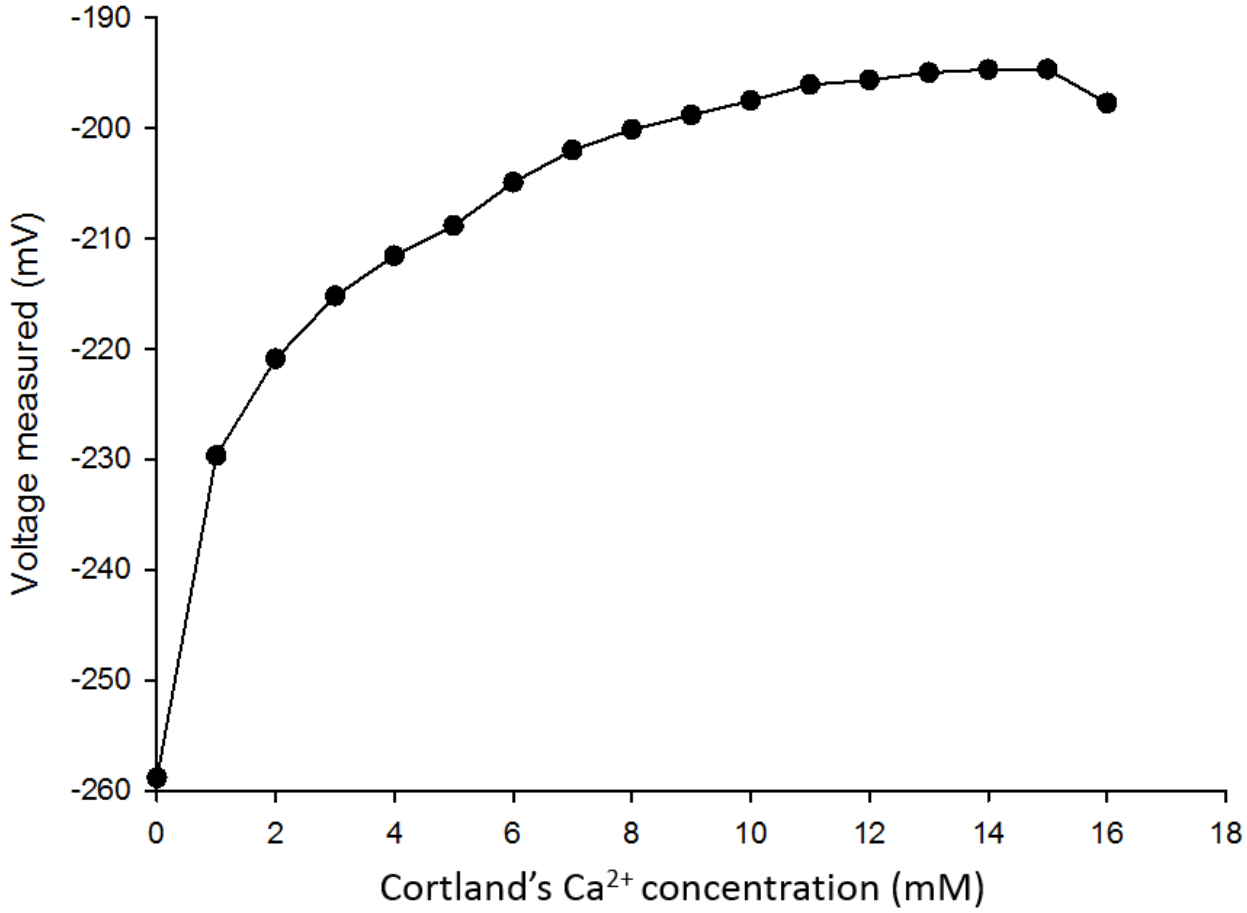

Figure 31: Magnesium ionophore selectivity for Ca^{2+}. A magnesium ionophore ISME was placed inside a Cortland's solution containing different concentrations of calcium (and a constant Mg^{2+} concentration of 1.9mM). All solutions used were made equimolar with the addition of meglumine.